Toe stability of rubble-mound breakwaters

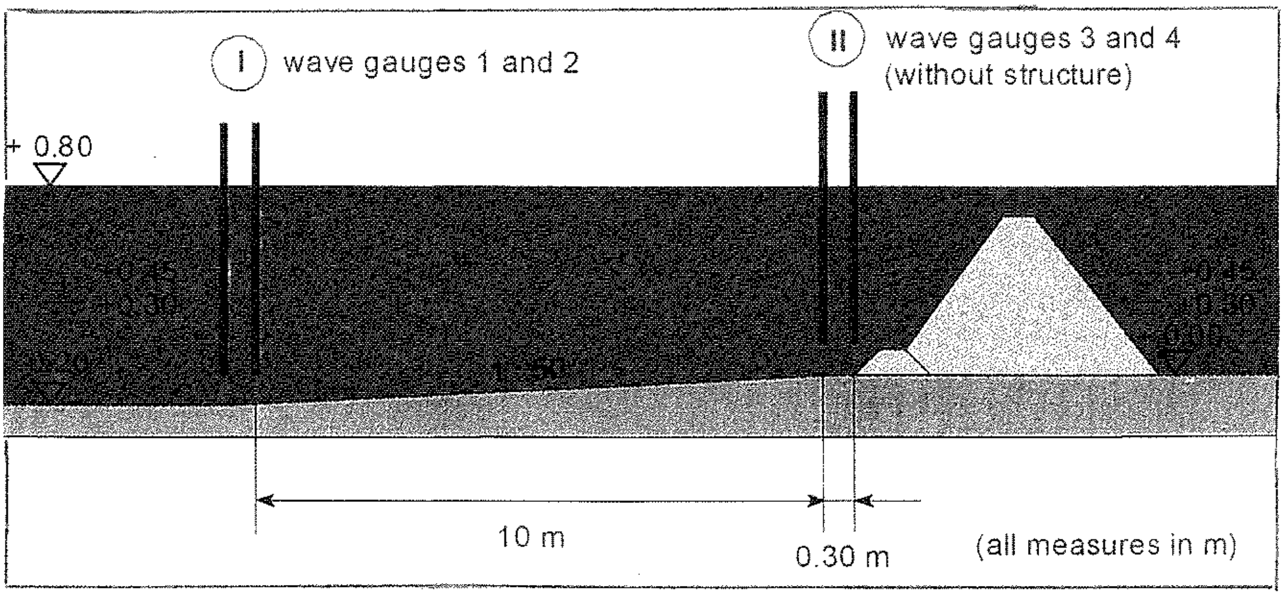

L. Docters van Leeuwen
Delft University of Technology
October 1996

Toe stability of rubble-mound breakwaters

The known is finite, the unknown infinite;
intellectually we stand on an island in the
midst of an illimitable ocean of inexplicability.
Our business in every generation is to reclaim
a little more land.

T.H.Huxley (1887)

Preface

This report contains a study on the stability of toe structures of rubble-mound break waters based on experimental research performed in the Laboratory of Fluid Mechanics of the Faculty of Civil Engineering of Delft University of Technology.
During the preparation of the tests a lot of people have been helpful.
First of all, Mr.L. Tulp of Delft Hydraulics "De Voorst" helped to collect all the materials needed.
During the construction assistants of the Laboratory of Fluid Mechanics were always willing to help with masonry or carpentry.
For the guidance in preparing my Master Thesis, I want to thank all the members of my commission who gave me all possible support to succeed. Especially T.van der Meulen who 'infected' me with his enthusiasm and who was of great help with his constructive criticism and ideas.
I'm also grateful to Dr.J.van der Meer and E.Gerding for answering my urgent questions and placing their valuable time at my disposal.
Last but not least I like to thank my parents and my friend for their patience and support in the past year.

Abstract

This Master Thesis contains a study on the stability of the toe structure of rubble-mound breakwaters based on small scale model tests performed in the large wave flume of the Laboratory of Fluid Mechanics of the Faculty of Civil Engineering of Delft University of Technology. In this report the study of Gerding (1993) on the stability of toe structures was continued. Gerding suggested a design relation for toe structures:

$$\frac{H_s}{\Delta D_{n50}} = (0.24 \frac{h_t}{D_{n50}} + 1.6) N_{od}^{0.15}$$

In his tests the density of the stone was not varied, although it is a parameter in the formula. The main purpose of the study at hand was to check the validity of the density in the Gerding-relation: therefore the stone mass density ρ_s in this research was varied: namely 1900, 2550 and 2850 kg/m^3, respectively the materials brick, porphyry and basalt.

Only one cross section of a rubble mound breakwater with various toe structures was investigated. The existing knowledge and the influence of all governing parameters is reviewed. The main variables were toe height, Z_t, water depth in front of the toe h_m, water depth above the toe, h_t, wave height, H_s, nominal stone diameter, D_{n50} and stone mass density ρ_s. Variation of the wave steepness wasn't of influence on the toe stability, because the range of values of the surf similarity parameter was such that the reflection coefficient was almost constant.

Existing knowledge is presented from which an analysis of the influence of the parameters involved followed. The tests are described and then the result of the measurements is analysed.

The data showed too much scatter and is therefore elaborated to one damage level N_{od} = 0,5 (start of damage). The influence of the relative density of the stone, Δ, was reproduced in the above mentioned Gerding-relation in the right way, because different stone mass densities gave similar results for $H_s/\Delta D_{n50}$ as a function of h_t/D_{n50}. The design curve by Gerding can be used for the design of toe structures, albeit that the designer must not forget the influence of h_m which is not mentioned in this relation. In the present study the same trend is found but the values from the present study show a higher stability of the structure than with the suggested relation of Gerding, which is more conservative.

Computations of toe stability were performed according to Shields and to Rance & Warren to get an analysis on analytical grounds, because empirically found results don't necessarily have to be right. Only the computations according to Rance & Warren could fit the results of the measurements with addition of a small amplification factor.
The parameter of the local water depth in front of the toe structure, h_m, had still an influence on the relation found between $H_s/\Delta D_{n50}$ and h_t/D_{n50}; this followed both from the tests and the computations. So it is risky to use the design curve for all h_m. The working-out of the computations must be improved and more experiments are needed to enlarge the knowledge of the influence of h_m and to simulate the measurements more accurate.

Between the present study and the research of Gerding large differences have been found. The damage estimated was on the avarage two times smaller than the damage Gerding had determined. The reason why this happened is still unknown. It is therefore recommended to perform further research to explain why this difference occurs.

More insight into toe stability may be found when the velocity distribution over the water depth in front of the toe structure is better defined and when the influence of the shape of the foreshore and of the reflection on the structure on toe stability would be taken into account.

CONTENTS

List of figures

List of tables

Notation

b_t	= width of the toe structure	[m]
C	= Chezy-coefficient	[-]
C_r	= reflection coefficient	[-]
D_{n50}	= nominal diameter $(M_{50}/\rho_s)^{1/3}$	[m]
D_{n85}	= diameter according to M_{85}	[m]
D_{n15}	= diameter according to M_{15}	[m]
D_{n85}/D_{n15}	= gradation	[-]
E	= wave energy density	[m²/Hz]
f_m	= mean frequency	[Hz]
f_p	= peak frequency	[Hz]
g	= accelaration of gravity	[m/s²]
h_m	= water depth in front of toe structure	[m]
h_t	= depth above the toe structure	[m]
H_i	= incoming wave height	[m]
H_{m0}	= significant wave height based on wave energy spectrum, $(m^0)^{1/2}$	[m]
H_r	= reflected wave height	[m]
H_s	= significant wave height, average of highest 1/3 of all waves	[m]
H_t	= transmitted wave height	[m]
$H_{2\%}$	= 2% wave height	[m]
L_0	= wave length at deep water	[m]
m^0	= zero-orderth moment of wave energy spectrum	[m]
M	= stone mass	[kg]
M_{50}	= 50% value on the mass distribution curve	[kg]
M_{85}	= 85% value on the mass distribution curve	[kg]
M_{15}	= 15% value on the mass distribution curve	[kg]
N_{od}	= damage number	[-]
s_{op}	= fictious wave steepness $(2\pi H_s)/(gT_p^2)$	[-]
T_p	= peak wave period of spectrum	[s]
T_m	= mean wave period	[s]
R_d	= wave run-down	[m]
R_u	= wave run-up	[m]
U_{orb}	= orbital velocity	[m/s]
U_*	= critical velocity	[m/s]
Z_t	= toe height	[m]
α	= angle of slope	[deg]
ν	= kinematic viscosity	[m²/s]
Δ	= relative mass density of stones (ρ_s/ρ_w-1)	[-]
ξ	= surf similarity parameter	[-]
ρ_s	= mass density of stones	[kg/m³]
ρ_w	= mass density of water	[kg/m³]

1 Introduction

1.1 General

This report contains a study on the stability of the toe structure of rubble-mound breakwaters based on small-scale model tests. Main purpose of the study was to extend the knowledge on toe structure stability. Although the stability of the toe of rubble-mound breakwaters is only a detail of a much more extensive design process, it may have a considerable influence on the cost of the structure.
This is especially the case when the yield of the quarry contains a limited fraction of suitable armour stone, so that it is important at what level the transition from armour stone to the lighter toe can be positioned.
The study was performed by L. Docters van Leeuwen, student at Delft University of Technology, as part of her Master's thesis, under guidance of Prof.ir. K. d'Angremond, Dr.ir. H.L. Fontijn, Ir. T. van der Meulen and Ir. G.J. Schiereck (all from Delft University of Technology).
In May, June and July 1996, the author performed a series of tests on toe structure stability at the Laboratory of Fluid Mechanics of the Faculty of Civil Engineering.

The study is restricted to staticly stable rubble-mound breakwaters. In a staticly stable breakwater the individual stones are stable and therefore the total breakwater is stable. Rubble-mound breakwaters consist of several layers and parts. The various parts are indicated in **Figure 1.1.**

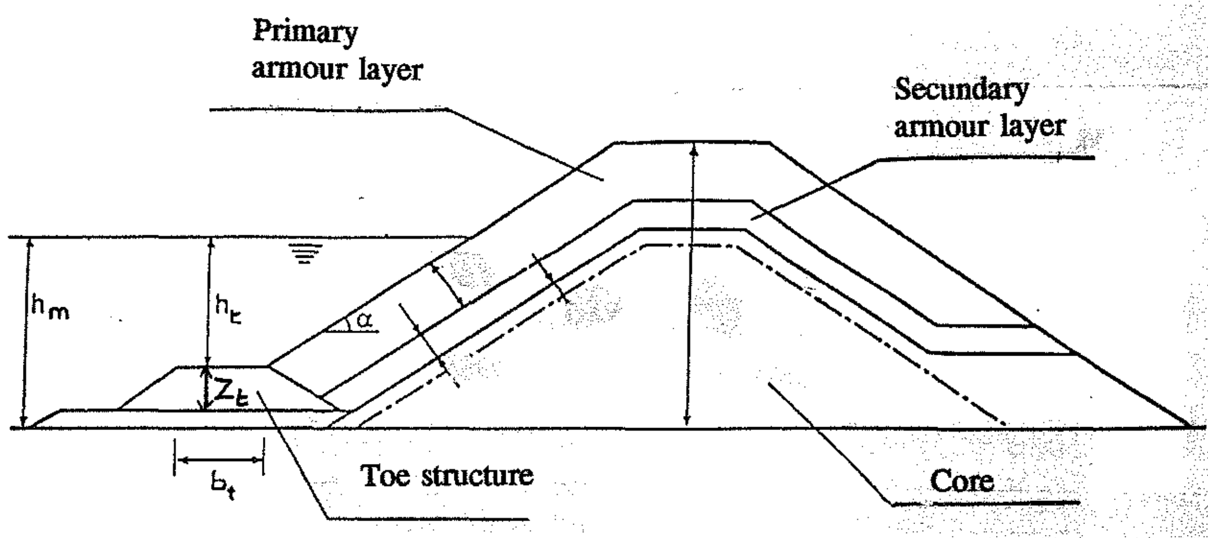

Figure 1.1 Various parts of a rubble-mound breakwater

Firstly the core material is dumped, this is often the cheapest available material. The function of the core is to support the covering armour layers in their proper position and the core must be impermeable for sand from the foundation layer. Above the core a filter layer is placed. This layer prevents penetration of core material in the secondary armour layer or the intermediate layer under the armour layer.

Each layer of the breakwater must be designed such that the adjacent layer of finer material cannot 'escape' by washing through its voids. At the top is the primary armour layer, which must resist the wave forces. The toe structure consists of light armour units to support the lower portion of the primary armour layer.

In Chapter 2 the physical processes involved with the toe structure will be given. In Chapter 3 the existing knowledge on toe stability is summed up. The present study is started in Chapter 4 with governing parameters, their influence and an approach to this study. Further, in Chapter 5 the description of the laboratory tests performed will be treated and in Chapter 6 a presentation of the test results follow.
After this presentation, the test results are analysed and the original data and data with fixed damage levels will be compared to existing formulae of Gerding and Van der Meer in Chapter 7.
The results from Chapter 7 can be simulated by computations based on analytical theory and a trial-and-error method given in Chapter 8.
Finally in Chapter 9 other parameters are considered and in Chapter 10 the conlusions and recommendations are discussed.

1.2 Aim of the research

In this research the study by Gerding (1993) on the stability of toe structures will be continued. Gerding suggested a design relation for toe structures:

$$\frac{H_s}{\Delta D_{n50}} = \left(0.24 \frac{h_t}{D_{n50}} + 1.6\right) N_{od}^{0.15} \qquad (1.1)$$

In the tests by Gerding the density of the stone was not varied, but kept constant at a value of 2680 kg/m^3. Consequently, the use of the relative density Δ in the design formula is rather based on judgement than on facts. In the present study, the density of the stone is varied between 1900 and 2850 kg/m^3. The results of this study must prove whether the Δ is represented correctly in the formula and control the values of the coefficients used.

2 Physical processes around the toe structure

2.1 Loads and strength

The physical processes can be described in terms of loads, the force on the stones, and strength, the resistance against the loads and the response of the structure. The load is caused by waves which reach the foreshore and move to the rubble-mound breakwater with a certain waveheight and orbital velocity. The stones of the toe structure move because lift, drag and shear forces are generated by the orbital velocities and the turbulence caused by the breaking of the waves on the breakwater.

The main hydraulic responses of rubble-mound structures to wave conditions are wave run-up and run-down, overtopping, transmission and reflection (see **Figure 2.1**).

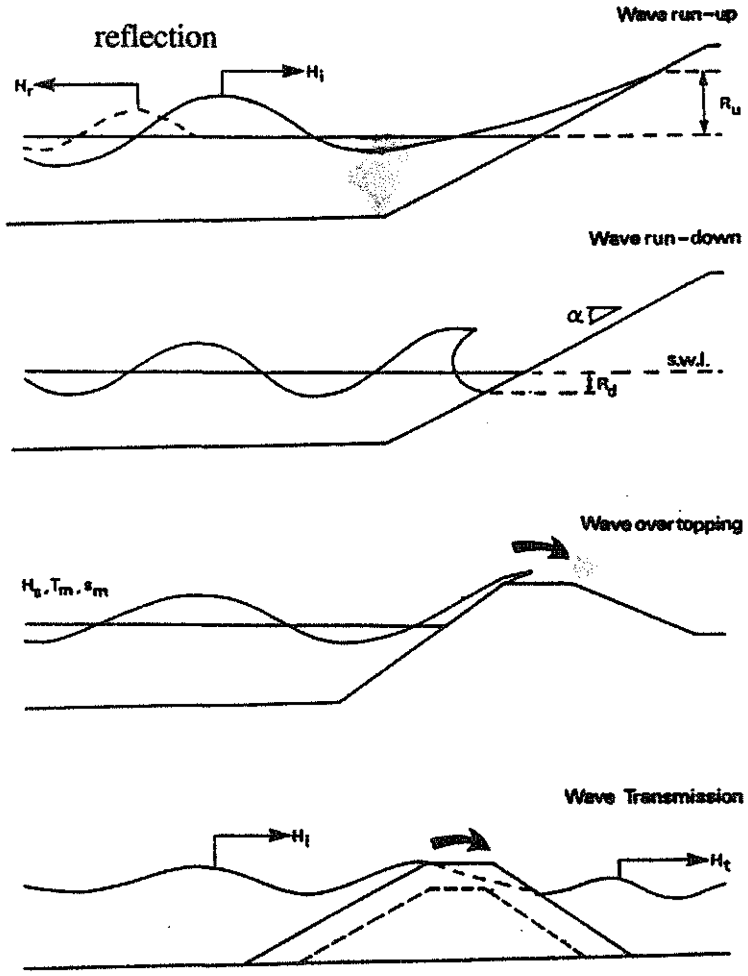

Figure 2.1 Hydraulic responses of a rubble-mound breakwater

In **Figure 2.1**, H_r, H_i are the reflected and incoming wave height; R_u and R_d are the run-up and run-down and H_t is the transmitted wave height.

The wave boundary conditions can be described by the wave height, H_s, and the period, T. For the stability of the toe structure the wave run-up and overtopping are not of importance, because the toe is situated at the bottom of the breakwater and not at the surface. The run-down influences the stability of the stones only, if it reaches the toe structure or comes close by it. The transmission reduces the loads on the structure, because wave energy is transported to the other side of the breakwater.

The orbital velocity, U_{orb}, depends on the local wave height and this wave height is related to the wave height at deep water. The shoaling at and the reflection of the foreshore and structure influence the local wave height. The larger the wave height, H_s, the larger the U_{orb}, so when the reflection would be added to the incoming wave height, both the H_s and the U_{orb} would increase. The U_{orb} depends also on the place in the vertical; this velocity distribution is also related to the local wave height. So with different water depths and wave heights the U_{orb} at the toe height level h_t will differ too, see **Figure 2.2**.

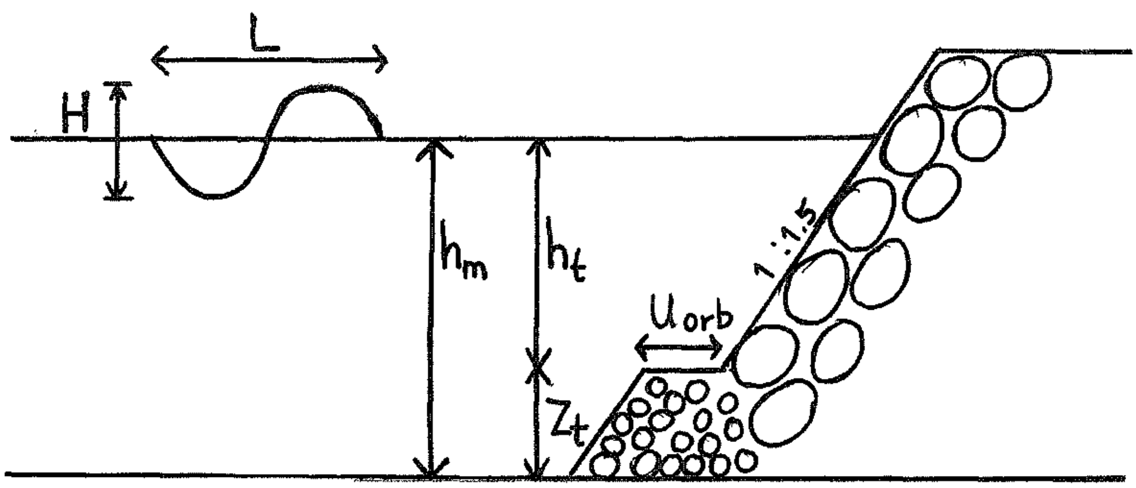

Figure 2.2 Physical processes around the toe structure

Gerding (1993) found that varying the wave steepness s_{op} had no influence on the damage occurring. The reason why this probably resulted from his tests will be explained in the following:

For smooth impermeable slopes Battjes (1974) experimentally found a relation given in (2.1) (see Eq.46) between the surf similarity parameter ξ and the reflection coefficient C_r:

$$C_r=0.1\xi^2 \qquad (2.1)$$

In ξ, the wave steepness $s_{op} = H_s/L_0$ is included:

$$\xi = \frac{\tan(\alpha)}{\sqrt{\frac{H_s}{L_0}}} \tag{2.2}$$

The structure in the present study has a rough permeable slope. Seelig (1983) distinguished a formula for smooth and a formula for rough permeable slopes see Eq.47 in **Figure 2.3**. Van der Meer (1988a) made a comparison of data on rock slopes and Postma (1989) gave a best-fit curve through these data points given in **Figure 2.3** as Eq.48. Both the slope angle and the wave steepness were treated separately and Postma derived the following relationship:

$$C_r = 0.071 P^{-0.082} \cot\alpha^{-0.62} s_{op}^{-0.46} \tag{2.3}$$

with: P = empirical permeability factor according to Van der Meer (1988a)

The values of the parameters in this study are : s_{op} = 0.04, $\cot\alpha$ = 1.5 and P = 0.4. The standard deviation of C_r is 0.036. The result of the calculation is a reflection coefficient 0.26 with margins 0.224 and 0.296. During the measurements the average C_r was 0.25 with minimum and maximum values of 0.185 and 0.315, so the values are well in line with the calculated values.

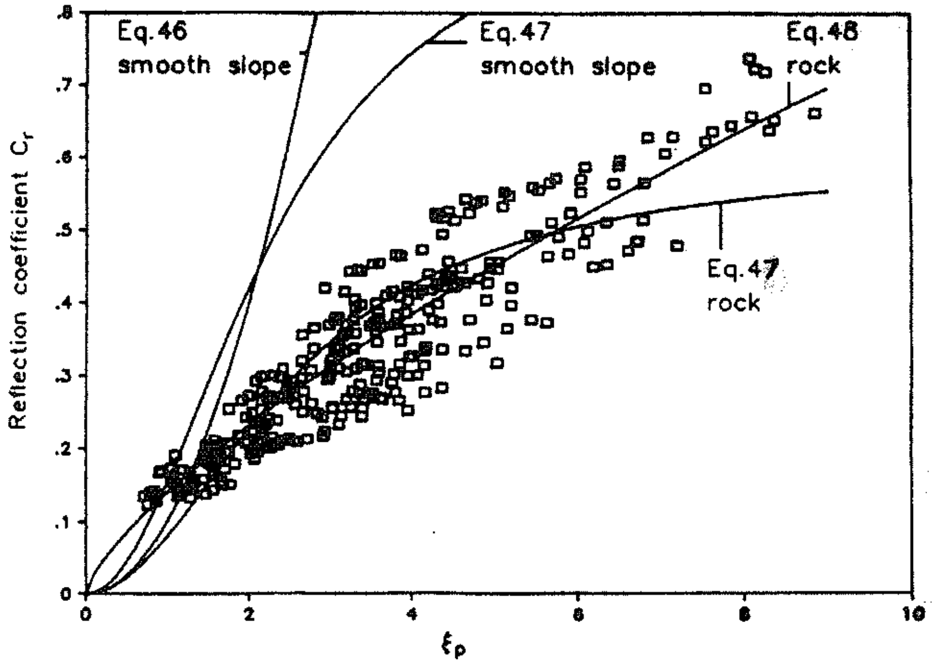

Figure 2.3 **Comparison of data on rock slopes by Van der Meer (1988a) with other formulae**

In practice $\cot\alpha$ of the slope of rubble-mound breakwaters is 1.5 or 2 (for economical reasons: the steeper the breakwater the less volume of material is used and that means less costs). With $\cot\alpha = 1.5$ and $s_{op} = 0.04$ results $\xi = 3.3$ and from **Figure 2.3** see Eq.48, it can be concluded that from this value of ξ an area starts where the C_r does not increase very fast. In this area the influence of the wave steepness on C_r does not change a lot. This is probably the reason why Gerding (1993) found that varying the wave steepness had no influence on the damage occurring. Therefore the value for s_{op} was held constant 0.04 in this research.

Four parameters involved with the damage at the toe structure can be mentioned, namely H_s, U_{orb}, h_t/h_m and $H_s/\Delta D_{n50}$. The stability of the toe structure depends on H_s and U_{orb} as coupled parameters for load and h_t/h_m as a geometric parameter and ΔD_{n50} as parameter for strength.
H_s and U_{orb} are not only coupled with each other, but also with the reflection and transmission, because the reflection and transmission influence the wave height (see figure 2.1) and the wave height determines U_{orb}.
Two examples of changes in the parameters are: if h_t/h_m becomes larger, the water depth above the toe structure becomes larger, so the load on the toe will diminish, but the strength will stay the same or when ΔD_{n50} becomes larger, then the structure can stand a larger H_s and U_{orb}, while the stability number, $H_s/\Delta D_{n50}$, stays constant.

Gerding (1993) empirically found a relation with h_t/D_{n50}, which can however theoretically not be affirmed.

In Chapter 3 the formulae with the parameter h_t/h_m will be handled and in Chapter 8 computations of orbital velocities are used to get more insight into toe stability.

3 Overview of existing knowledge

3.1 Overview of existing knowledge

If the rock in the toe structure has the same dimensions as the armour, the toe will be stable. However, one wants to reduce the rock size in the toe structure to reduce the costs of construction. When the yield of the quarry contains a limited fraction of suitable armour stone, it is important at what level the transition from armour stone to the lighter toe can be positioned. The Shore Protection Manual (SPM, 1984) gives design rules for the toe structure. The weight of the stones in the toe structure is related to the weight of the stones in the armour layer. According to the SPM the stones in the toe structure should have a weight of 1/10 of the weight of the stones in the armour layer. This is the same as 1/2 of the nominal diameter, D_{n50}, of the stones in the armour layer. The SPM also gives a width of the toe structure of 2 or 3 stones. Other measures for the toe structure are not given.

Little research into the stability of toe structures has been done. Following the work of Brebner and Donnelly (1962), given in the SPM (1984), who tested toes at vertically faced composite breakwaters under monochromatic waves, a relationship may be assumed between the ratio h_t/h_m and the stability number $H/\Delta D_{n50}$, where h_t is the depth of the toe structure below water level and h_m is the water depth in front of it (see for parameters Figure 2.1). A small ratio of h_t/h_m (0.3-0.5) means that the toe is relatively high above the bottom. A value $h_t/h_m = 0.8$ means that the toe is near the bottom. $H/\Delta D_{n50}$ values, using regular waves, of 6-7 are recommended if $h_t/h_m > 0.5$.

A relationship between $H_s/\Delta D_{n50}$ and h_t/H_s is assumed by Gravesen and Sørensen (1977), where a lower value of h_t/H_s should give more damage. They describe that a high wave steepness (short wave period) gives more damage to the toe structure than a low wave steepness. The above mentioned assumption was based on a few points only. This conclusion could not be verified (CIAD report (1985)). No relationship was found there between $H/\Delta D_{n50}$ and h_t/H_s. An average value $H_s/\Delta D_{n50} = 4$ was given for no damage and a value 5 for failure. The standard deviation around these values was 0.8, showing a large scatter.

A more in-depth study was performed by Van der Meer (CUR/CIRIA Manual, 1991), which gives a design graph on toe structure stability, based on a collection of site-specific tests at Delft Hydraulics and the Danish Hydraulic Institute, given in **Figure 3.1**.

Three damage classifications were established based on the number of removed stones expressed in a percentage of the total number of stones in the original toe structure:

0-3 %	no movement of stones (or only a few) in the toe.
3-10 %	the toe flattened out a little, but the function of the toe (supporting the armour layer) was intact and the damage is acceptable.
>20-30 %	failure; the toe lost its function and this damage level is not acceptable.

In almost all cases the structure was attacked by waves in a more or less depth-limited situation, which means that H_s/h_m was fairly close to 0.5. In the study by Van der Meer $H/\Delta D_{n50}$ is related to h_t/h_m. Figure 3.1 is therefore, applicable for depth-limited situations only.

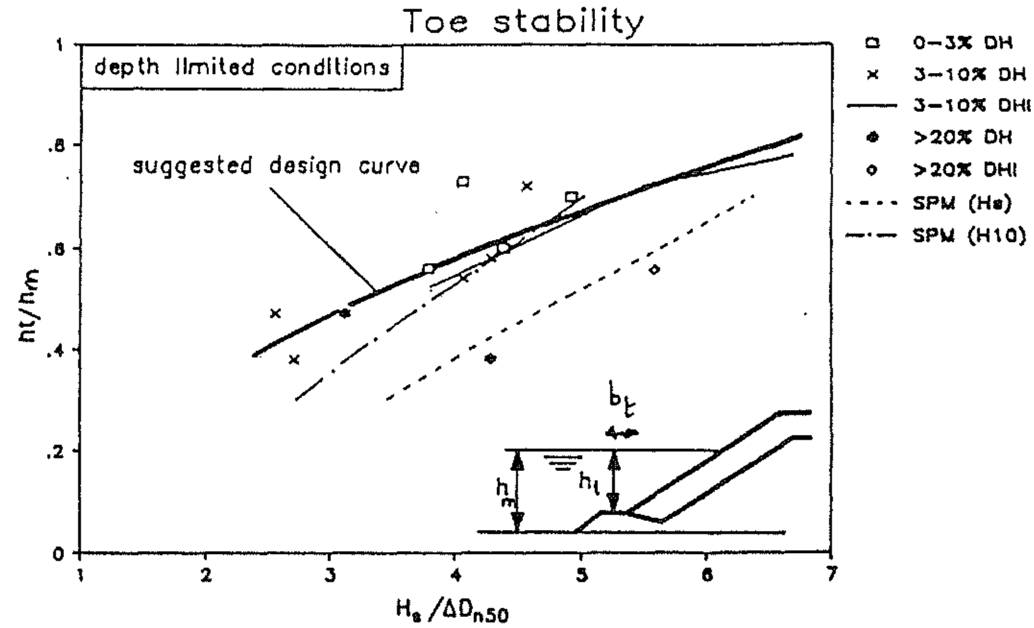

Figure 3.1 Design curves according to CUR/CIRIA

From Figure 3.1 it can be deduced that, if the toe structure is high above the bottom (small h_t/h_m ratio) the stability is much smaller than for the situation were the toe is close to the bottom. The results of DHI are also showed in the graph and correspond well with the 3-10% values of Delft Hydraulics.

A suggested line for design purposes is given in the graph. In general it means that the depth of the toe structure below water level is an important parameter. If the toe is close to the bottom the diameter of the rocks can be more than twice as small as when the toe is half-way the bottom and the water level. The design formula by Van der Meer for low and acceptable damage (3-10%) and for more or less depth-limited situations is (CUR,1991):

$$\frac{h_t}{h_m} = 0.22\left(\frac{H_s}{\Delta D_{n50}}\right)^{0.7} \tag{3.1}$$

Formula (3.1) is the suggested design curve presented in Figure 3.1. Three points are shown in this figure, which indicate failure of the toe structure, these points have more than 20% damage. The design curve (Fig. 3.1) is safe for values of $h_t/h_m > 0.5$ according to CUR/CIRIA,(1991). For lower values of h_t/h_m one should use the stability formulae for armour rocks described in the SPM (1984) or by Van der Meer (1988a). The ratio $h_t/h_m = 0.5$ indicates the transition from toe structure to armour layer.

Recent research on toe structure stability was performed by Gerding (1993). His tests were performed in order to establish the influence of wave height, wave steepness and water depth on toe stability.
One of the main conclusions was that the wave steepness had no influence.
His analysis resulted in an improved formula with regard to formula 3.1 and included the damage level N_{od}.

N_{od} = the number of stones removed from the toe structure divided by the number of stones in a strip with a width of 1 D_{n50}.

$$\frac{H_s}{\Delta D_{n50}} = \left(0.24\frac{h_t}{D_{n50}} + 1.6\right) N_{od}^{0.15} \tag{3.2}$$

In formula 3.2:

$N_{od} = 0.5$	hardly any damage
$N_{od} = 2$	acceptable damage, some flattening out
$N_{od} = 4$	unacceptable damage, complete flattening out

Formula 3.2 can be used in the range:	0.4	$< h_t/h_m$	< 0.9
	3	$< h_t/D_{n50}$	< 25

The suggested design curve is presented in **Figure 3.2.** The result demonstrates that the traditional SPM recommendations are specifically conservative for large submergence of the toe.

3.2 Comparison of formulae

The relation found by Gerding reads (3.2); With the test results of Gerding a relation with h_t/h_m could be found too.

$$\frac{H_s}{\Delta D_{n50}} = 6.5\left(\frac{h_t}{h_m}\right)^{1.2} N_{od}^{0.15} \tag{3.3}$$

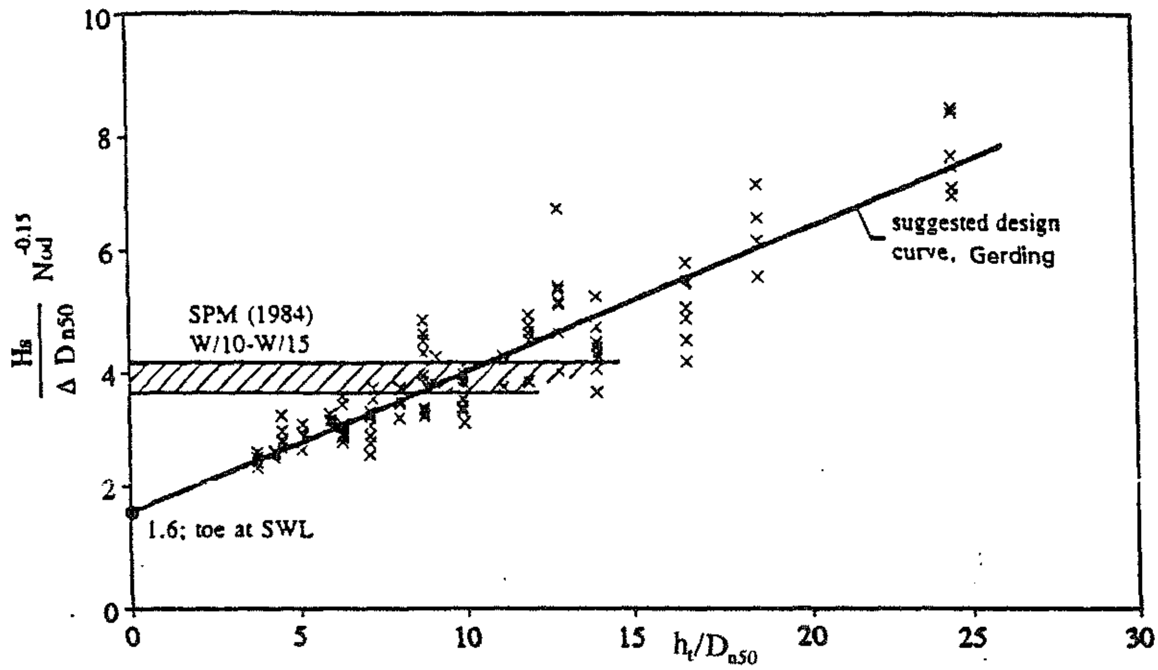

Figure 3.2 Suggested design curve by Gerding

The relation by Van der Meer (3.1) can be arranged in a different way:

$$\frac{H_s}{\Delta D_{n50}} = 8.7\left(\frac{h_t}{h_m}\right)^{1.43} \tag{3.4}$$

The relations (3.3) and (3.4) hold for $0.4 < h_t/h_m < 0.9$.

Because the damage level is not included in (3.4) it is assumed here that for the damage level N_{od} the value 2 can be used. The value 2 seems appropriate when the suggested damage levels are reviewed with $N_{od} = 2$ as a design criterion (acceptable damage) and also a correct value for a stable toe structure as suggested by Van der Meer, which is based on acceptable damage (3-10%).

When the value of $N_{od} = 2$ is used in the relation of Van der Meer (3.4) formula (3.5) results:

$$\frac{H_s}{\Delta D_{n50}} = 7.8\left(\frac{h_t}{h_m}\right)^{1.43} N_{od}^{0.15} \tag{3.5}$$

The only difference between (3.4) and (3.5) is a factor 1.1, the value of damage level $N_{od} = 2$ with power 0.15. So now the formulae from Gerding (3.3) and Van der Meer (3.5) can be compared, because they have the same parameters.

When the suggested design curve by Van der Meer (3.5) is compared with the design curve by Gerding (3.3) given in **Figure 3.3** (the points shown are measurements of the tests by Gerding), it can be concluded that for lower values of h_t/h_m the values of the two curves agree well. For higher values of h_t/h_m the difference between the two curves increases, see the difference in powers used: 1.43 and 1.2, although they show the same curve shape.
This means that the trend is the same for both curves and seems to be correct, only the values of the curves are different.

The way the damage is determined could be different for both data sets, which will result in different values and relations when the damage is included in the relation. The value of damage level chosen for the relation of Van der Meer (N_{od} = 2) is of influence on the position of the curve and it could be examined what value of N_{od} corresponds with the test results of Gerding.

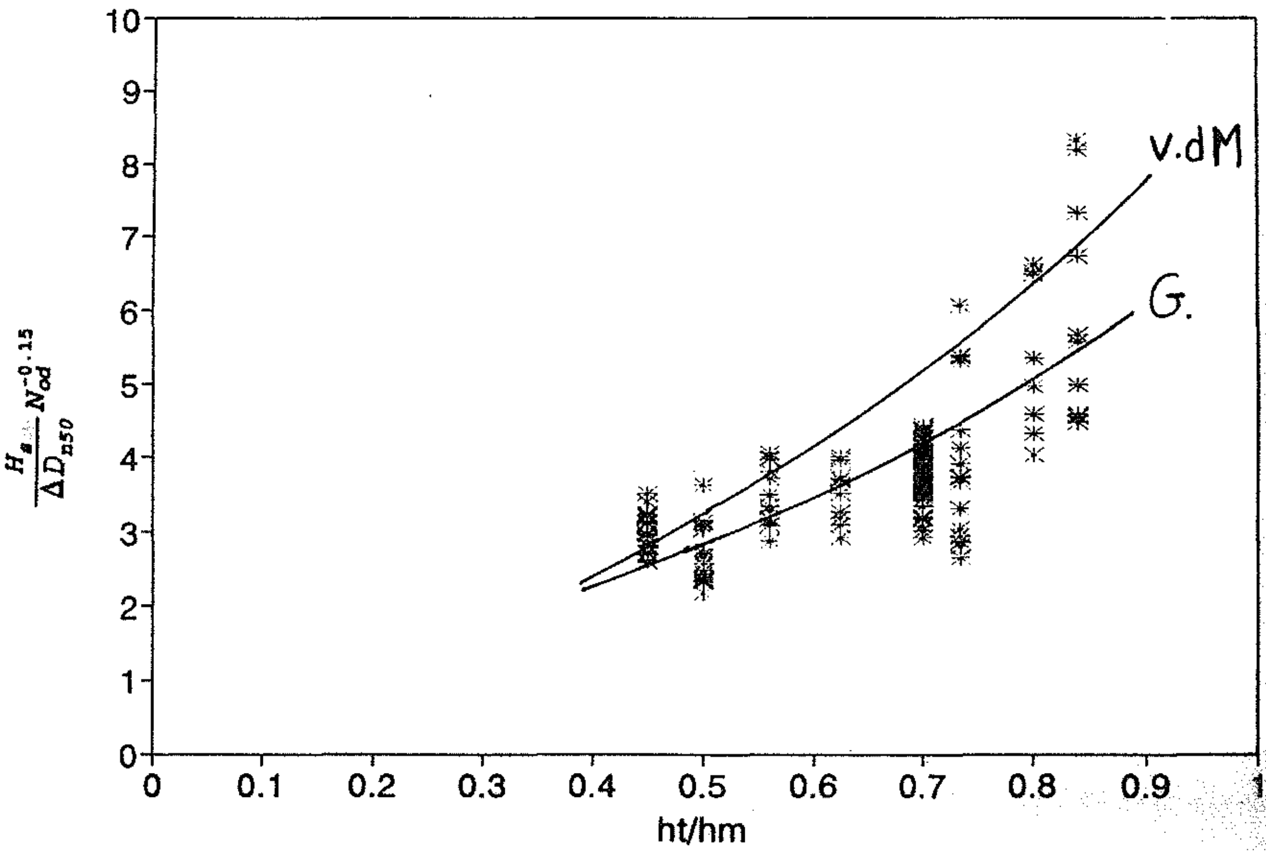

Figure 3.3 **Suggested design curve by Van der Meer compared to that by Gerding**

4. Present study

4.1 Governing parameters

The stability of the toe structure is influenced by several governing parameters. These parameters denoted in **Figure 4.1** are:

- Waves	- significant wave height	H_s (m)
	- significant wave height based on wave energy spectrum	H_{m0} (m)
	- 2% wave height, wave height exceeded by 2% of the waves	$H_{2\%}$(m)
	- peak period of spectrum	T_p (s)
	- orbital velocity	U_{orb} (m/s)
- Toe structure	- water depth in front of structure	h_m (m)
	- water depth above toe structure	h_t (m)
	- width of toe structure	b_t (m)
	- nominal stone diameter	D_{n50} (m)
	- mass density of stones	ρ_s (kg/m^3)
- Damage		N_{od}

From the governing parameters some other parameters can be deduced.
With dimension: - height of the toe $Z_t = h_m - h_t$ (m)
Dimensionless parameters: - wave steepness: $s_{op} = (2\pi H_s)/(gT_p^2)$
- relative density: $\Delta = (\rho_s - \rho_w)/\rho_w$

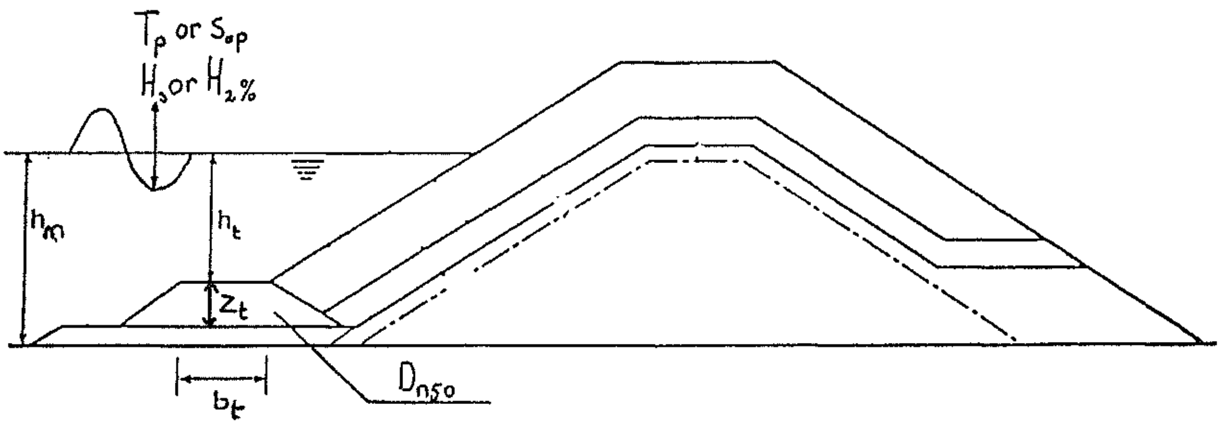

Figure 4.1 Governing parameters

The damage can be given as a percentage; in that case the number of stones displaced from the toe structure is given as a percentage of the total number of stones in the toe structure.
The disadvantage of this approach is that, if the same number of stones is displaced from different toe structures (a higher or wider toe),

the percentage changes but the amount of damage or the damage profile is actually the same.
For this reason the damage number N_{od} is used in this report. N_{od} is defined as the number of stones removed from the toe structure divided by the number of stones in a strip with a width of $1*D_{n50}$. The advantage of using the damage number N_{od} is that the damage is not related to height or width of the toe structure (i.e. in definition) and the same amount of moved stones give the same damage number for all kind of toe sizes. In this way the amount of damage is independent of the size of the toe structure. It should be noted, however, that the effect of a certain damage level on several toe structures differs with the size of the toe structure.

4.2 Influence of parameters

A brief review of the influence of the parameters from previous research is given for every parameter.

Significant wave height, H_s
Of course a higher wave gives more damage. From Van der Meer (CUR, 1991) this can be found in the stability number $H_s/\Delta D_{n50}$. The parameter shows that a larger stone is needed to maintain the same stability if a higher wave is introduced. In **Figure 4.2** a result of Gerding shows that higher waves cause more damage (the damage number N_{od} is larger) for a given configuration of the toe structure.

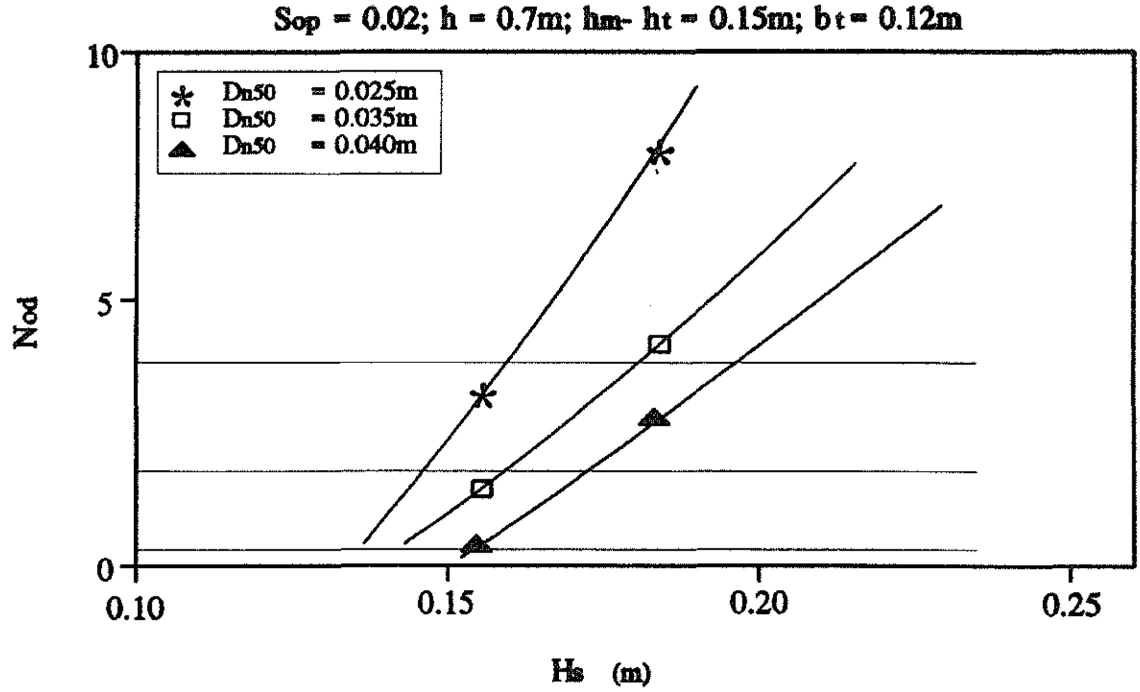

Figure 4.2 Damage level N_{od} as a function of H_s

2% wave height, $H_{2\%}$
As with H_s, a higher $H_{2\%}$ gives more damage. The advantage of using $H_{2\%}$ instead of H_s is that in $H_{2\%}$ the influence of a depth-limited situation is taken better into account.
The highest waves cause the damage to the structure. $H_{2\%}$ is nearer to the highest waves than H_s so the deviation from the highest waves is smaller when $H_{2\%}$ is used instead of H_s.

Local water depth, h_m
A larger water depth will give less damage. In Van der Meer (CUR, 1991) this can be found in the h_t/h_m ratio: if this parameter increases, this will lead to a larger stability, then a smaller stone diameter D_{n50} or a higher significant wave height H_s can be accepted.

Waterdepth above the toe, h_t
The impact of the waves and the largeness of the orbital velocity depends on the water depth above the toe. When h_t is large (the ratio h_t/h_m near to 1), the toe is relative near the bottom. In this case the orbital velocity computed from the local wave height is low. When h_t is small, the toe is closer to the still water level and will be heavily attacked by the waves. A large h_t, a value in the order of h_m, gives a lot of stability to the toe structure.

Armour size, D_{n50}
A larger stone leads to less damage. In Van der Meer (CUR, 1991) this can be found in the stability number $H_s/\Delta D_{n50}$. In this parameter a larger stone (larger D_{n50}) leads to a larger stability of the toe structure, because in that case a larger significant wave height H_s can be accepted. In **Figure 4.3** the relation between wave height H_s and D_{n50} for fixed damage levels is shown. When the diameter increases, a larger wave is necessary to cause the same damage as for a smaller diameter.

Mass density ρ_s
A higher mass density ρ_s leads to less damage. In Van der Meer (CUR, 1991) this can be seen from the stability number $H_s/\Delta D_{n50}$: where the density is in the Δ-parameter $((\rho_s-\rho_w)/\rho_w)$. If the Δ (and therefore ρ_s) is higher this will lead to a higher stability of the toe structure. This effect has only been found for the armour layer (Van der Meer, 1989) and is also assumed to hold for toe structures, although no research into this effect for toe structures has been performed.

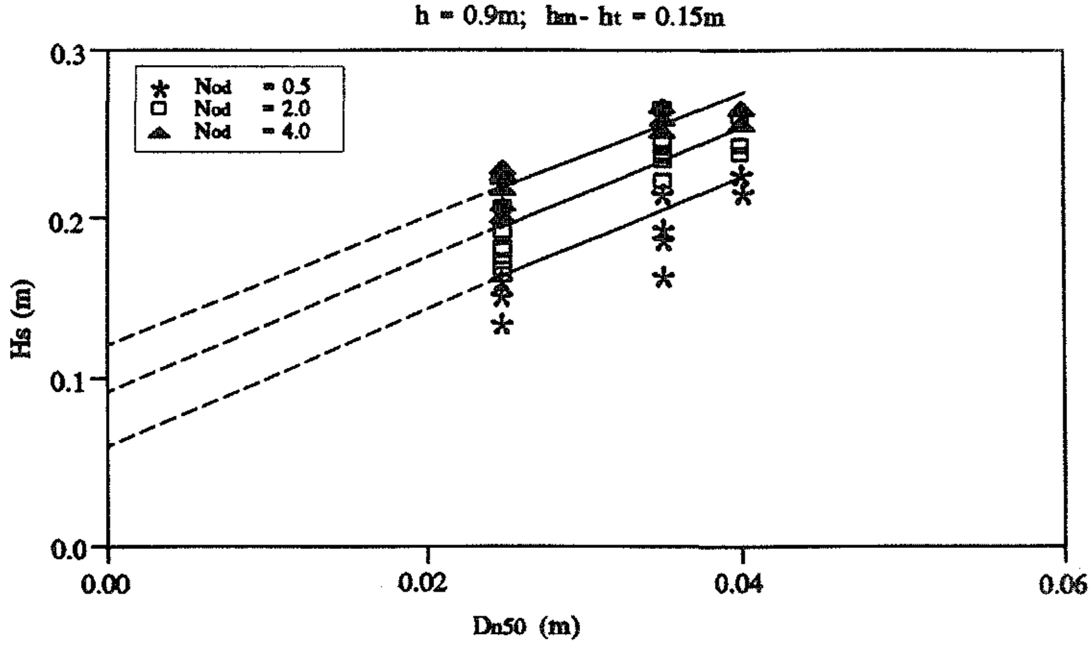

Figure 4.3 Relation between H_s and D_{n50} for fixed damage levels

Peak period, T_p and wave steepness, s_{op}
Gravesen en Sørensen (1977) described the influence of the period and wave steepness. They suggested that a high wave steepness or a short period gives more damage than a low wave steepness or a long period at the same wave height. Gerding (1993) found that the same damage occured, when different wave steepnesses were introduced. In Chapter 2 the explanation why the damage doesn't change is already given. When the slope is 1:1.5 or 1:2, which is mostly the case with rubble-mound breakwaters, the surf similarity parameter (indirectly the period) doesn't vary the influence on the reflection-coefficient.

Width of the toe structure, b_t
Gerding (1993) varied the width of the toe structure and the result was that the width in general had no influence on the damage. In some cases a wider toe was more stable. It is logical that using a wider toe more damage can be accepted, when the damage is determined with the damage number N_{od}. In **Figure 4.4** his results are shown. The width of the toe structure can be enlarged but the required wave height to cause the same damage level doesn't increase. So a wave height of 0.18 m cause the same damage to the toe widths 0.12, 0.2 and 0.3 m.

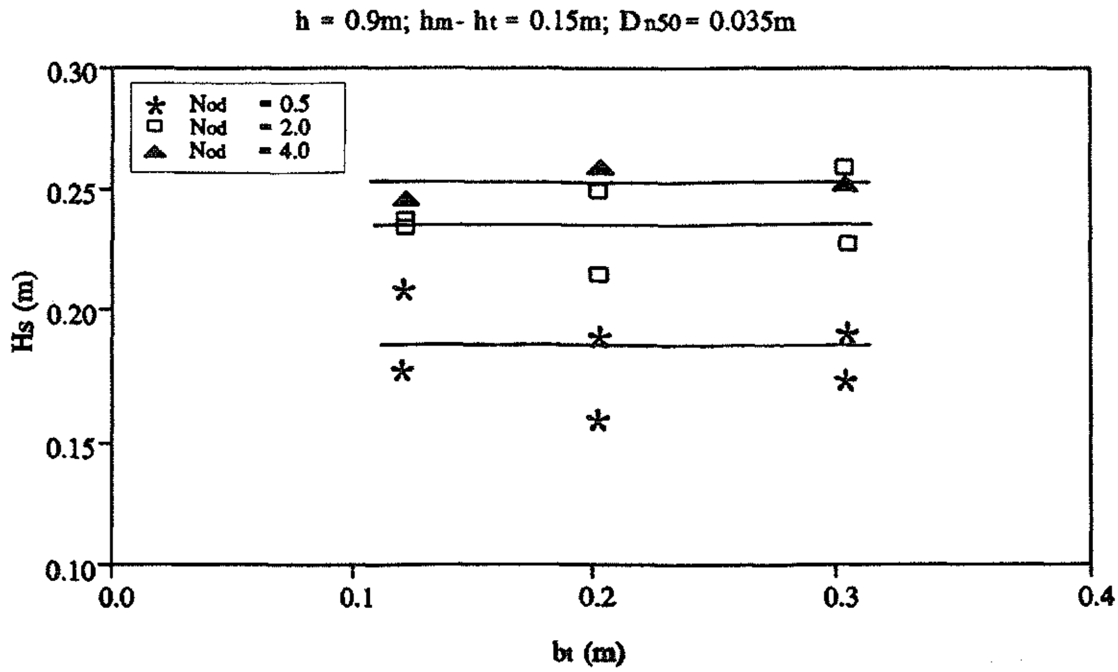

Figure 4.4 **Influence of toe width b_t on required wave height H_s to cause fixed damage levels N_{od}**

4.3 Approach

From Chapter 2,3 and the preceding sections of this Chapter an approach, a method, to perform the tests was determined.
The tests were executed in a wave flume with the following parameters as variables: H_s, h_m, Z_t, D_{n50}, and ρ_s. The s_{op} was hold constant just as the width of the toe structure b_t. The only parameter, that hasn't been investigated yet, but of the most importance for the aim of this research, is the stone mass density ρ_s; the stone mass densities varied are 1900, 2550 and 2950 kg/m^3. The materials used are: brick, porphyry and basalt. Only one cross section of a rubble-mound breakwater with various combinations of water depth, toe height and wave heights were investigated. The wave heights were measured and the damage of the toe structure for each condition was estimated.

The measured data is elaborated into the same dimensionless parameters as in Chapter 3, namely: h_t/h_m, h_t/D_{n50} and $H_s/\Delta D_{n50}$. In the analysis the parameters are put in a dimensionless form, to reduce the data and to become independent of scale factors. In this way the results become more clear.

This was performed to compare the results of the present study with the existing formulae of Gerding (1993) and Van der Meer (1991).

From local wave heights at the toe structure orbital velocities were computed; with those velocities the nominal diameters needed for a stable toe structure were determined. Then a comparison between the computations and measurements was made.

5 Description of laboratory tests

5.1 Wave flume

The tests were performed in the large wave flume of the Laboratory of Fluid Mechanics of the Faculty of Civil Engineering of the Delft University of Technology. The length of this flume is 30 m, the width 0.8 m and the maximal water depth is 0.9 m. An overview of the test set-up is given in **Figure 5.1**. For the tests a foreshore of 1:50 was constructed consisting of an underlayer of sand covered with a thin layer of cement. The length of the foreshore was 10 m. The breakwater and toe structure were placed at the end of the wave flume. The slope of the breakwater remained constant, 1:1.5.

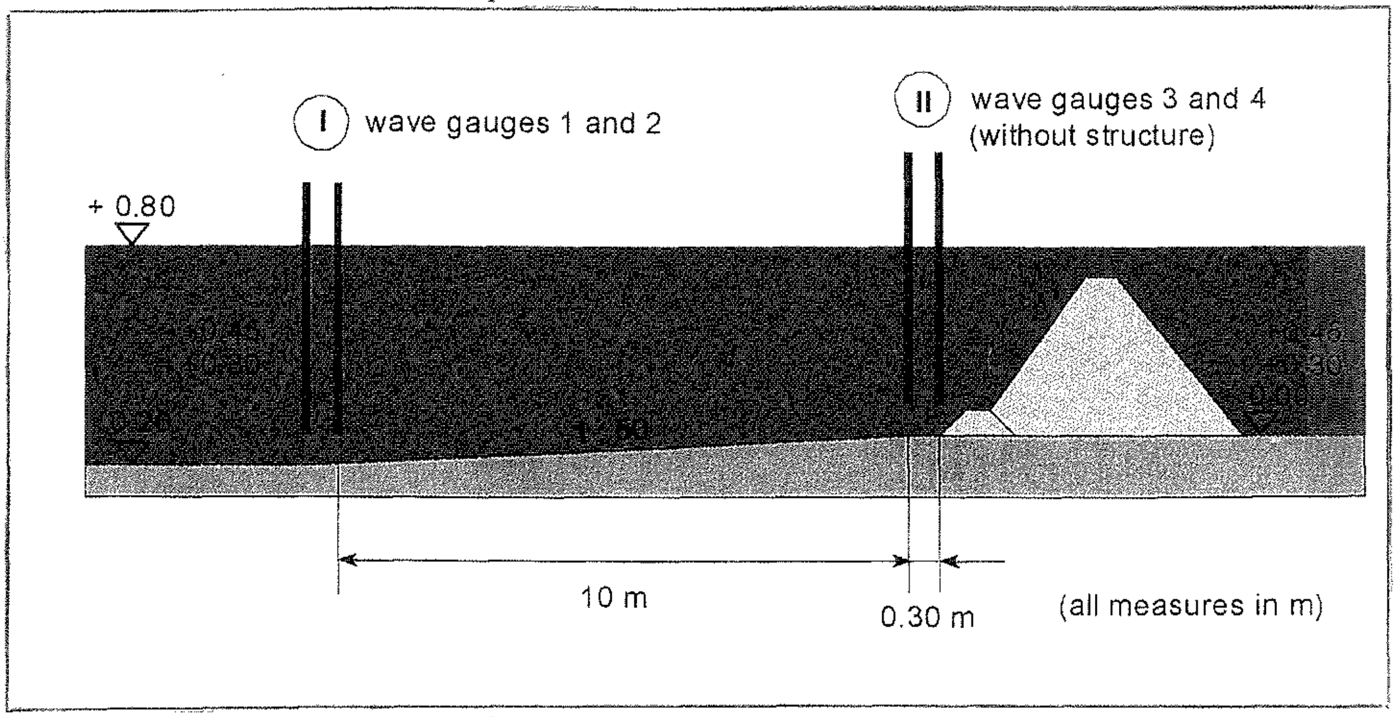

Figure 5.1 Overview of test set-up

5.2 Wave characteristics

Before performing tests with the structure in the flume, a set of tests were performed without the structure to determine the wave characteristics. For this purpose 4 wave gauges were placed in the flume, 2 gauges were placed about 0.5 m apart (the distance between the wave gauges was determined with the computer program DISTANCE of Delft Hydraulics) at the begin of the foreshore, so 10 m in front of the place where the breakwater in the actual tests would be placed, and 2 wave gauges were placed at the site of the structure.

This was done to determine the relationship between the wave height at the begin of the foreshore and the wave height at the place of the toe structure in absence of the breakwater structure for the two water depths: 0.5 m and 0.65 m (begin of foreshore = h) and 0.3 and 0.45 m (local water depth toe = h_m), respectively.

This procedure was necessary, because during the tests the waves would break at the structure. In the area before the breakwater the energy distribution then become non-linear and accurate measurements cannot be made. From the measurements taken at the begin of the foreshore in absence of the breakwater the occurring wave height at the toe structure can be deduced according to the graph of **Figure 5.2**. The wave heights are the incoming wave heights, so without the reflected components. The reflection is determined and subtracted from the measured wave height by the compute software REFLEC; more information about the software can be found in **Appendix A**.

For the generation of irregular waves a software package named AUKE/pc, was used. The software is able to generate a data-set, which fulfills certain predefined requirements, such as spectral shape, significant wave height and peak period. The data-set was translated from the computer to the wave-board controller by a 10 Volt D/A converter.

First, for all wave fields, a comparison had to be made between the measured wave characteristics and the input of the software in order to check whether they corresponded. In case the 'reflection compensation' is 'on': the maximum amplitude of the waveboard is 0.20 m and the input of large waves can not be realized. So the maximum wave height which can be generated with 'compensation on' is 0.18 m. For larger waves the 'compensation' was put 'off'. The results could be compared because differences in reflection didn't influence the damage see **Figure 5.3**.

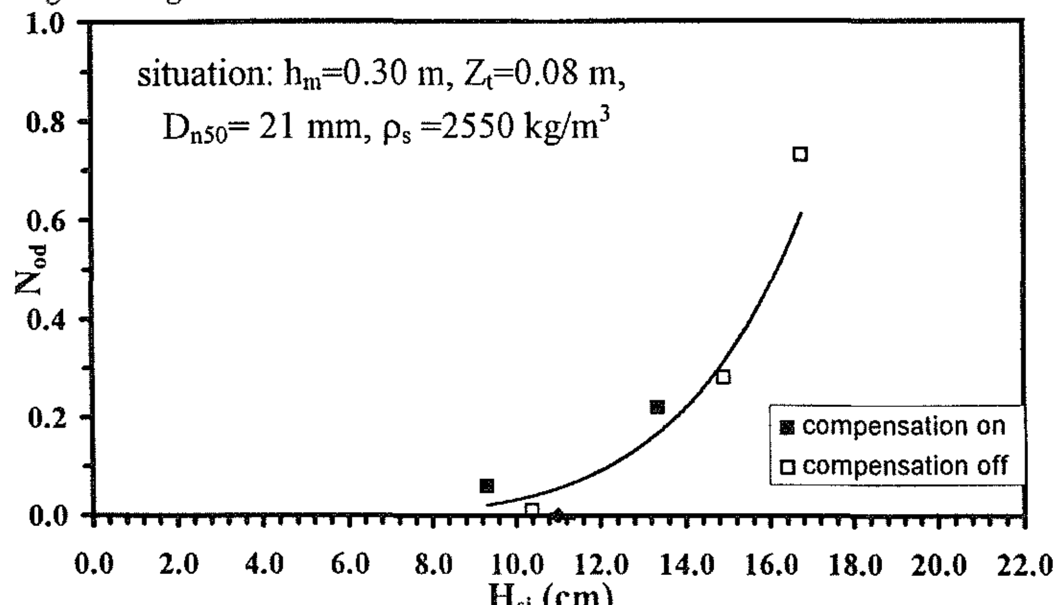

Figure 5.3 Reflection compensation

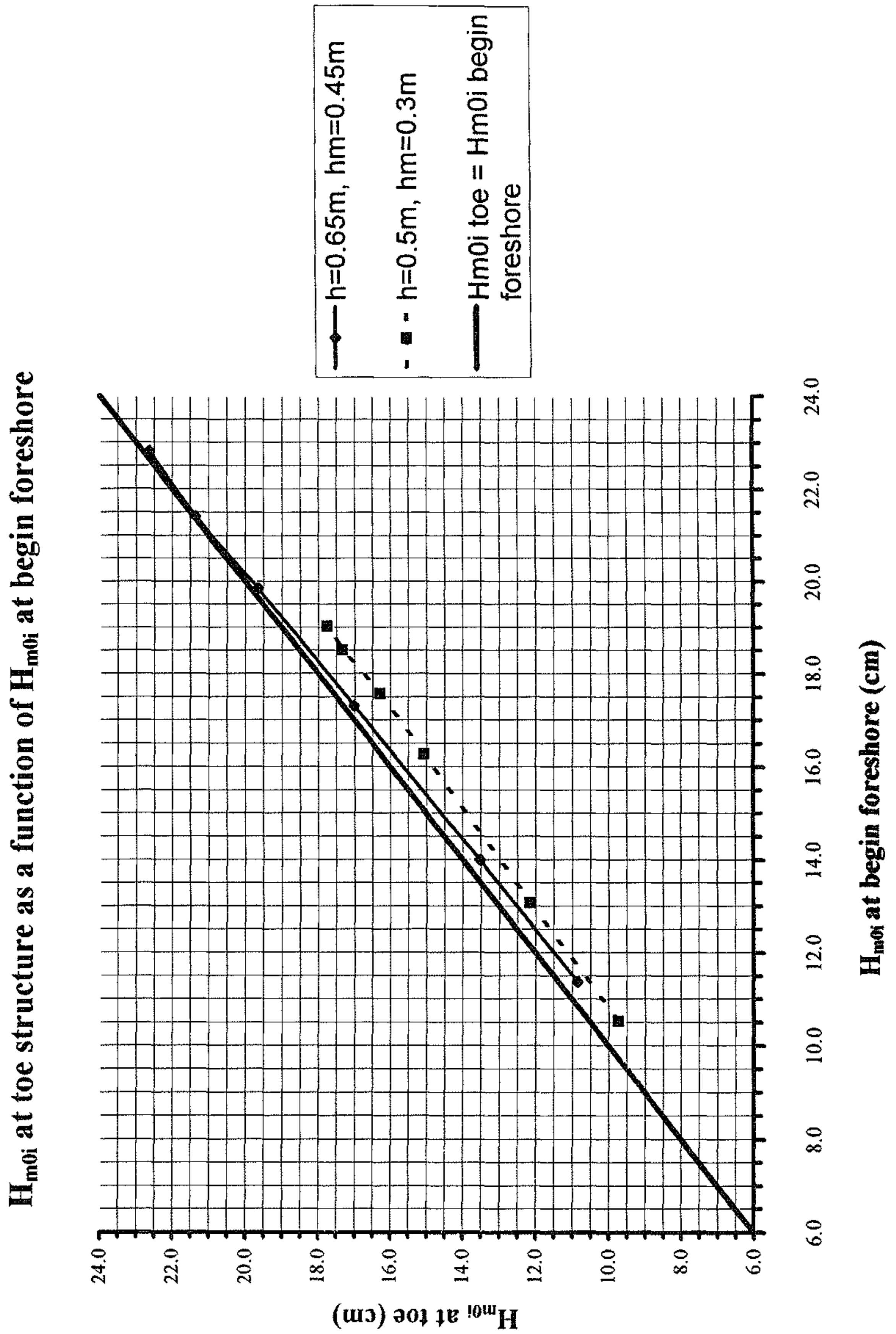

Figure 5.2 H_{m0i} **at toe structure as a function of** H_{m0i} **at begin foreshore**

There is a difference between H_s and H_{m0}. H_{m0} is based on the wave energy density spectrum and can be smaller than H_s (avarage of highest 1/3 of all waves). This depends on the shape of the foreshore and the wave steepness. In **Figure 5.4** the relation between H_{m0i} and $H_{1/3,i}$ (i means incoming without the reflected components) is shown for a foreshore 1:50 and several wave steepnesses. It appears that for s_{op} = 0.04 the wave heights are practically the same, so we assume H_{m0i} is H_{si}, further refered to as H_s.

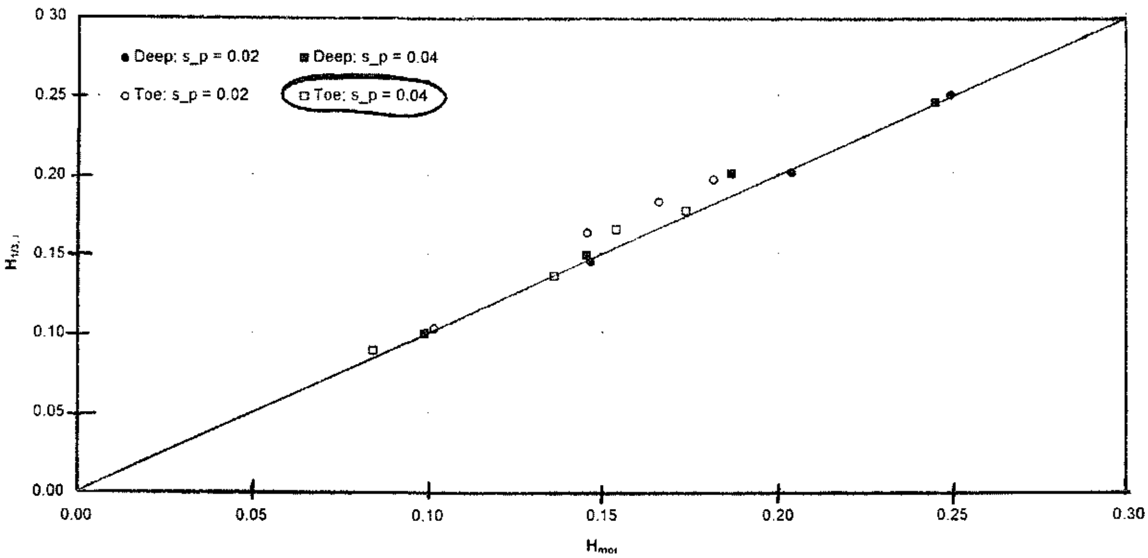

Figure 5.4 $\quad$ **$H_{1/3i}$ as a function of H_{m0i}, h_m = 0.30 m**

5.3 Wave energy density spectrum

For the description of random waves it is insufficient to use only a characteristic wave height and period, as for example H_s and T_p, because they do not fully describe the shape of the energy density spectrum. Therefore it is useful to describe an irregular wavefield by its energy density spectrum with respect to the surface elevations, which gives the distribution of the energy over the frequencies. Different wave spectra can be chosen for the description of irregular waves. A JONSWAP spectrum is chosen in the experiments for the irregular waves generated in this research. This type of spectrum is derived from measurements at the North Sea and it describes the energy density spectrum for a growing sea-state (Hasselman,K. 1973).
The JONSWAP energy density spectrum can be described with the **formula 5.1**:

$$E(f)=\alpha_f g^2(2\pi)^{-4}f^{-5}\exp[-\frac{5}{4}(\frac{f}{f_p})^{-4}]\gamma^{\exp\frac{-(f-f_p)^2}{2\sigma^2 f_p^2}} \tag{5.1}$$

with:

α_i = spectral parameter
f = frequency
f_p = peak frequency
γ = peak enhancement factor = 3.3
γ = 0.07 for $f \leq f_p$
= 0.09 for $f \geq f_p$

This is the shape of the Pierson-Moskowitz distribution multiplied by a so called 'peak-enhancement', the function $\gamma(f)$. In this study, the JONSWAP spectrum is the only spectral shape used.
In **Appendix A** an example of an input and an output is showed for the incoming wave. The spectrum of the output has lower energy than that of the input, because of the friction on bottom and walls of the flume, but the area's under the curve are almost equal. In the output there are some frequencies with very low and very high values; this results from reflections on the foreshore which can not be compensated by the wave-board. The peak frequency, f_p, and the wave steepness, s_{op}, stay the same as the input values.

5.4 Tests

5.4.1 Test set-up

The tests were concentrated on the governing parameters as described before. This means that variations were investigated of: water depth, wave height, stone diameter, stone mass density and toe height.
To make a comparison with the research by Gerding (1993) the dimensions and values he used were taken into account. The width of the toe and the wave steepness were considered to be constant: 0.12 m en 0.04, respectively. The value of the width of the toe was chosen to be 0.12 m because Gerding had a lot of data on a toe structure with a width of 0.12 m.

Different wave steepnesses don't infuence the damage in the domain of the slope angle of the breakwater (see Chapter 2, figure 2.2) and therefore the wave steepness is chosen 0.04. To get a good insight into the influence of all individual parameters, only one parameter was changed at a time. The tests were performed with a fixed toe composition (combination of stone diameter and mass density) for two water depths and four or five wave heights. The toe structure was divided over the width of the flume into two parts. In this way two toe compositions could be tested in one test set-up.

In **Figure 5.5** a sketch of the breakwater cross section is presented with the tested parameters: water depth and toe height of the breakwater. An overview of all test variations is given in a matrix (see **Table 5.1**).

Variables	Values
Slope angle, α	1:1.5
Wave steepness, s_{op}	0.04
Stone mass density, ρ_s	basalt= 2850 kg/m^3, Δ = 1.85 porphyry= 2550 kg/m^3, Δ = 1.55 brick= 1900 kg/m^3, Δ = 0.90
Stones used	bas D_{n50}= 0.0102 m grad = 1.40 bas D_{n50}= 0.0151 m grad = 1.20 por D_{n50} = 0.0098 m grad = 1.34 por D_{n50} = 0.0144 m grad = 1.31 por D_{n50} = 0.021 m grad = 1.26 bri D_{n50} = 0.0231 m grad = 1.45 Total number of materials: 6
Local water depth at toe, h_m	0.30 m 0.45 m
Toe height, Z_t	0.08 m 0.15 m
Wave height, H_s	ca.0.10 m, 0.14 m, 0.17m 0.20 m
Total amount of tests	6x2x2x4 = 96

Table 5.1 Matrix of test variations

Every toe structure composed of basalt, porphyry and brick and with different stone diameters was tested for each of the 16 combinations. This resulted in a basic test set of 96 experiments. Two tests were performed at the same time. Tests may be deleted when a large wave height results in zero damage.

The damage was obtained by counting the number of stones removed seaward on or over a white painted line at the bottom of the flume, see **Figure 5.6**. The damage number N_{od} was obtained by dividing the number of stones removed from the original structure by the number of stones in a strip with a width of one D_{n50} (number of stones per 0.39 m width perpendicular of the wave flume).

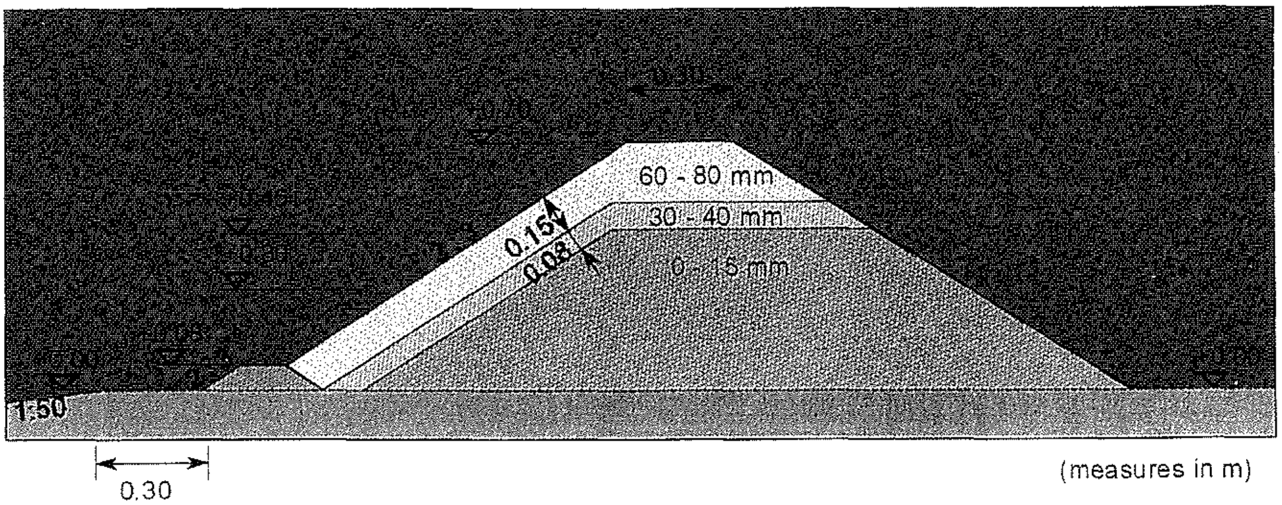

Test variations
in height of
toe structure:

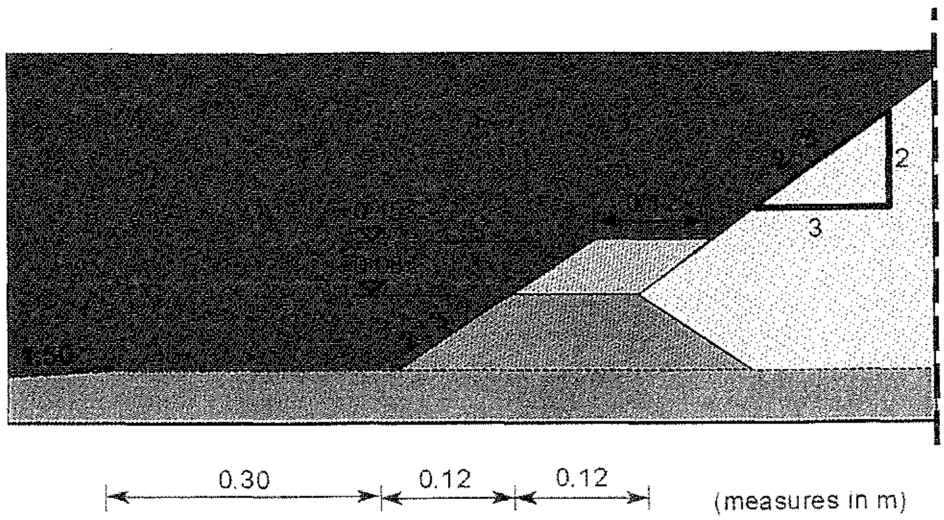

Figure 5.5 **Breakwater cross section with variable parameters**

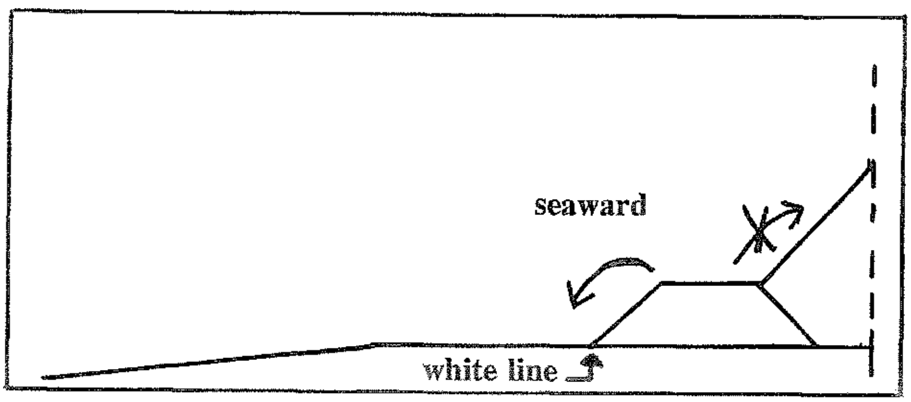

Figure 5.6 **Determination of damage**

5.4.2 Test procedures

1 Build the toe structure of the required composition, the first 0.08 m comes under the armour layer.
2 Assure that the stones are lying in the right profile (according to the indication on the side-wall of the flume).
3 Fill the wave flume gently until the required depth is reached.
4 Calibrate the wave gauges.
5 Start the test by imposing the calculated, irregular steering signal on the wave-board.
6 Take the measurements at the required positions.
7 Stop the test after 2000 waves.
8 Count the number of stones displaced on and over marked line.
9 Let the water out of flume; if needed, repair the damage of the toe structure.

5.5 Materials

5.5.1 Study on the use of bricks

In order to improve the reliability of the research a material with a smaller relative density than basalt or porphyry was needed. The material must have the following qualifications: sharp, because round material would roll too easily under wave attack; the right dimension, or it must be possible to break it into usable pieces; it may not dissolve in water. Three kinds of bricks were tested on these qualities. The codes of these stones were: NEE 27, NW 24 and NCC 32.

Each brick was broken into pieces with a hammer. This resulted in a lot of stones and some rubbish. To compare the results and to select one of the bricks for use in the research on toe stability, the amount of usable stones and the amount of waste from one brick was determined.

NW 24 (soft)
Easily to break into pieces. The amount of usable stones was 98. The waste had a weight of 339 gr.

NCC 32 (hard)
More difficult to break, more strokes where needed to get pieces which were small enough. The amount of usable stones was 76. The waste had a weight of 379 gr.

NEE 27 (in between soft and hard)
Easily to break into pieces. The amount of usable stones was 87. The waste had a weight of 413 gr.

The NW 24 was selected, because this gave the best results for the three criteria formulated, namely the most usable stones, easily to break into pieces and the least waste.

5.5.2 Stone mass density and nominal diameter

Now the stone mass density of the broken bricks had to be determined. The stones were put into water and after one hour the weight of some stones was measured. Half an hour later this was done again to check if the stone was saturated with water. When the mass didn't increase anymore, 600 gr of stones was put into 400 ml of water. The volume of water increased to 715 ml. The mass density could be deduced:
600 gr / (715-400) ml = 1900 kg/m^3.

The nominal stone diameter was determined as follows: first 100 stones were weighed and arranged according to there weights from low to high. The total mass of the stones was counted. In the row of arranged weights the M_{50} is that weight where the cumulative weight is half the total weight. M_{50} is 21.8 gr.
With the **formula 5.2** the nominal stone diameter D_{n50} could be determined. The resulting D_{n50} = 0.023 m.

$$D_{n50} = \sqrt[3]{\frac{M_{50}}{\rho_s}} \qquad (5.2)$$

For the other two materials, basalt and porphyry, the stone mass density and the nominal diameter were determined in the same way. Only for these materials it wasn't necessary to saturate the stones with water. The result is showed in a matrix of test variations (see Table 5.1).
In a sample of natural quarry blocks there will be a range of block masses and in this sense all rock material is, to some extent, graded. The particle mass distribution is most conveniently presented in a percentage lighter by a mass cumulative curve, where M_{50} expresses the block mass for which 50% of the total sample mass consists of lighter blocks (i.e. the median mass); M_{85} and M_{15} are similarly defined. The overall steepness of the curve indicates the grading width; a commonly used quantitative indication of grading width is the M_{85}/M_{15} ratio or its cubic root, which is equivalent to the D_{85}/D_{15} ratio determined from the cumulative curve of the equivalent cubes or sieve diameters of the sample. The mass distributions and gradation of the materials are given in **Appendix A** together with photographs of the materials.

All gradations are in the range of narrow gradation, this means less than 1.5. The mass distribution curves are linear between M_{15} and M_{85}, which merely implies that there are no significant gaps in material sizes over the total width of the grading. Brick has the largest gradation of 1.45; its mass distribution curve is not completely linear especially around M_{15}.

5.6 Measurements and data processing

5.6.1 Instruments and equipment

Surface elevations were measured by means of conductivity-type wave gauges. The gauges consist of two metal rods which measure the conductivity of the water body between them. A reference electrode at the foot of the gauges corrects for the effects of conductivity fluctuations caused by for instance temperature fluctuations, so the conductivity is only dependent of the immersion depth. After cleaning, the gauge was mounted and stood in the water for at least half an hour before the measurements were started.
The wave gauges were connected to a computer. The analog signals from the wave gauges were digitezed by an A/D converter. With the computer this signal was sampled; the data were collected and stored in files. Data files as well as calibration files were collected with this computer.In **Figure 5.7** and **5.8** photographs of the wave gauges and measuring equipment are presented.
The elaboration of data and the programs used are given in **Appendix A.**

5.6.2 Calibration

Before a test was started, the wave gauges had to be calibrated in still water. After the instruments were put on zero a measurement was taken at five different immersion depths, viz. at the depths: +0.10 m, +0.05 m,
0 m, -0.05 m and -0.10 m. The five measurements were used to calibrate the wave gauges by using the calibration program EDFM, a least-squares method program. The slope and the offset found with this calibration were used to elaborate the data. With this calibration file the data files of the measurements were "translated" into the correct values.

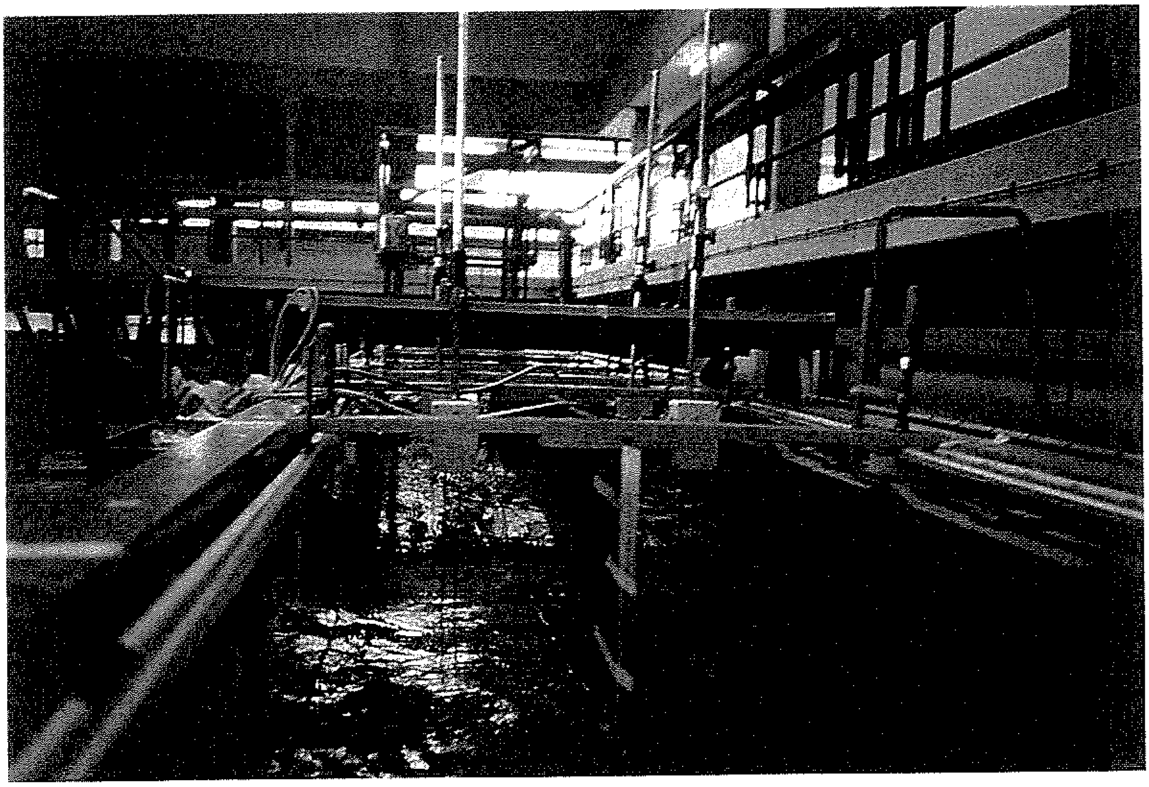

Figure 5.7 Wave gauge

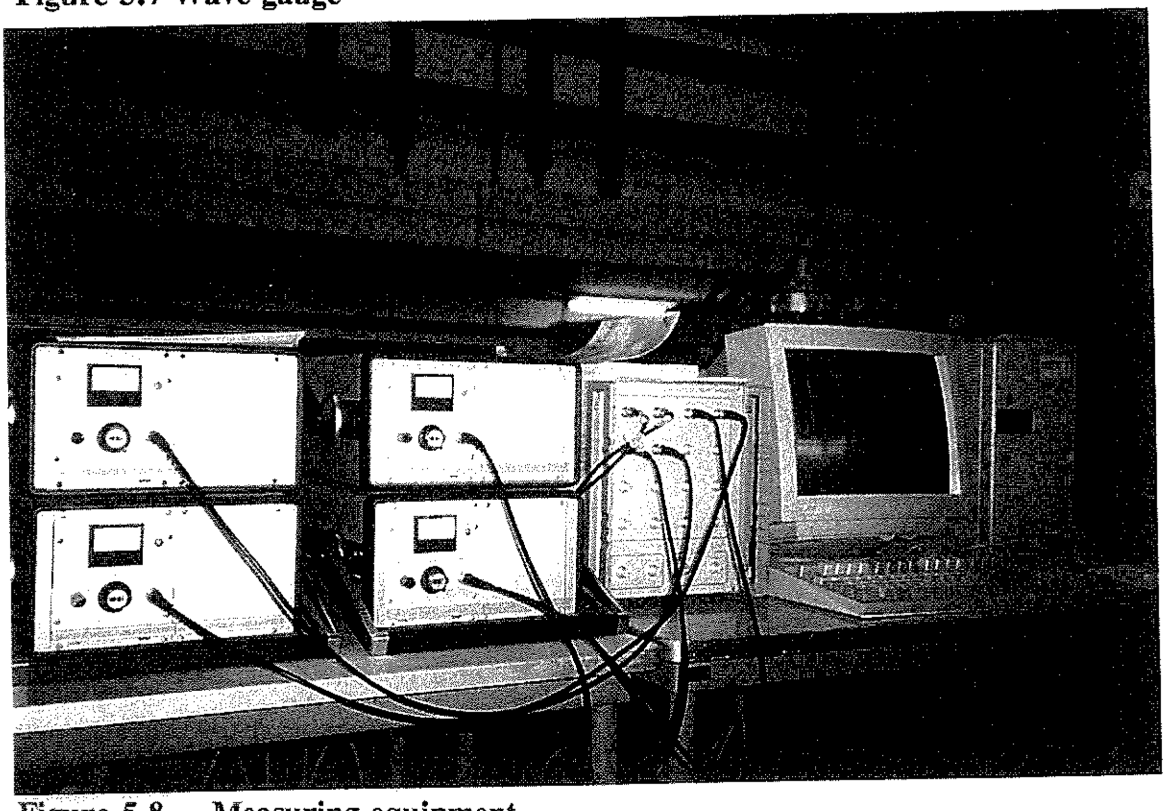

Figure 5.8 Measuring-equipment

6 Presentation of results

6.1 Introduction

The data obtained in the laboratory tests as described before will be used for an analysis of the influence of the governing parameters, but first a visual description of the tests about the way the damage of the toe structure developed will be given in section 6.2. In the sections 6.3 to 6.6 a presentation of the results is presented and explained by the curves presented in **Figure 6.2**; this figure is divided into the curves a, b, c and d. These curves give N_{od} as a function of H_s and belong to the four variations of h_m and Z_t.

6.2 Description of damage levels

The stones move because lift, drag and shear forces are generated by orbital velocities and the turbulence caused by the breaking of the waves on the breakwater. The stones rolled downward in most of the cases but sometimes a movement upward took place. The damage started at the sharp angle from berm to the down slope or there where a stone rose a little above other stones close by. This stage can be seen as damage level N_{od} = 0.5. The damage developed by stones rolling from the berm or the top of the toe structure down to the bottom. The shape of the structure changed, the slope became less steep, the width of the toe diminished but still remained in tact. This phase includes the damage levels N_{od} 1 to 3. Finally the toe width became zero and a slope of a small angle started directly from the breakwater down to the bottom: a lot of stones were displaced seaward from the white line painted at the bottom. In **Figure 6.1** the development of the damage is given with the damage levels and the amount of stones which were displaced in the several phases.

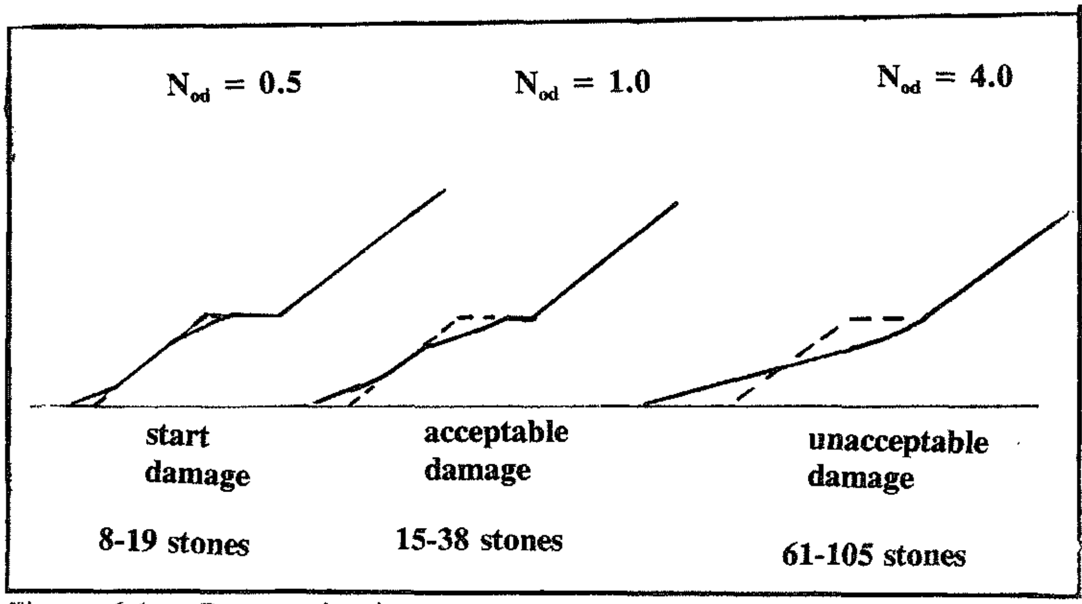

Figure 6.1 Damage levels

6.3 Influence of the local water depth h_m

It turns out that with a larger water depth a larger wave height is required to cause the same level of damage. This seems logical, because with a higher water level the toe structure is deeper under water and waves have to be higher to have the same effect and to cause the same damage to the toe structure at that depth. When the damage at the different local water depths h_m = 0.30 m and h_m = 0.45 m is compared (Figure 6.1: compare the curves of a to those of b and the curves of c to those of d); it is clear that the most damage occurs when the water depth is 0.30 m.

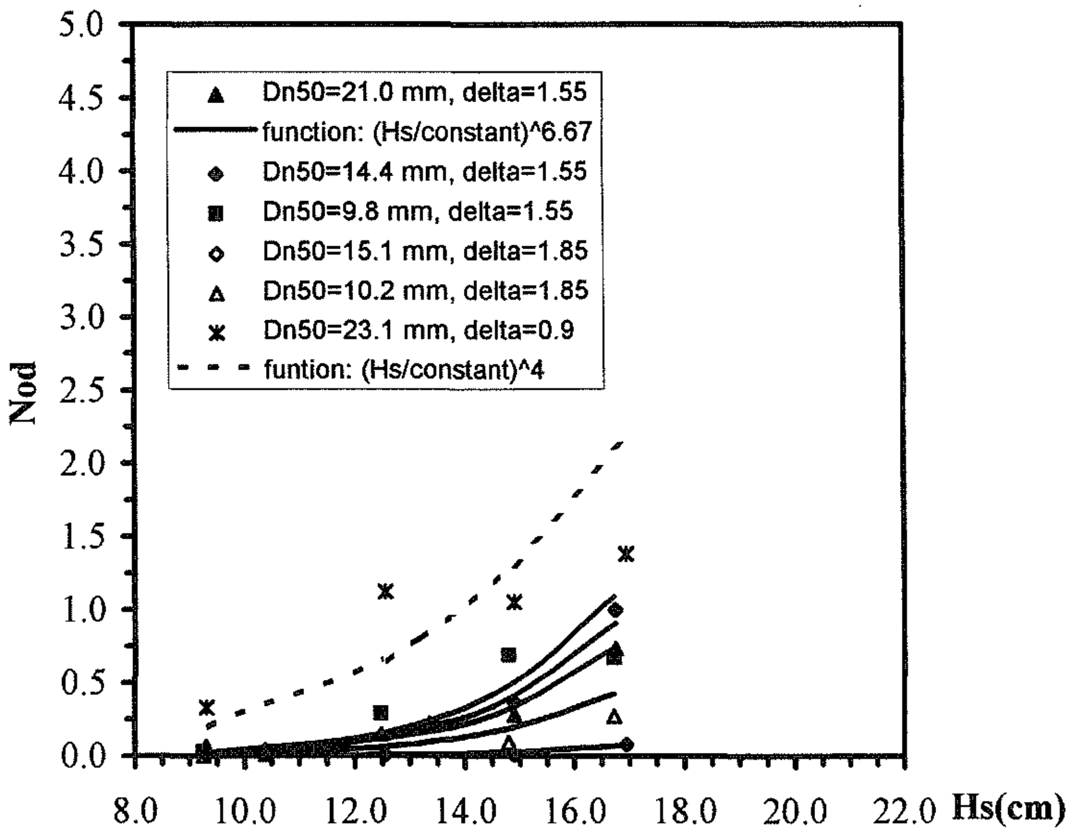

Figure 6.2a h_m = 0.30 m and Z_t = 0.08 m

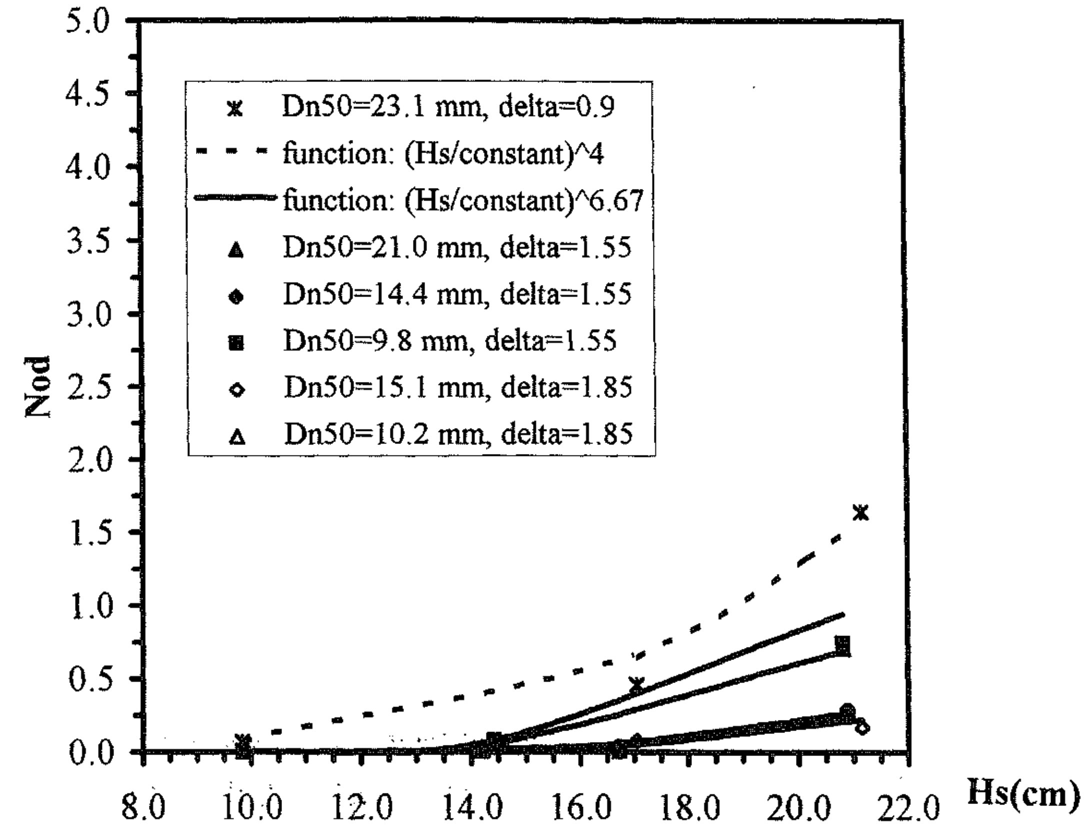

Figure 6.2b h_m = 0.45 m and Z_t = 0.08 m

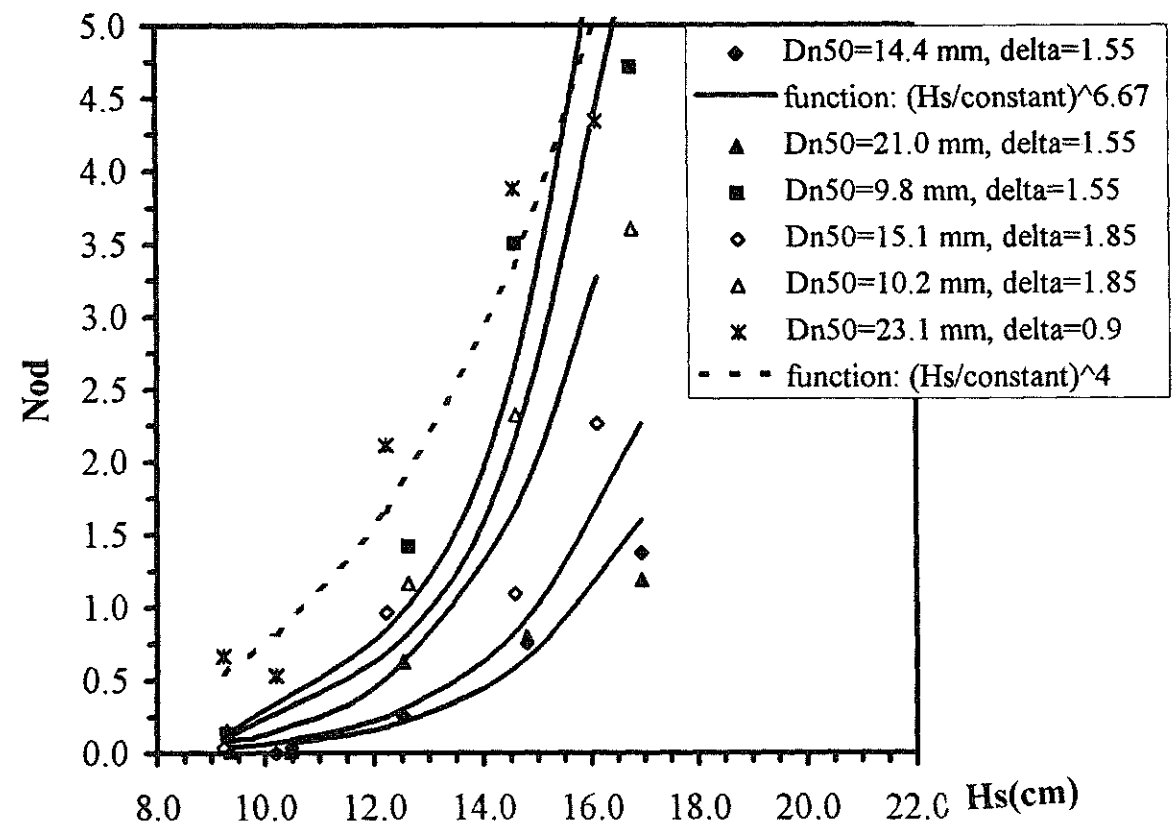

Figure 6.2c h_m = 0.30 m and Z_t = 0.15 m

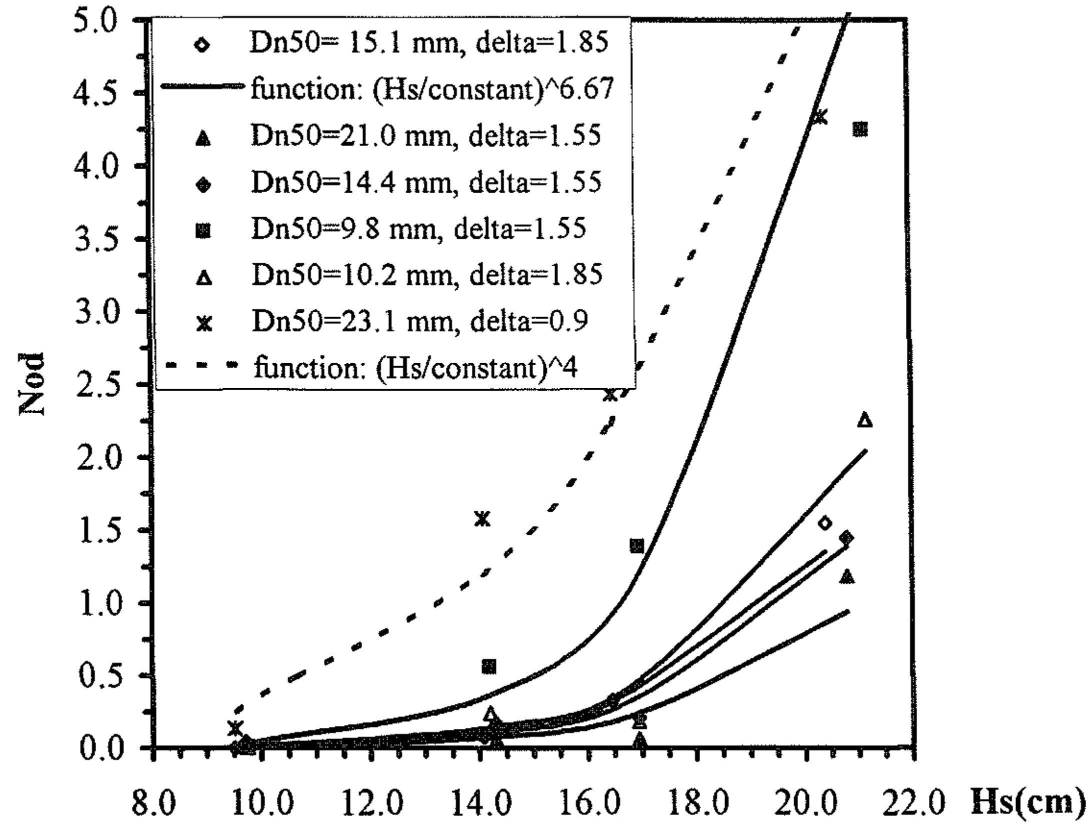

Figure 6.2d $h_m = 0.45$ m and $Z_t = 0.15$ m

6.4 Influence of the toe heigth Z_t

It can be concluded that a higher elevation of the toe structure gives more damage to the toe. The explanation for this trend is the same as for the influence of the local water depth h_m. If the toe structure is closer to the water level, the influence of the waves is larger than if the toe structure would be deeper under water and closer to the original bottom level.
Now a smaller wave height is sufficient to cause the same damage.
When the damage at the different toe heights $Z_t = 0.08$ m and $Z_t = 0.15$ m is compared (Figure 6.1: compare the curves of a to those of c and the curves of b to those of d); there's obviously more damage when the toe is higher.

6.5 Influence of the stone mass density ρ_s

The measurements show more damage for material with a small stone mass density. So brick shows the most damage, porphyry somewhat less and basalt the least. However, sometimes gives porphyry of a small diameter more damage than brick of a large diameter. Here the influence of the diameter is larger than the influence of the density of the stones.

When the damage number N_{od} is presented as function of H_s, the curve through the measuring points is a power function. For porphyry and basalt the power is 6.67, but for brick the power is 4. These curves are given in Figure 6.1. The damage for brick is larger, but the development of damage proceeds less fast than for porphyry and basalt.

As an explanation of the difference in the development of damage differences in roundness of the stones can be mentioned. Both the broken bricks and the basalt had got more sharp edges than the porphyry stones. Also the surface of the brick was more rough than that of the basalt and porphyry. When the roundness is of importance, the internal angle of friction of the materials may be different. This was tested.

In a self-made box (see **Figure 6.3**) a board with two layers of stones (one layer was glued on the board) was put under an angle at which a lot of stones moved down, to determine the angle of friction. This procedure was performed for all six stone diameters and three mass densities. The two largest diameters had also the largest internal angle of friction namely 50°. The other diameters had an angle of ca.45°. Unfortunately the smaller diameters were partly sunk away in the glue. The angle of friction would have been larger if the stones were not sunk away in the glue, because the surface then would have been rougher. Thus the differences between the respective angles of friction of the six diameters is in reality small.

6.6 Conclusion

The influence of the stone mass density is twofold. From the difference in power between the curves in the figures 6.2 an influence on the growth of the damage follows and from the same curves it can be concluded that the damage for brick is the largest of all test variations.
When the curves of a-b and c-d are compared (see figure 6.2), then there is little difference visible: the influence of the water depth in front of the toe structure is small.

The parameter which caused the largest influence is the toe height Z_t. The damage in case of a $Z_t = 0.15$ m is much more than for $Z_t = 0.08$ m, as the curves c and d show.

In **Appendix B** N_{od} is presented as a function of $H_s/\Delta D_{n50}$, the dimensionless stability parameter, to show some repeated tests. Now the influence of Δ and D_{n50} are already included.

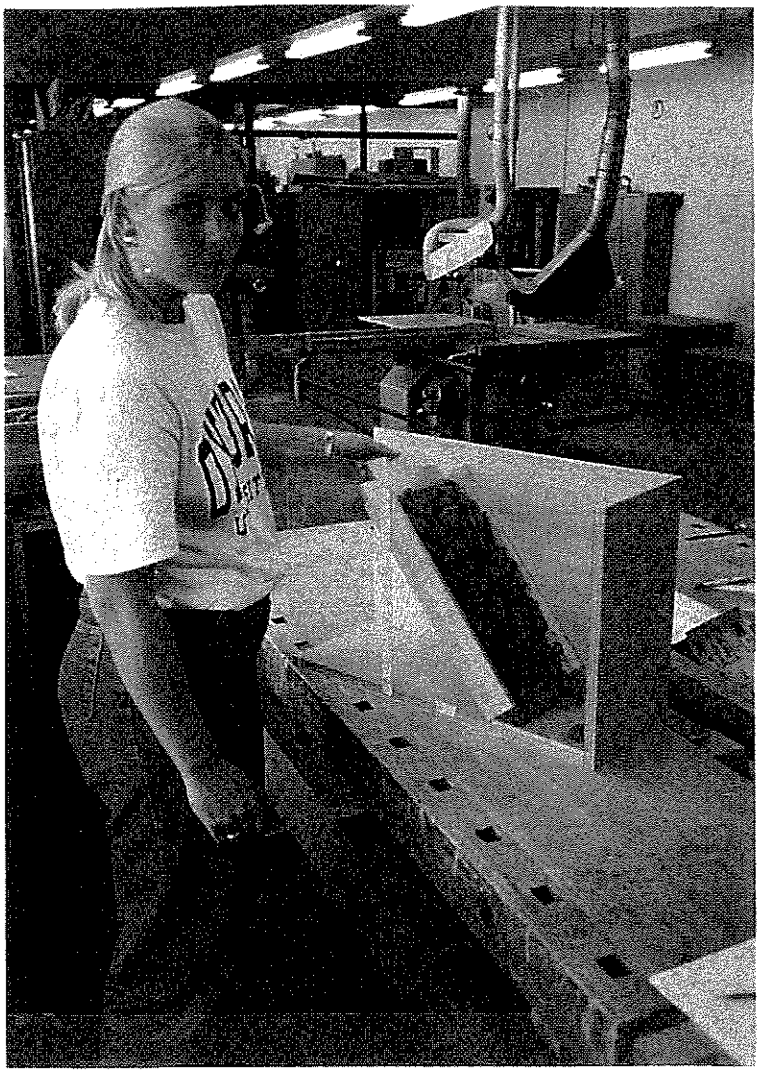

Figure 6.3 Determination of the angle of friction

7 Results compared to existing formulae

7.1 Original data set

All measurements were elaborated according to the recent study of Gerding (1993) to prove whether the relative density was represented correctly in his design formula and control the values of the coefficients used.

$$\frac{H_s}{\Delta D_{n50}}=(0.24\frac{h_t}{D_{n50}}+1.6)N_{od}^{0.15} \tag{7.1}$$

The elaborated data is given in **Appendix C.** Now $(H_s/\Delta D_{n50})/N_{od}^{0.15}$ should be a function of h_t/D_{n50} according to Gerding. **Figure 7.1** shows the original data set in which the measurements are subdivided into the three materials used: brick, basalt and porphyry.

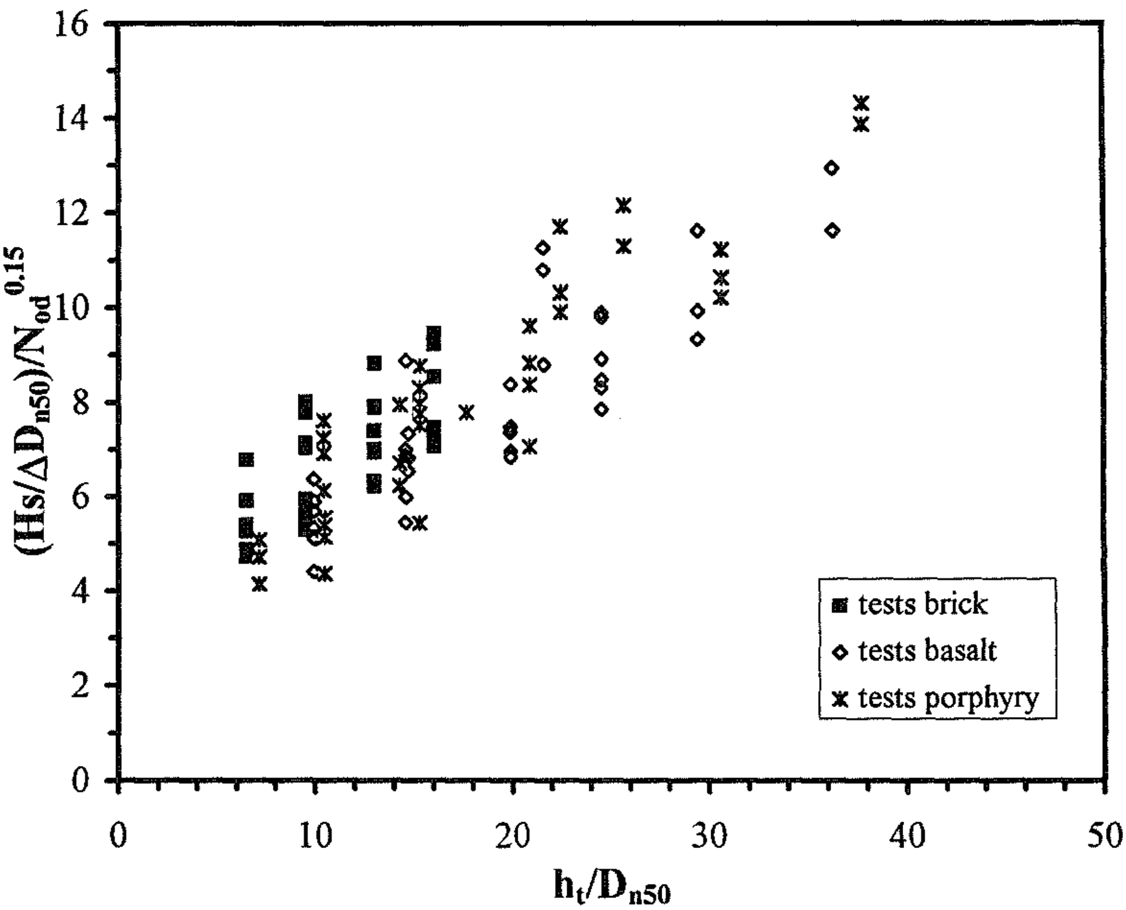

Figure 7.1 Original data set

The measured points of different mass density are well mixed and overlap each other in the figure. Especially the mass density of the natural stones that are normally used for rubble-mound breakwaters: basalt and porphyry. However, even the points which belong to the broken brick fit in the area of the other materials. From this it can be concluded that the formula of Gerding may be used for all stone mass densities. The scatter of the points from the original data set is too large to make further conclusions based on figure 7.1.

The scatter is large because the damage level that was reached at the end of the tests differed at each variation of parameters. When the results of these tests are compared, different damage situations are compared and a lot of scatter results. To investigate the influence of the parameters involved in the process of toe structure stability, the following operation was needed: fixed damage levels were introduced to compare the right data .

7.2 Data with fixed damage levels

7.2.1 Computation of fixed damage levels

For each variation of h_m and Z_t tests were done with several wave heights as load. At the end of the test the damage was established and a N_{od} number was determined. Then the N_{od} was presented as a function of H_s. Through three or four points in the graph a power curve which best fit was drawn. The wave height that caused a certain damage level could now be read. For N_{od} = 0.5 and N_{od} = 1.0 this was done, but in some cases (especially for N_{od} = 1.0) extrapolation of the power curve was necessary what makes the outcome less accurate. The values for all test variations are given in **Appendix C.** In **Figure 7.2** and **Figure 7.3** the measurements are given for the two determined damage levels 0.5 and 1.0 with $H_s/\Delta D_{n50}$ as a function of h_t/D_{n50}. In the following sections the influence of the governing parameters is discussed for the damage level N_{od} = 0.5.

7.2.2 Influence of the relative density Δ

From figure 7.1 it was concluded that the relative density was allowed to be used in the design formula. In **Figure 7.4** with a fixed damage-level N_{od} = 0.5 the function at the vertical axis changed into $H_s/\Delta D_{n50}$ but the parameter at the horizontal axis stayed the same. In figure 7.4 are less measuring points, but the figure has a lot of resemblances with figure 7.1. The three materials are still well-divided and are at the same place as before, except for the fact that the scatter has been diminished. There is less scatter so through the points a fictious curve can be drawn (see Eq.7.2); the direction coefficient is the same.

$$\frac{H_s}{\Delta D_{n50}} = 0.24\frac{h_t}{D_{n50}} + 2.9 \tag{7.2}$$

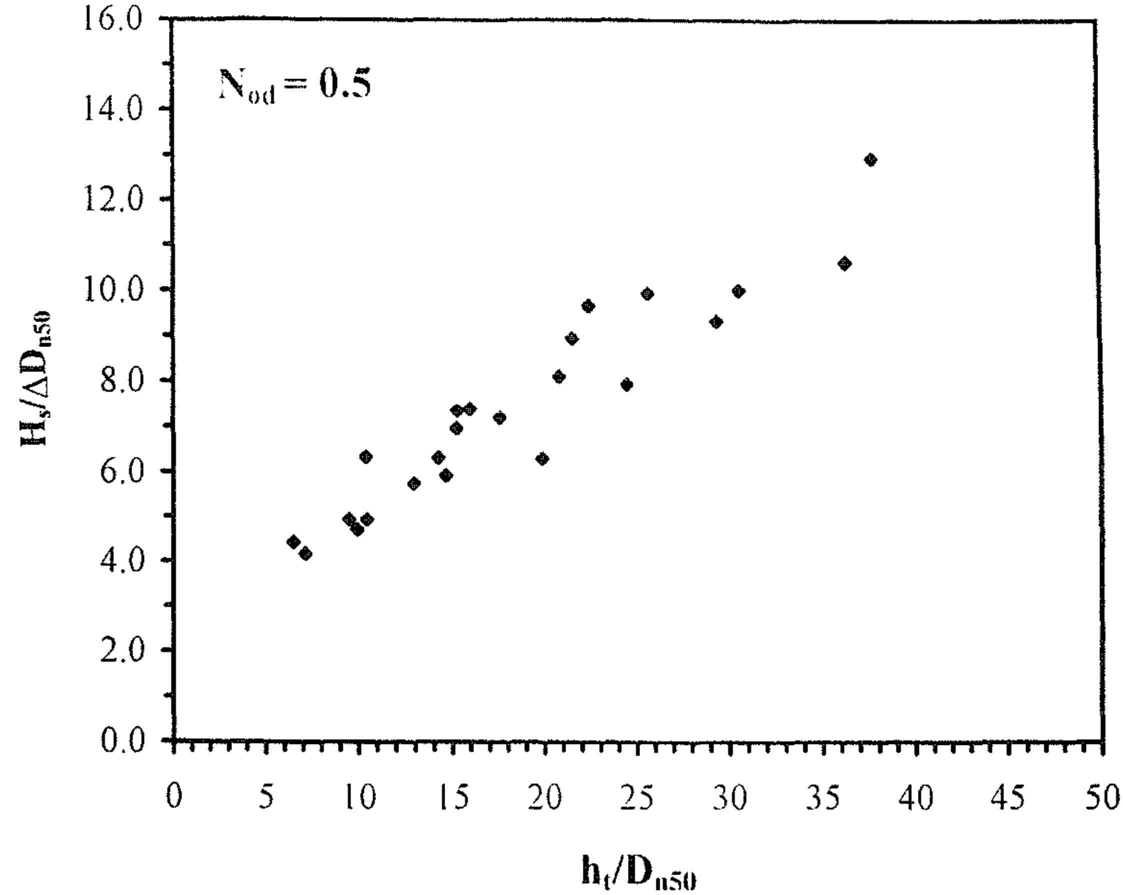

Figure 7.2 **Damage level $N_{od} = 0.5$**

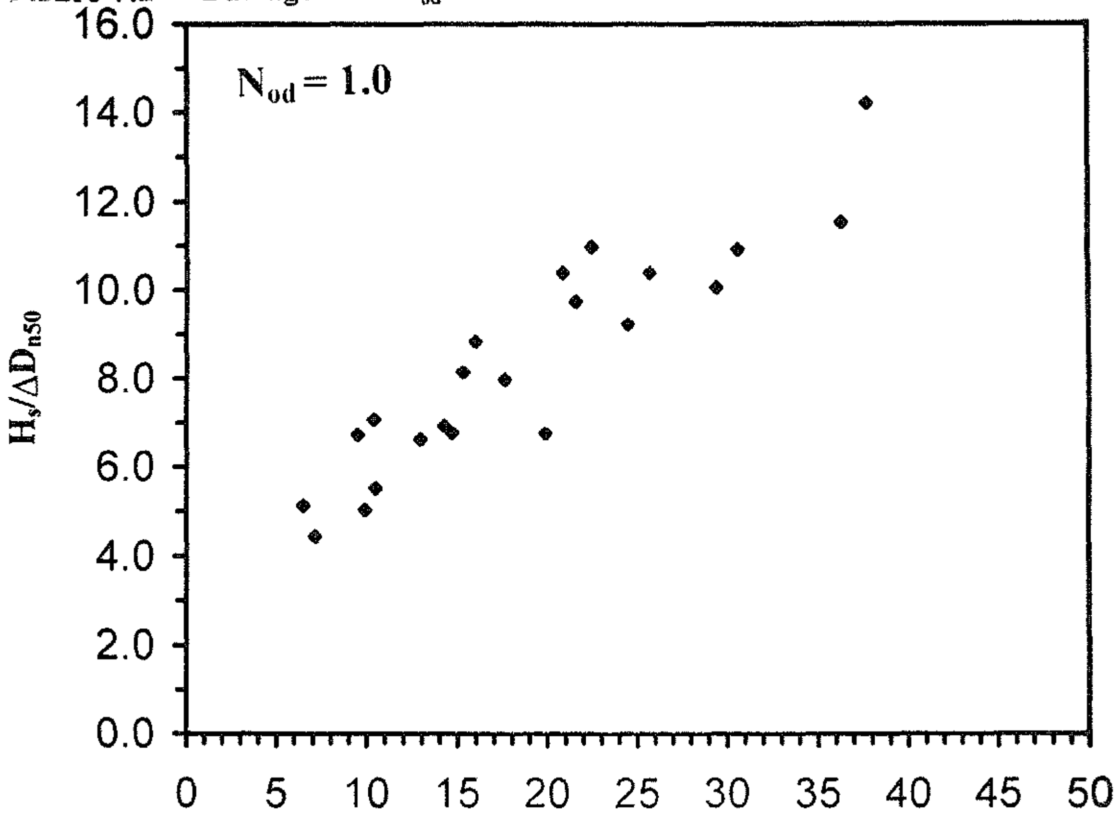

Figure 7.3 **Damage level $N_{od} = 1.0$**

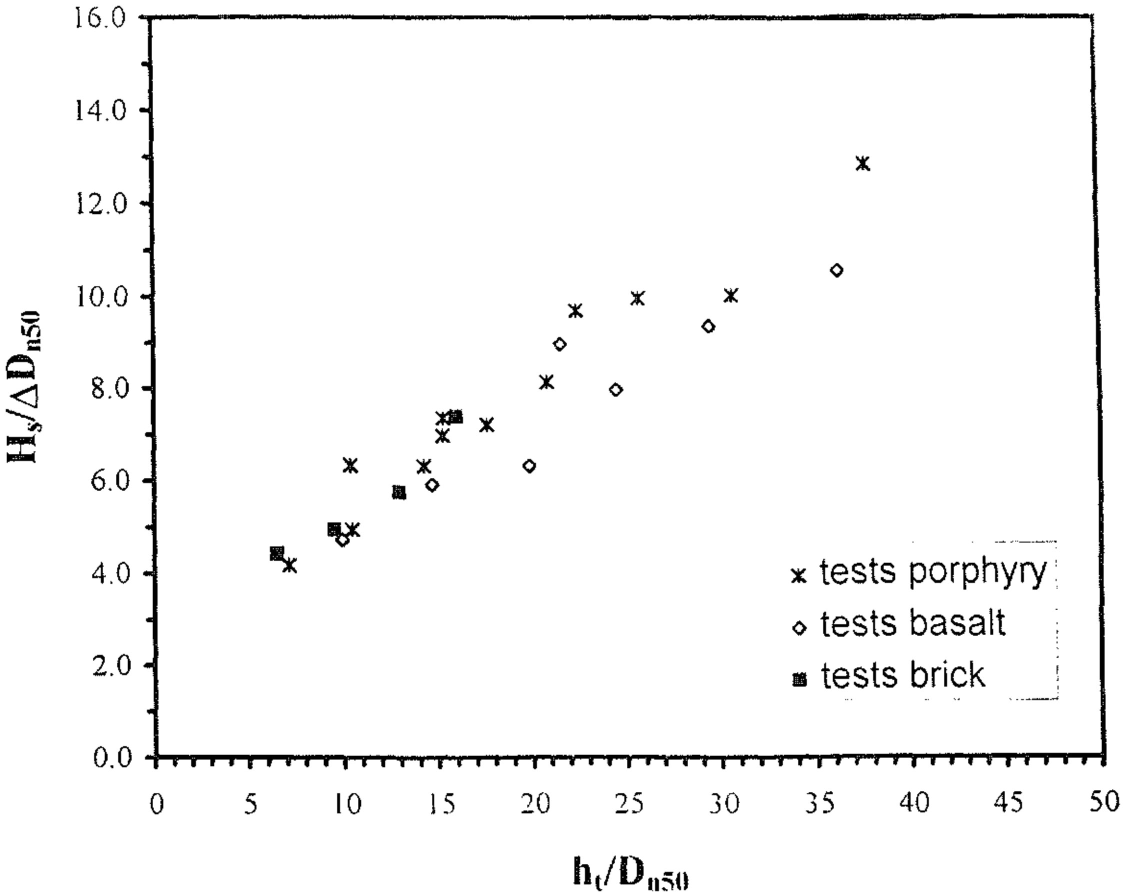

Figure 7.4 $H_s/\Delta D_{n50}$ as a function of h_t/D_{n50}

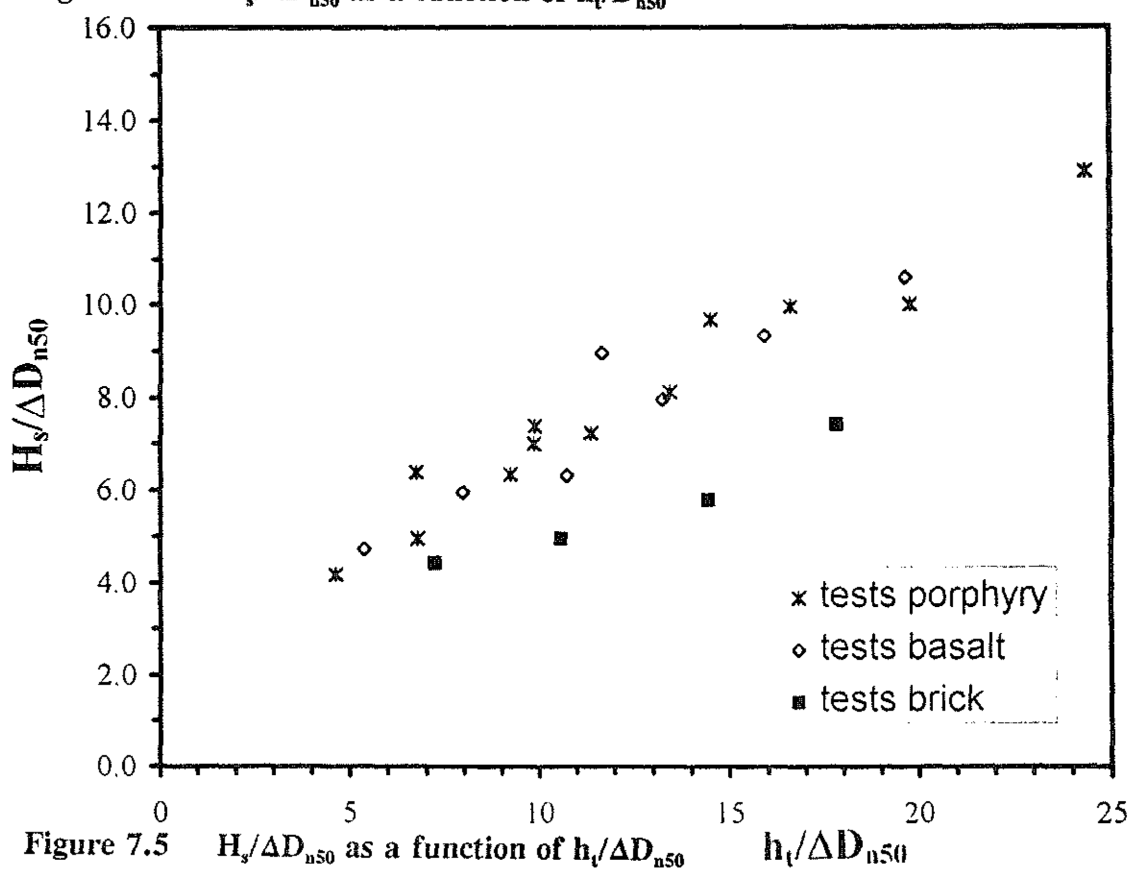

Figure 7.5 $H_s/\Delta D_{n50}$ as a function of $h_t/\Delta D_{n50}$

The relative density Δ could play a more important role if there existed a relation between $H_s/\Delta D_{n50}$ and $h_t/\Delta D_{n50}$. The result is shown in Figure 7.5 and it is obvious that the relation becomes worse, because the points of brick fall out of the area of the other material points and do increase the scatter too.

7.2.3 Influence of the toe height Z_t

The influence of Z_t can be found by sorting out the measuring points with respect to the toe height. So there are two possibilities Z_t = 0.08 m or Z_t = 0.15 m. When the same function of section 7.4 is considered, it turns out that the points of different toe heights are well-mixed, which means that the influence of Z_t is already included in the given relation (see **Figure 7.6**). An improvement could be when the stability parameter $H_s/\Delta D_{n50}$ is shown as a function of h_m/D_{n50}. In **Figure 7.7** the result shows a division into two groups, so this relation is worse than that of figure 7.6. In figure 7.7 the influence of the toe elevation isn't considered. Also the measuring points have a large scatter, that's the second reason why h_t/D_{n50} is preferred.

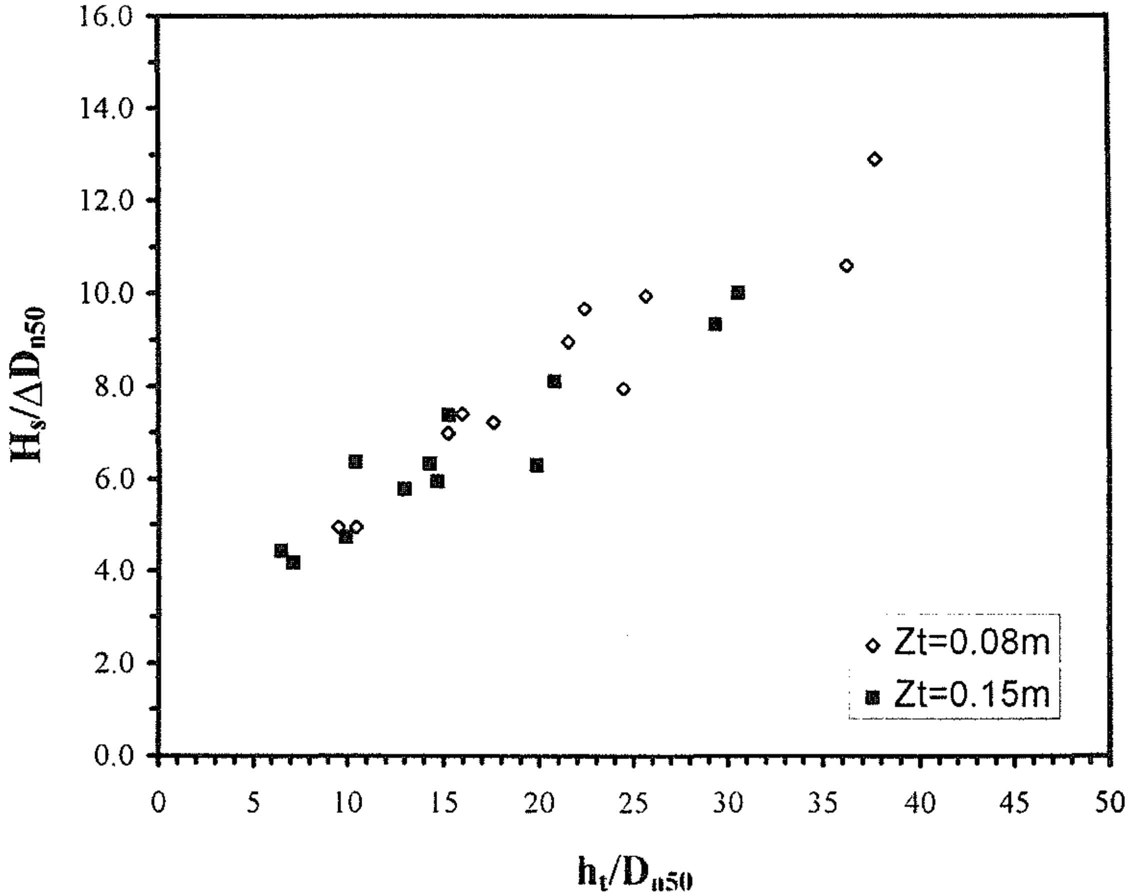

Figure 7.6 $H_s/\Delta D_{n50}$ as a function of h_t/D_{n50} sorted out after Z_t

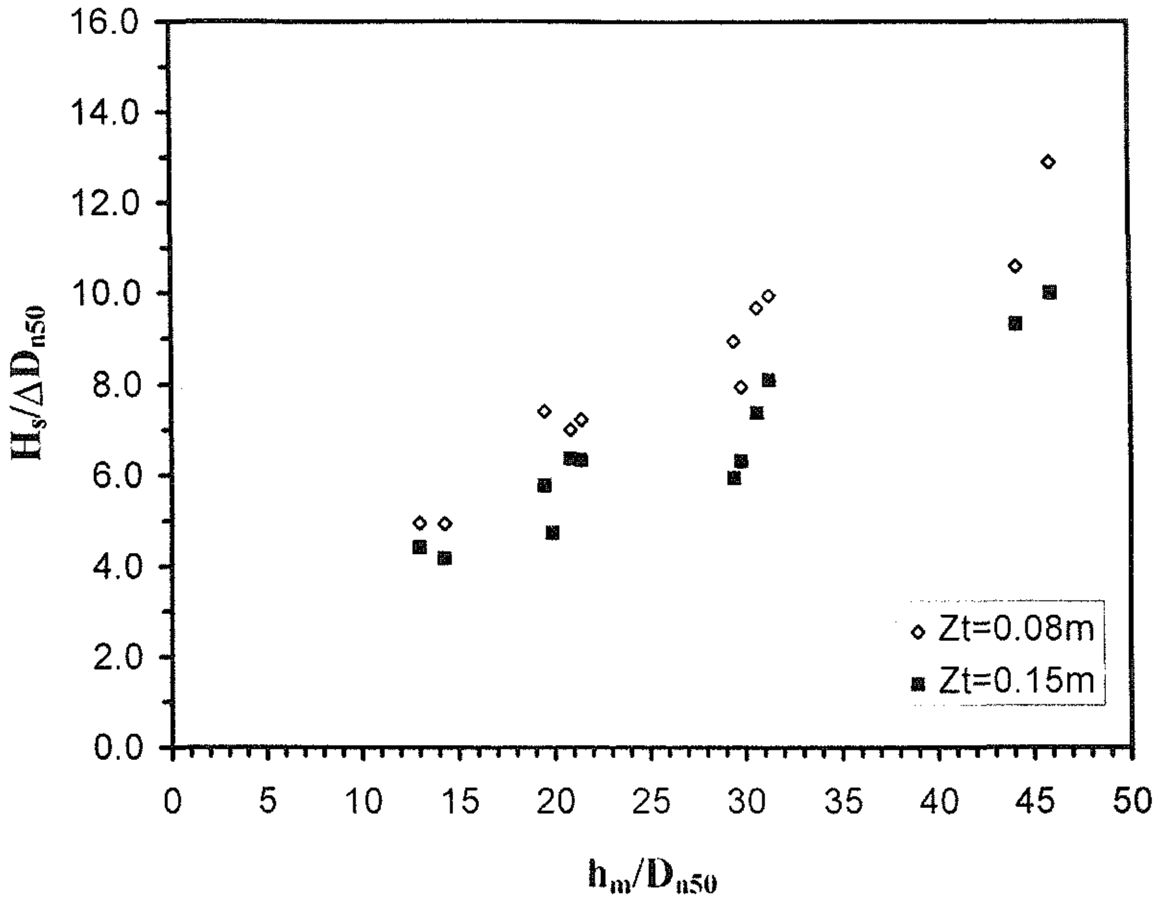

Figure 7.7 $H_s/\Delta D_{n50}$ **as a function of** h_m/D_{n50} **sorted out after** Z_t

7.2.4 Influence of the local water depth h_m

The influence of h_m can be found in the same way as the influence of Z_t. The measuring points are now sorted out with respect to h_m. In **Figure 7.8** the points which belong to h_m = 0.30 m or h_m = 0.45 m are divided. It looks as if the points for h_m = 0.45 m are a continuation of those for h_m = 0.30 m, but when the linear trends of the groups are taken apart an angle between the curves becomes visible (see **Figure 7.9**). From this it can be concluded that h_m has still an influence on the process of toe structure stability which isn't fully taken into account. For each h_m an equation can be deduced see (7.3) and (7.4):

$$h_m = 0.30m: \frac{H_s}{\Delta D_{n50}} = 0.33 \frac{h_t}{D_{n50}} + 1.9 \tag{7.3}$$

$$h_m = 0.45m: \frac{H_s}{\Delta D_{n50}} = 0.24 \frac{h_t}{D_{n50}} + 2.8 \tag{7.4}$$

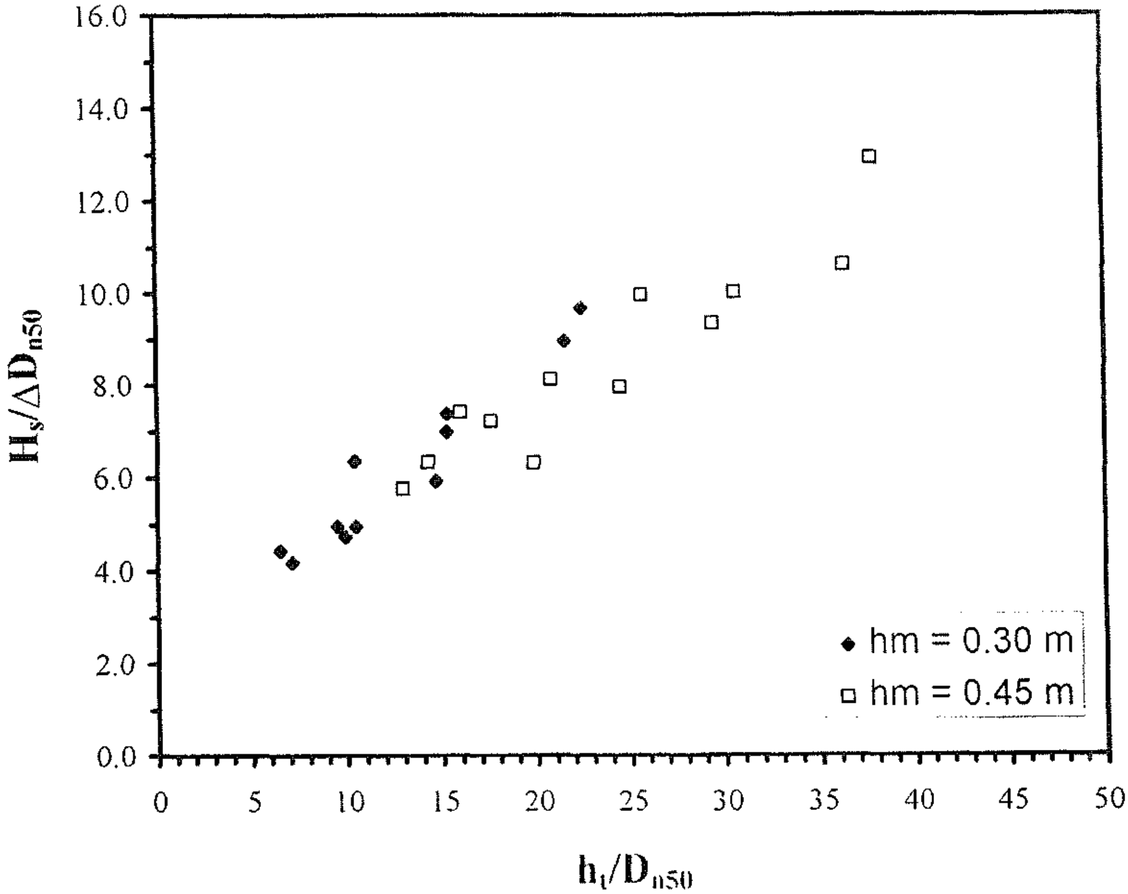

Figure 7.8 $H_s/\Delta D_{n50}$ as a function of h_t/D_{n50} sorted out after h_m

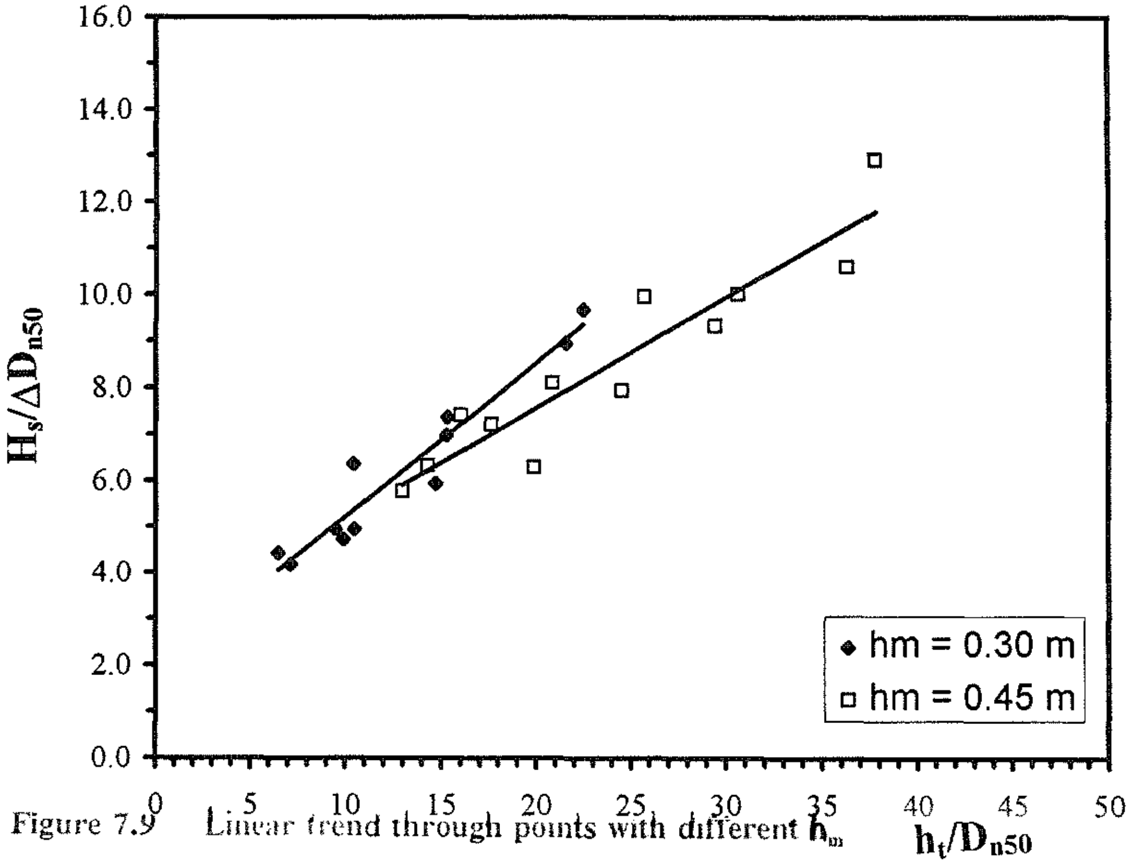

Figure 7.9 Linear trend through points with different h_m

7.2.5 Conclusion

From the sections 7.2.2 to 7.2.4 it can be concluded that $H_s/\Delta D_{n50}$ is a function of h_t/D_{n50}, by which the influences of both the relative density and the toe elevation are included. However, the influence of h_m is not fully taken into account. So there must be found a way to add this influence to the relation already given. The toe structure could be seen as an obstacle for the incoming wave. Then the parameter Z_t/h_m could play a part as shape factor. When Z_t/h_m is large, the wave would cause an impact force on the toe structure; when Z_t/h_m is small, the wave would barely notice the presence of the toe structure. When the shape factor is added as $(h_t/D_{n50})*(Z_t/h_m)^{0.2}$ to the parameter at the horizontal axis the influence of h_m remains (see **Figure 7.10**).

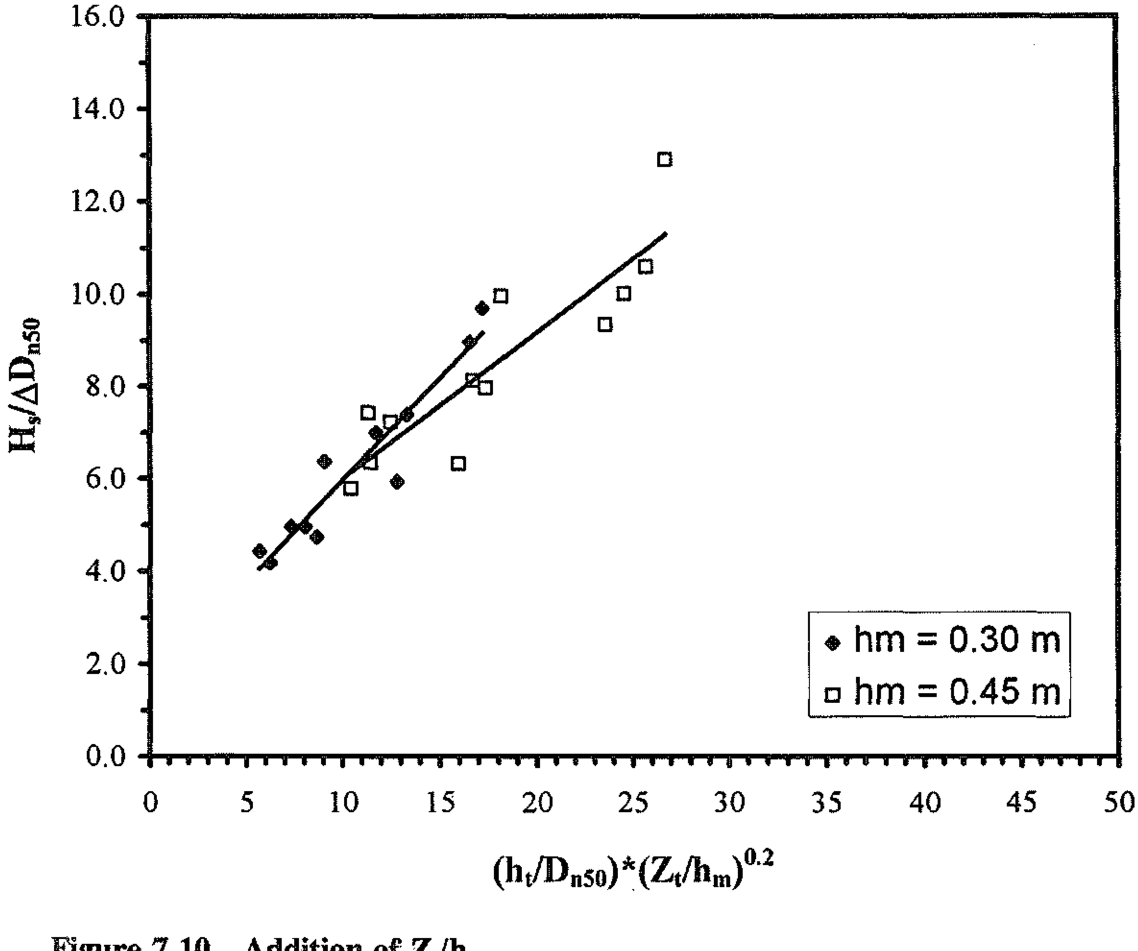

Figure 7.10 Addition of Z_t/h_m

From this trial-and-error approach and chosing dimensionless variables it can be concluded that there are too many physical processes (see Chapter 2) involved in toe structure stability to yield a relation which includes the influences of each governing parameter. It is risky to look for a relation only on an empirical basis; that's the reason why in Chapter 8 simple computations on an analytical basis are performed to increase the insight into the processes involved.

7.3 Comparison with existing formulae

7.3.1 Comparison with Gerding

7.3.1.1 Differences in test set-up

In the execution of the test series there were some differences between the way Gerding's test were performed and the present tests were done. Firstly Gerding generated 1000 waves and now 2000 waves were generated. As a result of this the damage should be 1.4 times greater (the damage grows with the root of the multiplication of wave number), but this can not be observed from the measurements. Further Gerding counted the damage both landward and seaward, but in the new tests only the seaward damage was taken into account. This fact became known too late to adjust to. The tests were already done when this extra information arrived.

As a consequence of this difference the damage measured was less than the damage in the tests performed by Gerding. The error is the largest when the local water depth h_m = 0.3 m and the incoming waves are relatively high at the toe structure : H_s = 0.15m, H_s = 0.17 m and H_s = 0.21 m. The percentage of the error can not be given, but from communication with Gerding it seemed that his landward damage was never more than 30% of the total damage.

7.3.1.2 Growth of damage

In the research of Gerding a power for the growth of the damage was determined. When N_{od} is shown as a function of the significant wave height H_s, a curve can be drawn through the points of the measured damage. This curve has the average power 0.15. When this power of growth also fits for the measurements of the present tests, the damage increases in the same way.

For the materials with nearly the same stone mass density as used by Gerding (viz. porphyry and basalt) this seems to be right. For brick a power 0.25 seems more accurate. When the power for brick is changed from 0.25 to 0.15, the results in the actual relation differ just a little. In section 6.4 the factors that influence the growth of the damage are explained more thoroughly.

7.3.1.3 Suggested design curve according to Gerding

In **Figure 7.11** $H_s/\Delta D_{n50}$ is given as a function of h_t/D_{n50} for the measurements of the present study and the suggested design curve of Gerding is added. There is a great difference in the results. The damage found in the present tests is much smaller (almost two times) than Gerding's.

One reason is the already mentioned fact that only the stones displaced seaward were counted as damage, while Gerding added the landward damage as well. But this is might not be the only cause of the large difference. There could be a difference in the way the breakwater was constructed or the packing of the stones; the permeability could also be different.

Another fact is that the tests by Gerding were performed in the "Schelde" flume at Delft Hydraulics and the present tests in the large wave flume of the Laboratory of Fluid Mechanics at the Faculty of Civil Engineering. The results differ so much that it is recommended to perform exactly the same tests in the two wave flumes to find out where 'the shoe pinches'. This should be done by one and the same person to exclude misinterpretations.

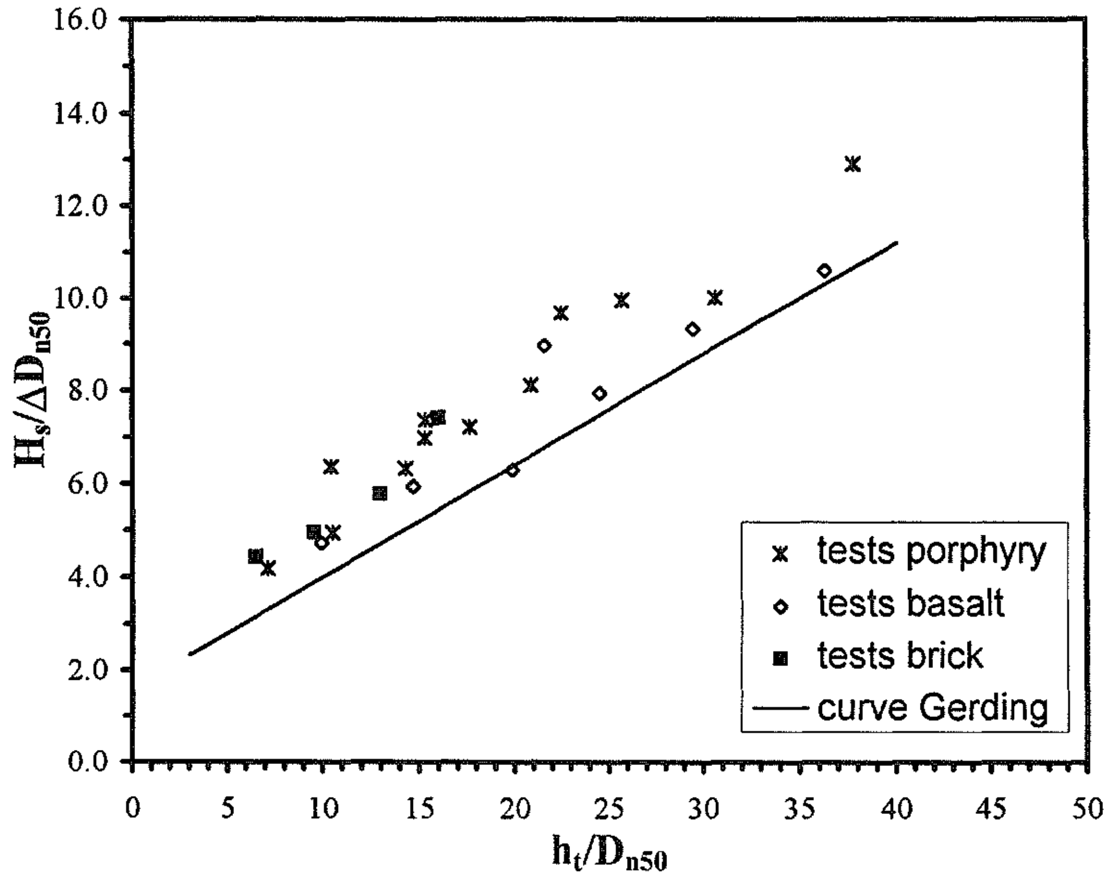

Figure 7.11 Comparison with suggested curve by Gerding

Although a difference in damage is found between Gerding's and this study, it is useful to check, if his data also has an influence of the local water depth h_m. In **Figure 7.12** and **Figure 7.13** data is sorted out after h_m. Three variations were measured. In Figure 7.12 different levels of N_{od} are presented. Here is more scatter visible than in Figure 7.13, because in Figure 7.13 only the data from N_{od} = 0.5 is shown. From Figure 7.13 it can be concluded that Gerding too, had an influence of h_m in his measuring results.

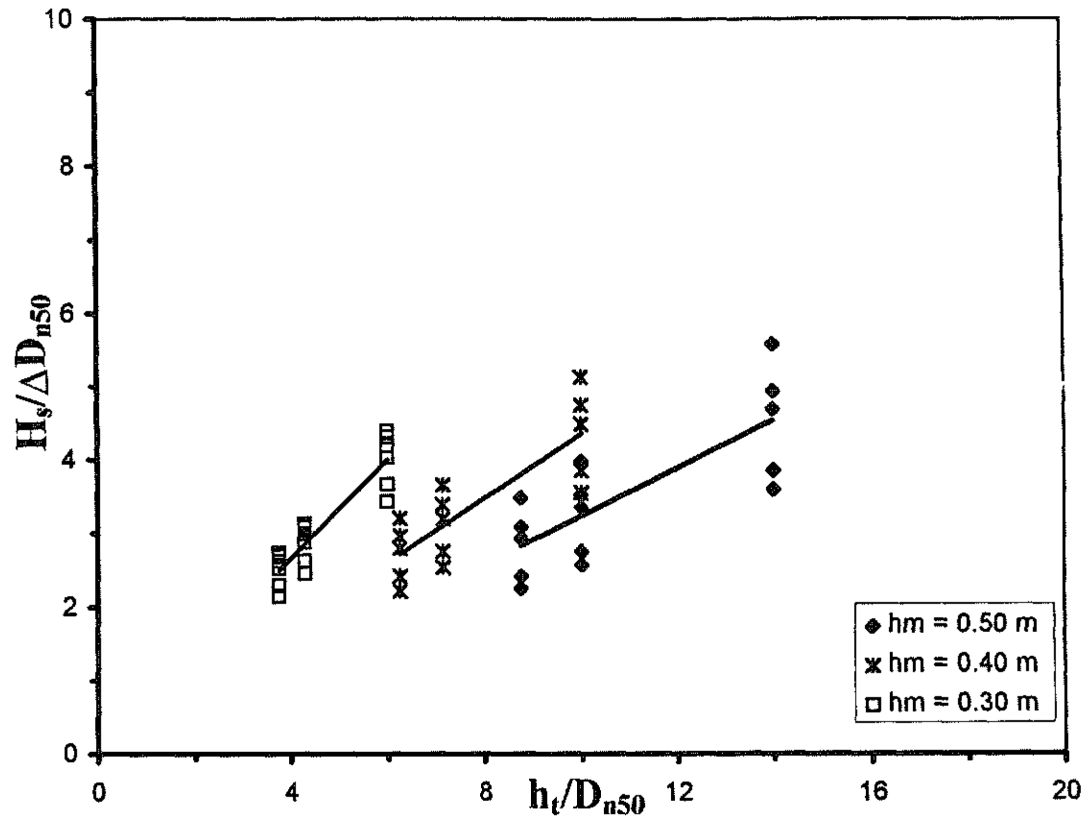

Figure 7.12 **Original data of Gerding(1993) sorted out after h_m**

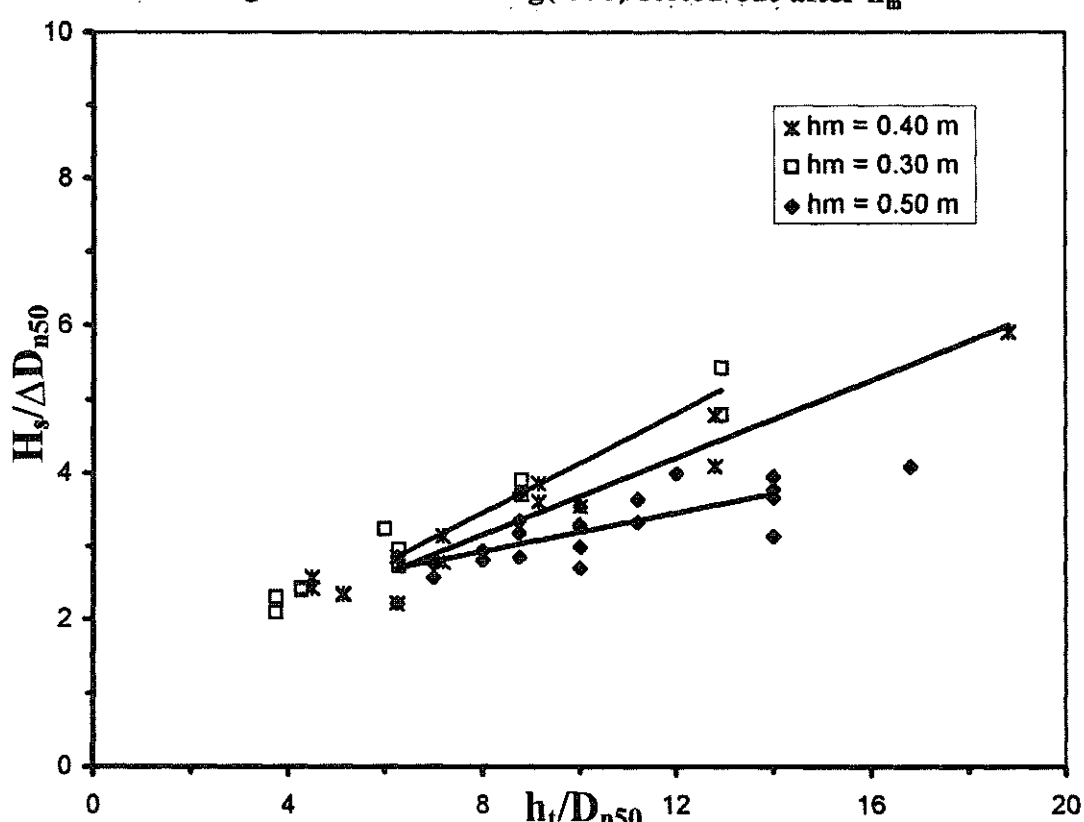

Figure 7.13 Data of Gerding(1993) with N_{od} = 0.5 sorted out after h_m

7.3.2 Comparison with results by Van der Meer

In **Figure 7.14** $H_s/\Delta D_{n50}$ is given as a function of h_t/h_m for the present test results and the suggested design curve by Van der Meer is added. For this relation the dispersal is even greater with respect to a representation of $H_s/\Delta D_{n50}$ versus h_t/D_{n50}. The design curve by Van der Meer is also under the actual data. The influence of h_m is here not fully implemented, because the points for h_m = 0.30 m have consequently lower values and a fictious curve through these points lies lower than a curve through the points for h_m = 0.45 m. This agrees with the result of section 7.2.4 where also an influence of h_m was found.

The accuracy of the results in figure 7.14 decreases, when the parameter h_t/h_m increases. For example, if h_t/h_m = 0.5, the difference between the minimum and maximum value of $H_s/\Delta D_{n50}$ equals 3.2, while the difference for h_t/h_m = 0.82 has increased upto 5.7. A restriction follows: the use of h_t/h_m is only allowed below h_t/h_m = 0.9.

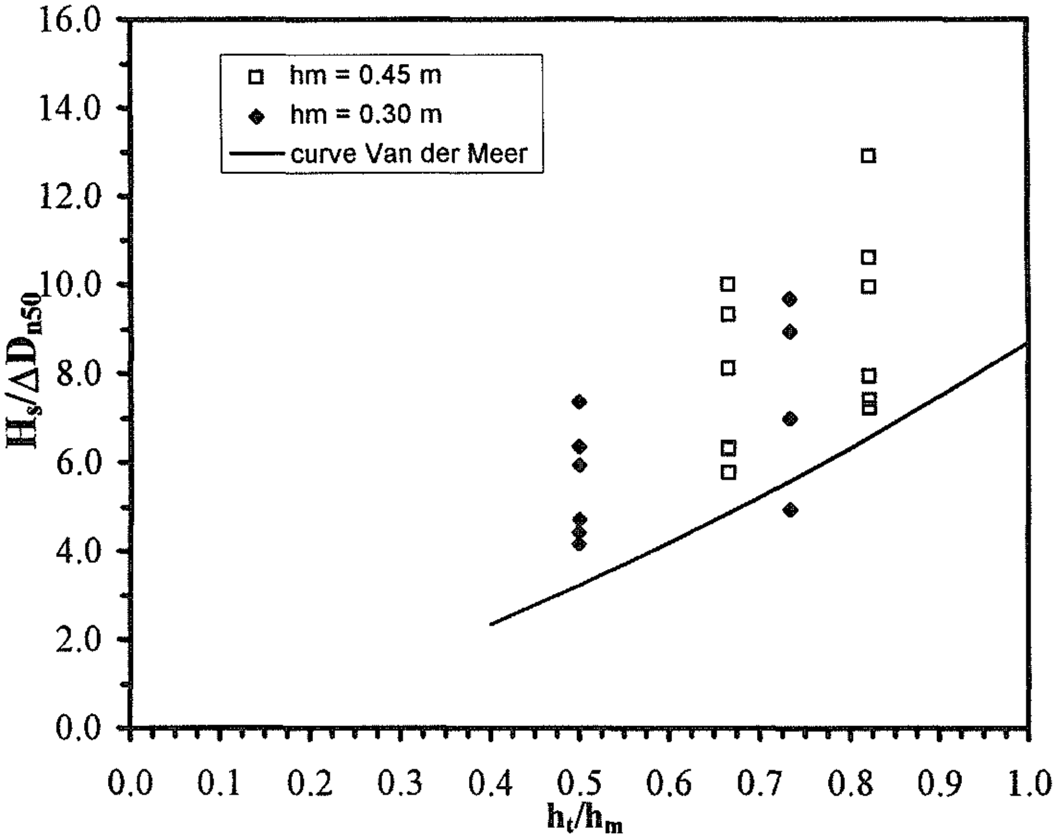

Figure 7.14 Comparison with suggested curve by Van der Meer

When another dimensionless parameter h_t/Z_t is tried out, a graph of the same shape as in figure 7.14 results (see **Figure 7.15**).Here is also the influence of h_m visible.
The measuring points which belong to h_m = 0.30 m have smaller values for the stability parameter $H_s/\Delta D_{n50}$ than the points for h_m = 0.45 m. The qualitative analysis is exactly the same as for figure 7.14, but this time with another parameter at the horizontal axis. The use of the parameter h_t/Z_t was just an empirical experiment to see whether a useful relation could be found or not. The outcome doesn't satisfy, because the scatter is too large; so the result is only of importance to enlarge the insight into the governing parameters.

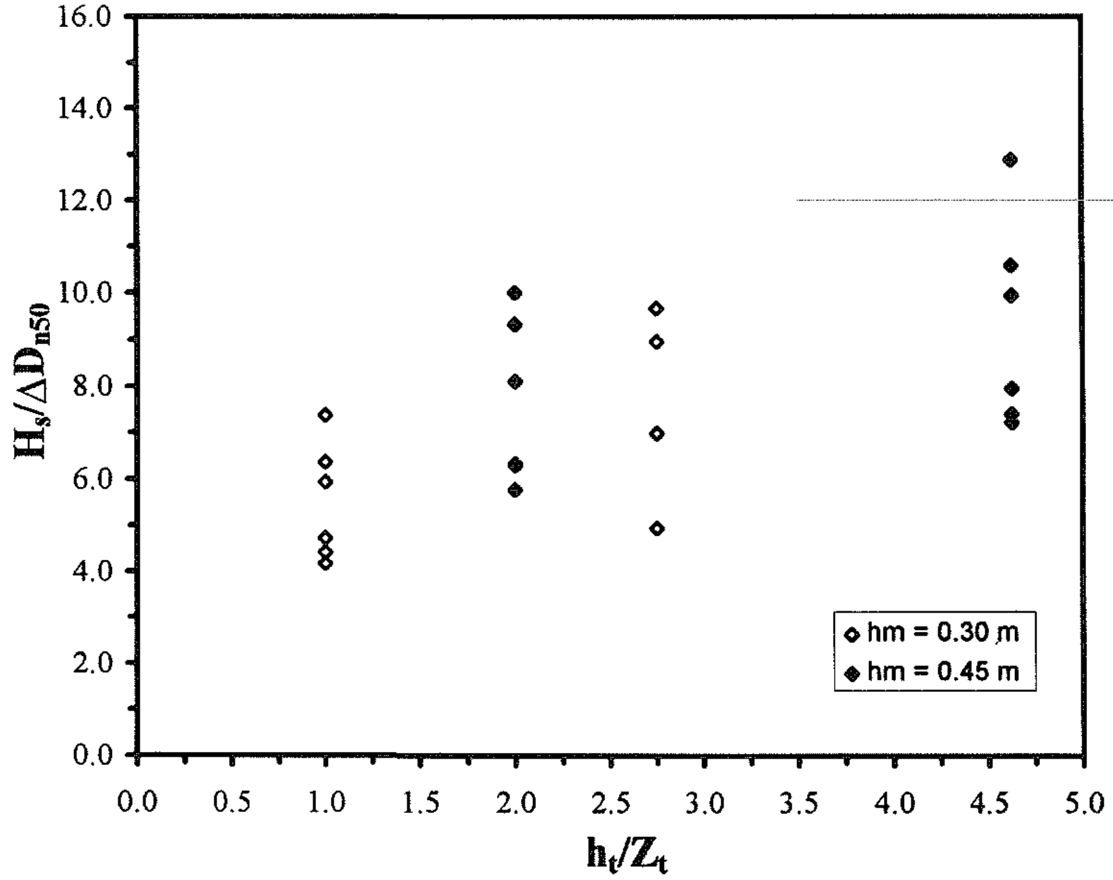

Figure 7.15 $H_s/\Delta D_{n50}$ **as a function of** h_t/Z_t

8 Computations

8.1 Introduction

In the present study there is a relation found between the load $H_s/\Delta D_{n50}$ and h_t/D_{n50} on the analogy of stability of stones in horizontal flow from Shields (1936), who also used h/D as parameter of roughness.
Although waves cannot be compared to flow, it is tried to make some computations with the orbital velocity, U_{orb}, instead of the wave height, H_s, as load on the toe structure. At a certain critical velocity the stones will start to move; in this study this is indicated as damage level N_{od} = 0.5.

Shields (1936) has a theory on the stability of stones in uniform flow, in which the critical velocity, U_*, shows a dependence on the Chezy-friction coefficient, C, and C depends on the water depth, h, see formula (8.1) and (8.2).

$$U_*=\frac{\sqrt{g}U}{C} \tag{8.1}$$

$$C=18\log 6\frac{h}{D_{n50}} \tag{8.2}$$

Now a relation is found between the load by the critical velocity, U_*, and the water depth over the roughness height, h/D_{n50}.

Rance & Warren (1968) and Sistermans (1993) (from Schiereck a.o. 1995) have studied the stability of stones in oscillating flow. The basic phenomenon in stability under non-breaking-waves is assumed to be the shear stress due to oscillatory flow, which depend both on the wave height H and period T. For breaking waves, the same mechanism is assumed to work. But due to a complete change in the velocity field and the turbulence in a breaking or broken wave, it can be expected that some amplification factor on the computional results has to be applied to fit experimental data.

It can be assumed that the velocity in a wave on a slope is proportional to the velocity in shallow water with the wave height as a representive measure for the water depth: before breaking, the speed of the front is $\sqrt{(gh)}$, with h of the same order as H_s; which indicates that U_{orb} and H_s are coupled: $U_{orb} \sim \sqrt{H_s}$.

However, in the linear wave theory another connection is assumed: $U_{orb} \sim H_s$, this is a simplification of what is really happening. The values can serve as an indication; therefore, it is useful to make some computations based on analytical equations to compare their results with the empirically found results.
All computed values are given in **Appendix C**.

8.2 Orbital velocities as critical velocity according to Shields

The velocities are computed with the linear wave theory for the measured incoming wave heights H_s, which are necessary to cause damage level $N_{od}=0.5$ (start of damage) and can be seen as critical velocities, at which the movement of stones will start at the toe, so at the level of the water depth h_t (a uniform flow condition is assumed). The following equations are needed:

$$L=g\frac{T^2}{2\pi}\tanh[2\frac{\pi}{L}h_m] \tag{8.3}$$

$$T=\sqrt{\frac{H_s}{\frac{g}{2\pi}*s_{op}}} \tag{8.4}$$

$$U_*=\omega\frac{H_s}{2}\frac{\cosh k(h_m-h_t)}{\sinh kh_m} \tag{8.5}$$

$$\frac{U_*^2}{\Delta g D_{n50}}=function(\frac{U_* D_{n50}}{\nu}) \tag{8.6}$$

$k=2\pi/L$, $\omega=2\pi/T$ and $\nu=1.10^{-6}$

Approach of the computations

With the aid of the computed velocities, nominal stone diameters will be determined which will be stable under the attack of the load generated by these velocities. Now $H_s/\Delta D_{n50}$ and h_t/D_{n50} can be computed from the found diameter and given wave height H_s. These values can be compared to the empirically found relation between $H_s/\Delta D_{n50}$ and h_t/D_{n50}. The computations are repeated with different values for the function of Reynolds (8.6) until they fit the results of the measurements. Afterwards it is checked, if the factor needed to make the computations fit is physically right.

In **Figure 8.1** the computed values and the measured values are compared. The values don't overlap each other and the computed stability numbers are higher. For the computations in Figure 8.1 a value of 1 for the function of Reynolds was used. Normally this value holds between 0.03 and 0.06, so no conclusions can be deduced from the computations according to Shields, because the amplification factor is too large to agree with reality. The computations according to Rance & Warren may fit better, because their theory is valid for stability in oscillating flow.

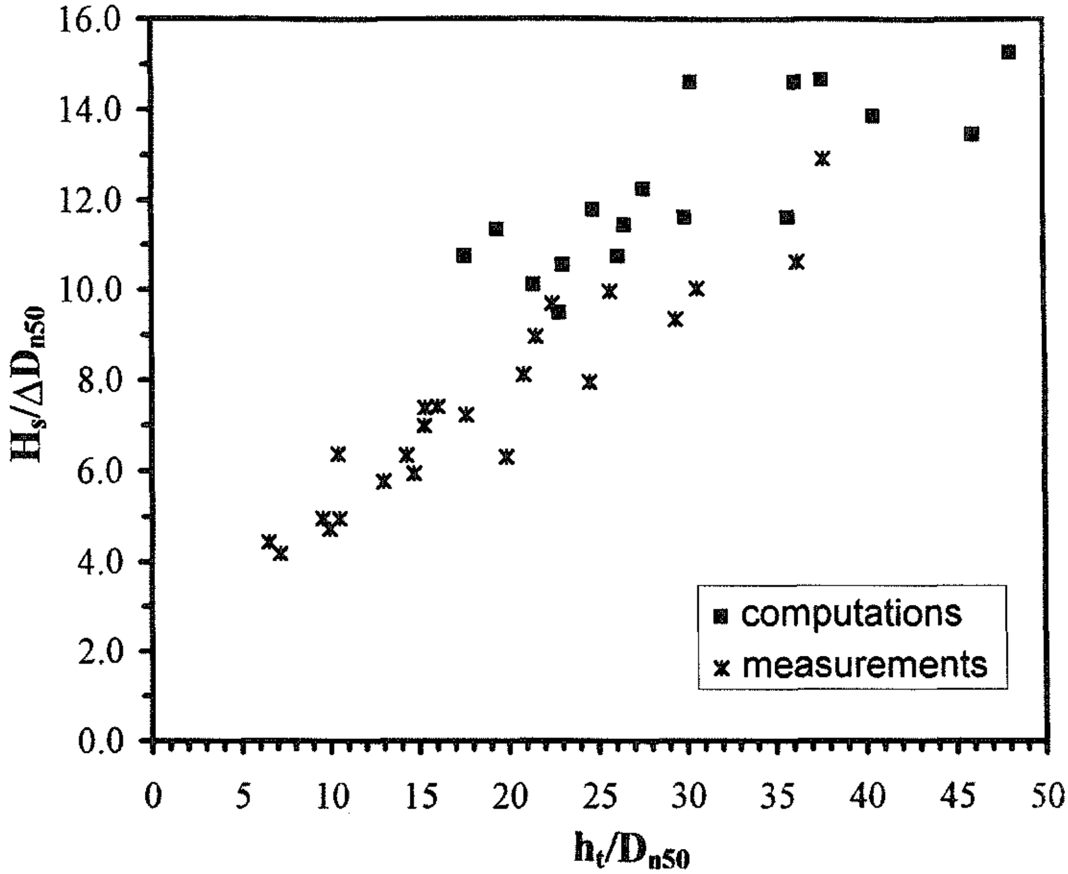

Figure 8.1 **Computations according to Shields compared to measurements**

8.3 Orbital velocities as critical velocity according to Rance & Warren

For the computations according to Rance & Warren based on experimental data another equation to determine the nominal diameter is used. The equations of section 8.2, with exception of (8.6), are still valuable. The equation for the diameter becomes:

$$D_{n50} = \frac{2.15 U_{orb}^{2.5}}{T^{0.5}(\Delta g)^{1.5}} \tag{8.7}$$

The computations were performed in the same way as in section 8.2 with the measured incoming H_s as input to compute the velocities. H_s, however, is only one characterization, while the damage is caused by the highest waves, for example $H_{1\%}$. This wave is 1.5 times larger than H_s. That's why the velocity is multiplied by an amplification factor to include the effect of higher waves.

In **Figure 8.2** the points of the computations and the measurements are well mixed and both groups show a comparable scatter. A factor of ca. 6.5 was needed to compare the computations with the measurements, but 6.5 divided by $1.5^{2.5}$ (factor of $H_{1\%}$), only a factor of 2.3 remained. Figure 8.2 shows that a simple computation with some adjustments can approach the results from experimental tests.

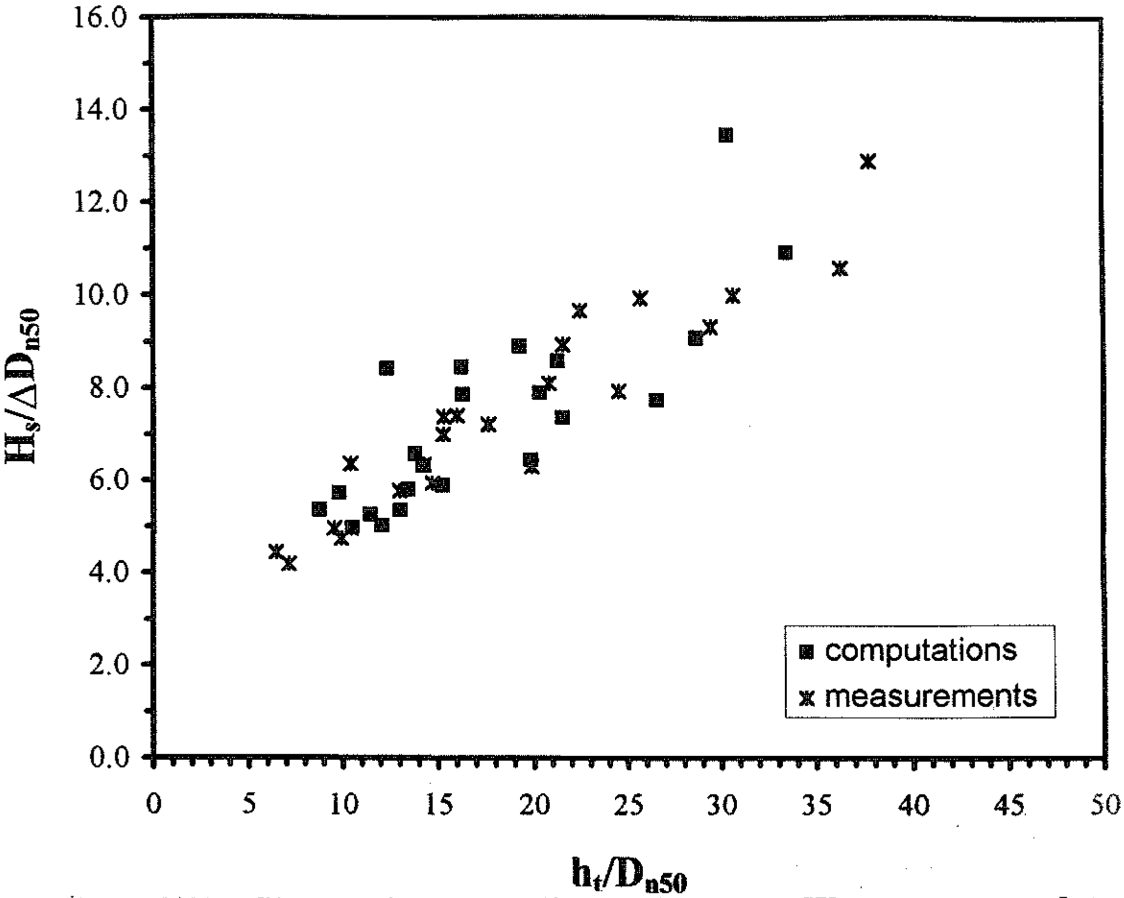

Figure 8.2 Computations according to Rance & Warren compared to measurements

Now that the relation between $H_s/\Delta D_{n50}$ and h_t/D_{n50} has been simulated by computations according to Rance & Warren, the influence of the local water depth h_m will be investigated. In **Figure 8.3** the respective computations are sorted out after the water depths h_m they belong to. From this figure of the computations it follows that there is indeed an influence and two linear curves can be fitted through the computed points in the same way as the curves in figure 7.9 were fitted.

The reflection coefficient was included in a factor in the computations up to now. The effect of the reflection C_r can be better presented in the equation of the velocity (8.5) as follows, with C_r measured during the tests (given in **Appendix C**):

$$U_{orb} = \omega C_r \frac{H_s}{2} \frac{\cosh k(h_m - h_t)}{\sinh k h_m} \tag{8.8}$$

The results of the computations with the reflection coefficient included are given in **Figure 8.4.** The trend of the curves in figure 8.4 is the same as that in figure 8.3, but the scatter has increased. The absolute values of the stability number has also changed. The scatter is caused by the range of C_r, the values differed between 1.2 and 1.32, which influenced the result of the computations. It is recommended for further research to determine the damage according to the H_s with the reflection included to see if the results will improve.

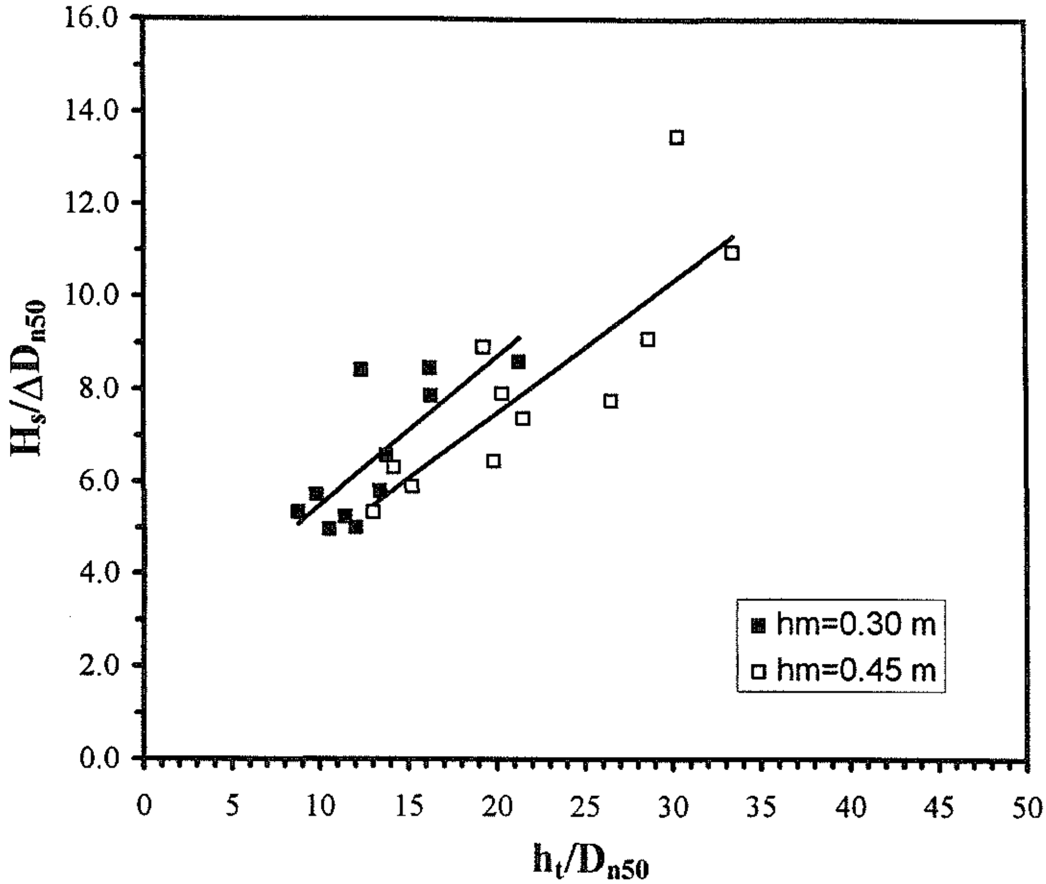

Figure 8.3 **Computations according to Rance & Warren sorted out after h_m**

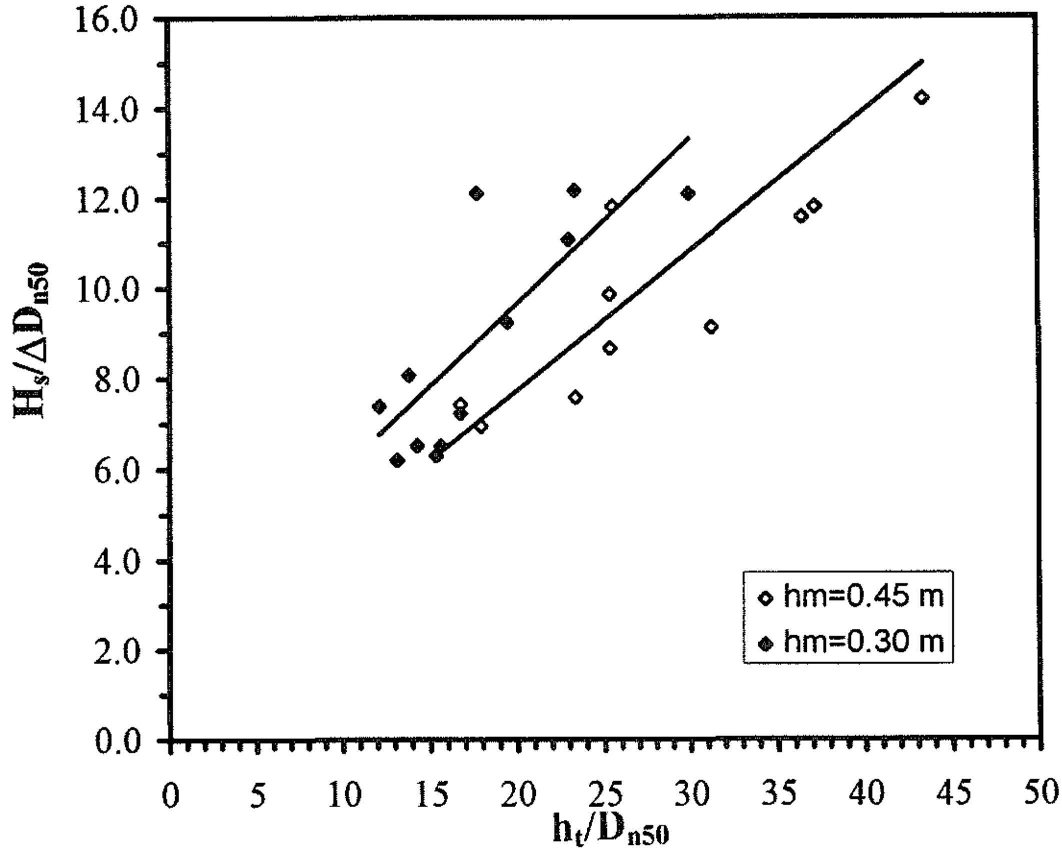

Figure 8.4 **Computations according to Rance & Warren with C_r**

8.4 Conclusion

The simple computational approach according to Rance & Warren with analytical equations described the processes involved with the stability of toe structures very well, because the results can be compared to the outcome of the measurements. However, it must not be forgotten that some factors had to be added to achieve this results.
In this case the velocities are deduced from the measured wave heights with the linear wave theory; if the distribution of the velocity could be determined with more accuracy, the results could be improved to simulate the actual processes better.

From the computations it can be deduced that the stability of the toe structure with a water depth h_m = 0.30 m in front of it, is higher than that with a water depth of 0.45 m see figure 8.3. The same results followed from the measurements see figure 7.9 and 7.14. The reason why this happened may be that the highest waves broke on the foreshore, so that lower wave forces resulted on the structure.

For a designer it is important to take the influence of h_m into account, when he designs according the suggested design formula of Gerding (1993). But how the effect of this should be dealt with in a design, is not clear yet; more computations and experimental research are necessary to investigate the influence of h_m and how to include this influence in design formulae.

9 Other parameters

In the present test series a few parameters were not taken into account for practical reasons.
Firstly the shape of the foreshore was not varied. The shape of the foreshore is of influence on the stability of the toe structure, because the foreshore influences the breaking point of the waves. It is recommended to investigate the influence of the foreshore on the toe stability.
The shape of the breakwater itself is another parameter that was not considered here. Especially the steepness of slope is supposed to have an influence on the damage to the toe structure. A steeper slope will probably lead to more damage than a less steep slope, due to the deeper run-down of the waves. However, a fact is that only few shapes are normally used in breakwater construction. Slopes with $\cot\alpha$ 2 or 1.5 are most common, because the steeper the slope the less volume of material is needed. So varying the slope of the breakwater is only interesting for theoretical reasons.
The last parameter that should be better investigated is the reflection. When only the incoming wave is considered to cause the occuring damage, the extra part of the wave height, the reflected part is hidden in the results. This reflection is of influence on the stability of the toe structure, because it leads to larger loads on the toe structure.
In the present study the reflection increased with larger water depths, what indicates that there is a dependence between those parameters.
It is recommended to investigate the influence of the parameters disregarded in the present study on toe stability.

10 Conclusions and recommendations

1. The influence of the relative density Δ was reproduced in the right way in the formula (10.1) of Gerding (1993), because different stone mass densities gave similar results for $H_s/\Delta D_{n50}$ as a function of h_t/D_{n50}.

$$\frac{H_s}{\Delta D_{n50}} = (0.24 \frac{h_t}{D_{n50}} + 1.6) N_{od}^{0.15} \tag{10.1}$$

2. The design curve by Gerding (10.1) can be used for the design of toe structures. In the present study the same trend is found but the values from the present study show a higher stability of the structure than with the suggested relation of Gerding, which is thus more conservative.
   The relation is empirically determined, so it can only be used in the tested range: $0.4 < h_t/h_m < 0.9$
   $3 < h_t/D_{n50} < 40$

   The damage levels can be classified as:
   $N_{od} = 0.5$ start of damage, used as fixed level in the present study
   $N_{od} = 2$ acceptable damage, design criterion of Gerding
   $N_{od} = 4$ unacceptable damage

3. The parameter of the local water depth in front of the toe structure, h_m, had still influence on the relation found between $H_s/\Delta D_{n50}$ and h_t/D_{n50}; this followed both from the tests and the computations. Because this parameter is not mentioned in the formula, it is risky to use the design curve for all h_m. The designer must not forget to take the influence of h_m and its tested range into account. The computations must be improved and more experiments are needed to enlarge the knowledge of the influence of h_m and to simulate the measurements more accurate.

4. It is recommended to perform further research into the influence on toe stability of the shape of the foreshore; a steeper foreshore may cause more damage to the toe stucture because the higher waves will break closer to the structure.

5. Further, it is recommended to take the influence of the reflection on toe stability into account, because up to now only the incoming wave height, so without the reflected component was considered as load. When the reflection is added to the wave height, a larger force will result as load on the toe structure and the coefficients in the relation between $H_s/\Delta D_{n50}$ and h_t/D_{n50} will change.

6. Between the present study and the research of Gerding large differences have been found. The damage estimated was on the avarage two times smaller than the damage Gerding had determined. The reason why this happened is still unknown.
   It is therefore recommended to perform exactly the same tests in the two wave flumes the "Schelde" flume at Delft Hydraulics, where Gerding performed his test, and the wave flume of the Laboratory of Fluid Mechanics of the Faculty of Civil Engineering of the Delft University of Technology, where the present tests were performed. This should be done by one and the same person to exclude misinterpretations.

7. The last recommendation is to determine the velocity distribution of the water depth in front of the toe structure and also to determine the development of damage more precisely to get more insight in the processes involved with the stability of toe structures. With a better description of the velocity field, the computations for the stability will become more precise.

References

d'Angremond, K.(1994)
Breakwater design, lecture notes F5, Faculty of Civil Engineering,
Delft University of Technology

Battjes, J.A.(1974)
Computation of set-up, longshore currents, run-up and overtopping due to wind-generated waves. Comm. on Hydraulics, Dept. of Civil Eng.
Delft University of Technology, Report 74-2

Brebner, A. and Donnelly, P.(1962)
Laboratory study of rubble mound foundations for vertical breakwaters.
Engineer Report No. 23, Queen's University Kingston, Ontario, Canada

Burger, G.(1995)
Stabiliteit golfbrekers met lage kruin.
Msc Thesis, Faculty of Civil Engineering, Delft University of Technology.

CIAD, Project group breakwaters (1985)
Computer aided evaluation of the reliability of a breakwater design.
Zoetermeer, The Netherlands

CUR/CIRIA Manual (1991)
Manual on the use of rock in coastal and shoreline engineering.
CUR report 154/CIRIA, Gouda, The Netherlands.
CIRIA special publication 83, London, United Kingdom

Gerding, E.(1993)
Toe structure stability of rubble mound breakwaters.
Msc Thesis, Faculty of Civil Engineering, Delft University of Technology
Also: Delft Hydraulics report no. H 1874

Gravesen, H. and Sørensen, T.(1977)
Stability of rubble mound breakwaters. Proc. 24th Int. Navigation Congress

Hasselman, K.(1973)
Measurements of wind-wave growth and swell decay during the Joint North Sea wave project (JONSWAP)

Postma, G.M.(1989)
Wave reflection from rock slopes under random wave attack.
Msc Thesis, Delft University of Technology, Faculty of Civil Engineering

Schiereck, G.J.(1992)
Introduction to bed, bank, shore protection, engineering the interface of soil and water. Lecture notes F4, Faculty of Civil Engineering, Delft University of Technology

Schiereck, G.J. a.o.(1995)
Stability of rock on beaches, Proc. 24th ICCE Kobe, Japan, Oct 1994, Vol.2

Seelig, W.N.(1983)
Wave reflection from coastal structures.
Proc. Conf. Coastal Structures '83. ASCE, Arlington

SPM,(1984)
Shore Protection Manual. Coastal Engineering Research Centre.
US Army Corps of Engineers.

Van der Meer, J.W.(1988a)
Rock slopes and gravel beaches under wave attack.
Doctoral thesis. Delft University of Technology.
Also: Delft Hydraulics Communication No.396.

Van der Meer, J.W.(1993)
Conceptual design of rubble mound breakwaters
Delft Hydraulics publication no. 483

Appendix A

Contents

A1 Elaboration of data

The type of measuring file is dependent on the used program. In the Laboratory of Fluid Mechanics two programs are in use: DACON and DASY*Lab*. During some try-outs it became clear that the measuring files from DASY*Lab* couldn't function as input for the processing program AUKE/pc (which is used for typical wave-parameter processing). Therefore the older program DACON was used, which functioned very well. The output files were of the type test.log, where test is a chosen filename. For the conversion of .log-files to a legible form, there is a program called DACONVER. With this program the header can be erased and the file is ready to function as input for AUKE/pc. Here follows a short description of the elaboration in AUKE/pc. A file exists of two different parts: test.dat and test.seq. The .dat-file contains the measuring data and the .seq-file contains information about the format and scale of the .dat-file. The file from DACONVER has an output test.was; this file can be renamed to test.dat. The .seq-file must be made up by the user. The file test can now be analyzed by all AUKE-programs. The programs used are: SPECTRUM, FILTER, REFLEC and ASCII. The commando files are called *.pcf and the results are shown in *.out. The incoming wave heights were determined with REFLEC. The other programs were used to get graphs in EXCEL for wave energy density spectra.

A2a

Mass distribution curve: $D_{n50} = 9.8mm$ $\rho_s=2550\ kg/m^3$ gradation = 1.34

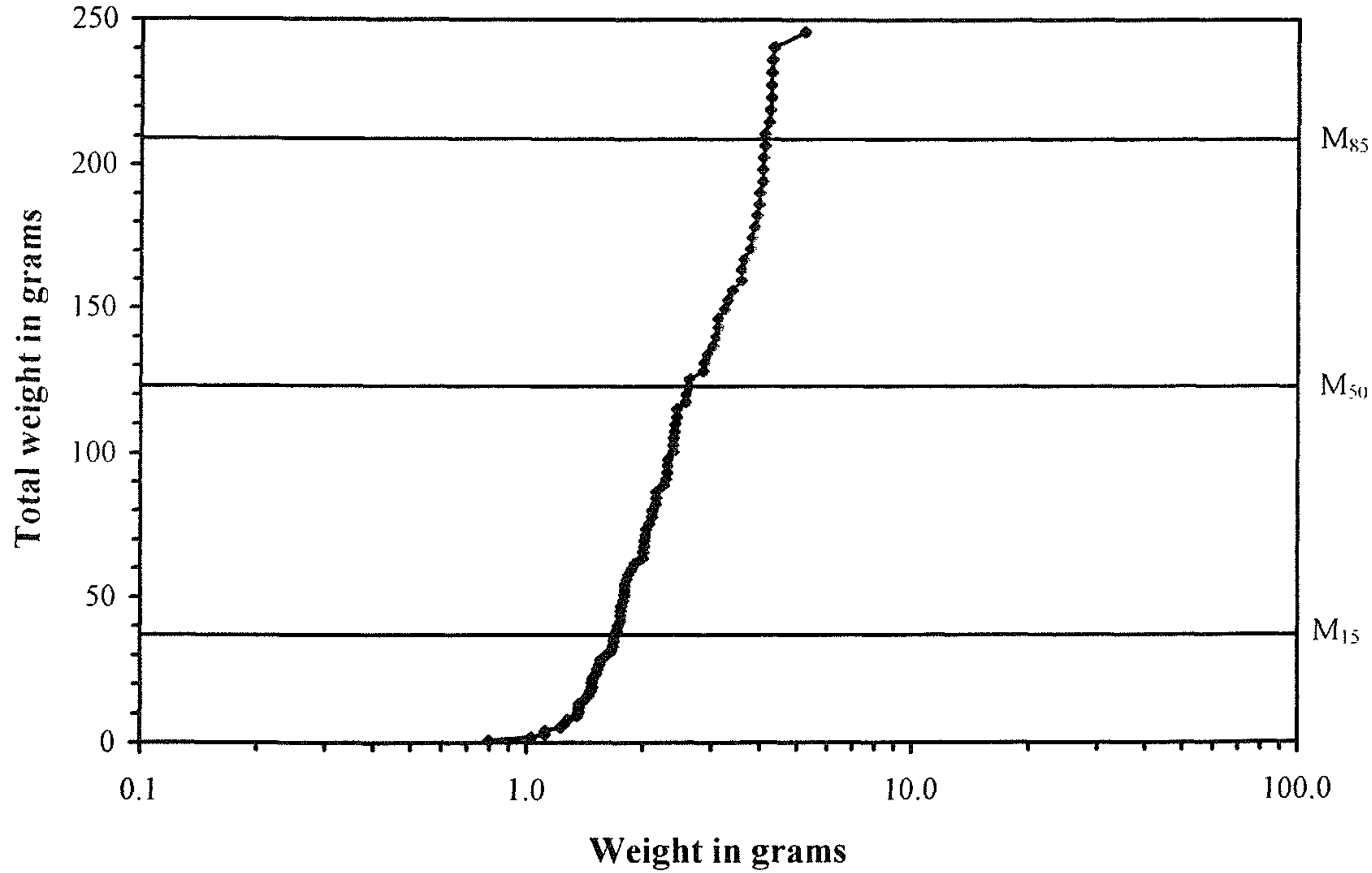

A2b

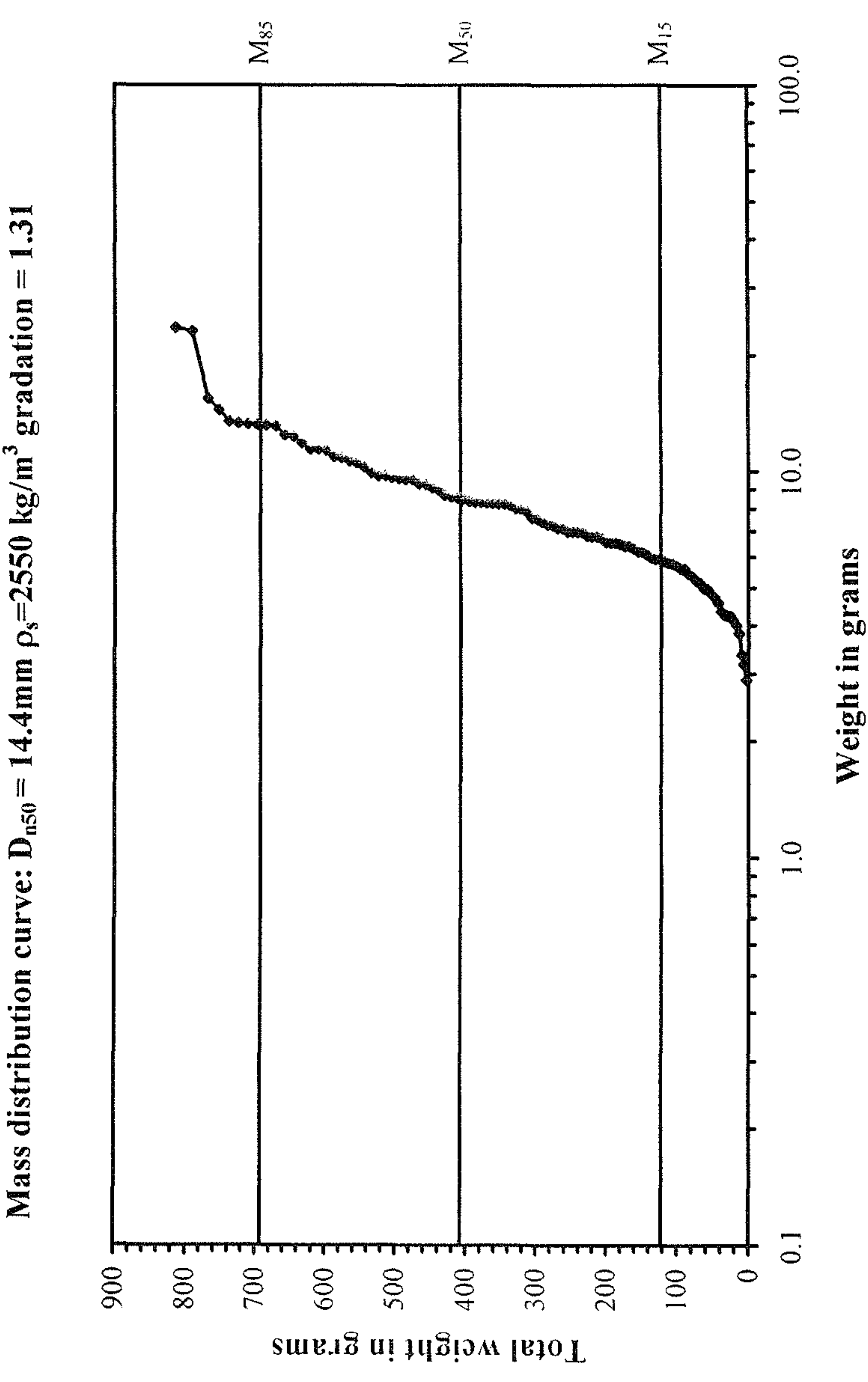

Mass distribution curve: D_{n50} = 14.4mm ρ_s=2550 kg/m^3 gradation = 1.31
M_{85}
M_{50}
M_{15}
900
800
700
600
500
400
300
200
100
0
Total weight in grams
0.1
1.0
10.0
100.0
Weight in grams

Mass distribution curve: Dn50 = 21.0mm ρs=2550 kg/m3 gradation = 1.26

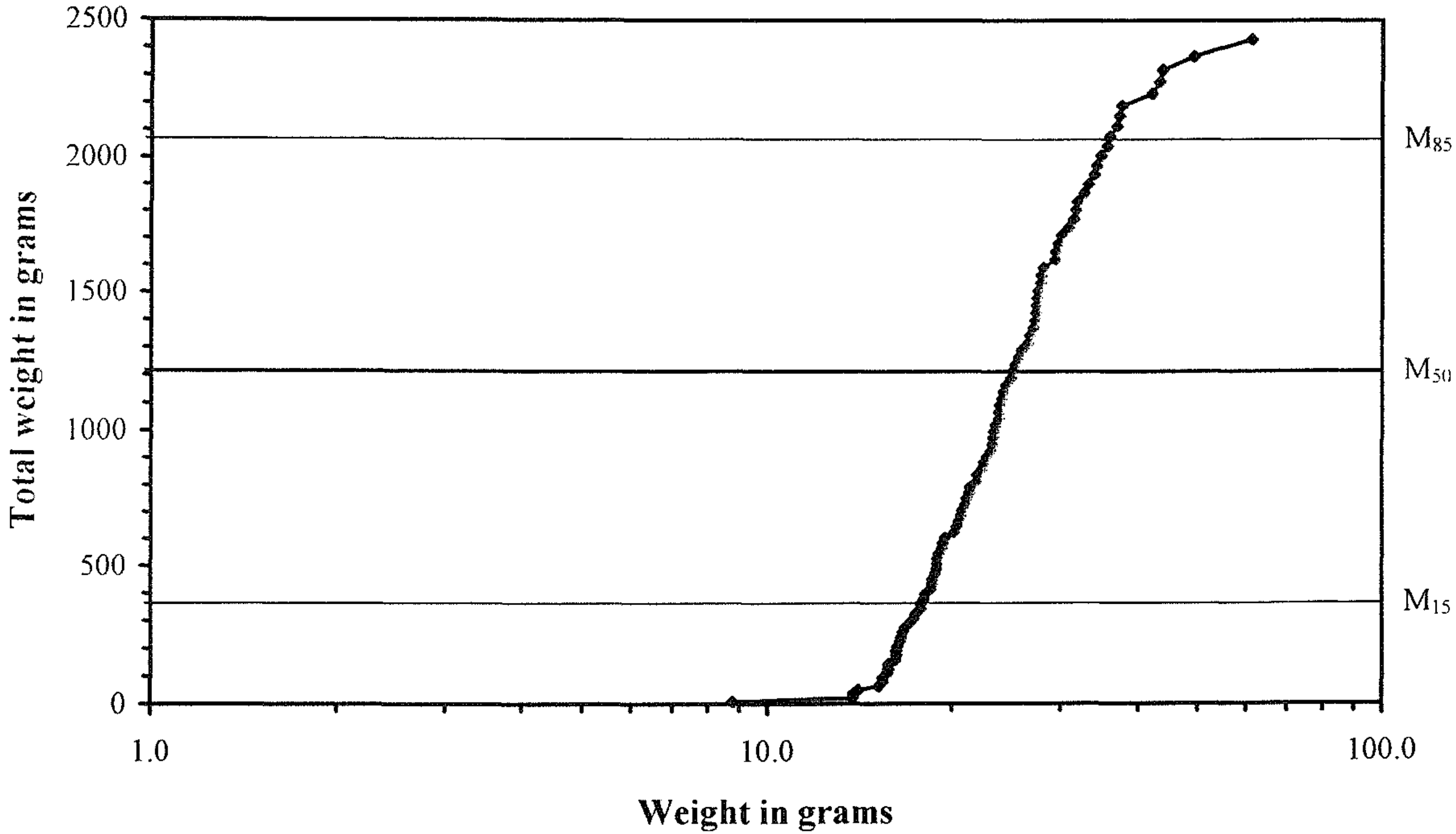

A2d

Mass distribution curve: Dn50 = 10.2mm ρs=2850 kg/m3 gradation = 1.40

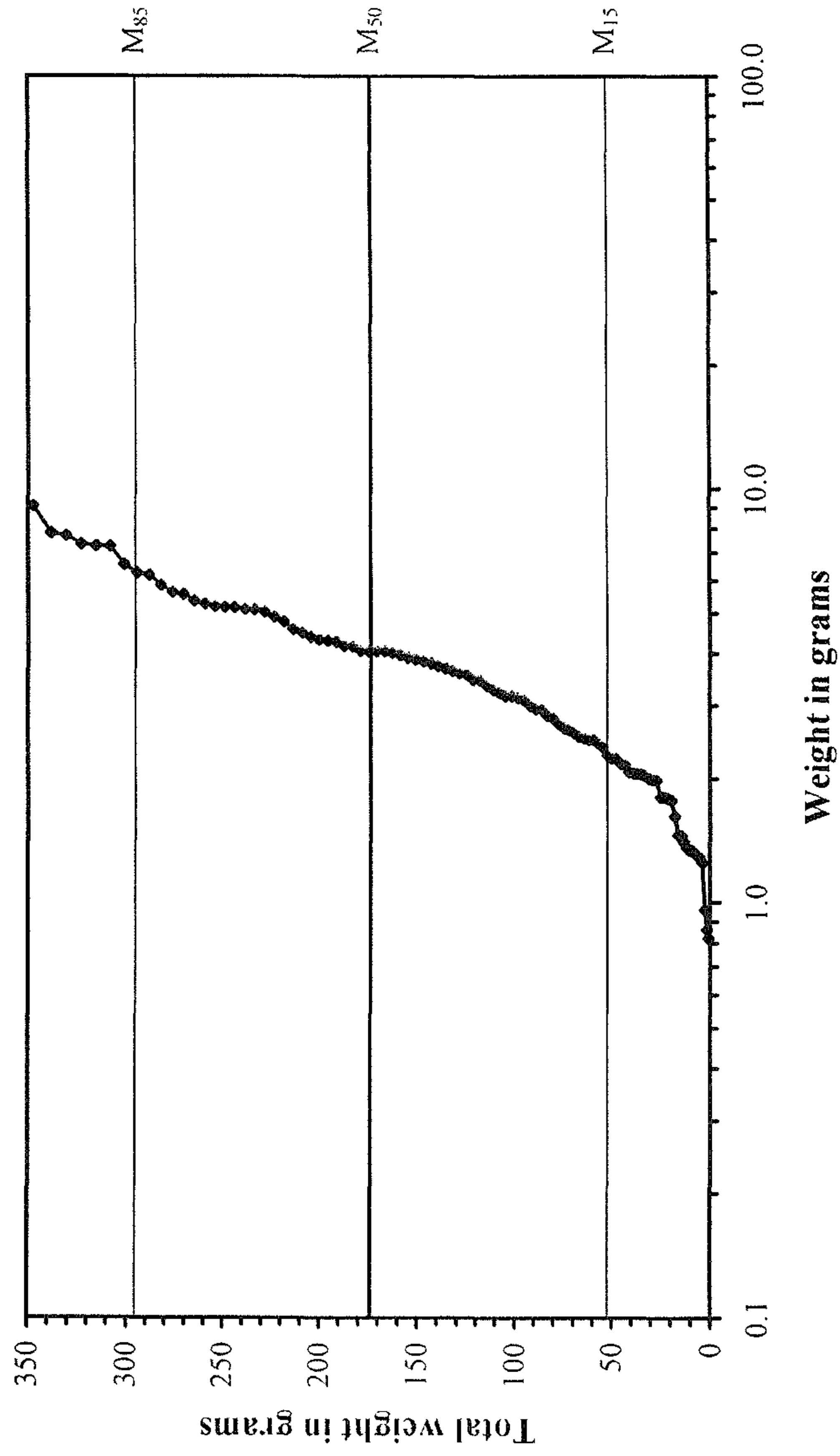

Mass distribution curve: Dn50 = 15.1mm ρs=2850 kg/m3 gradation = 1.20

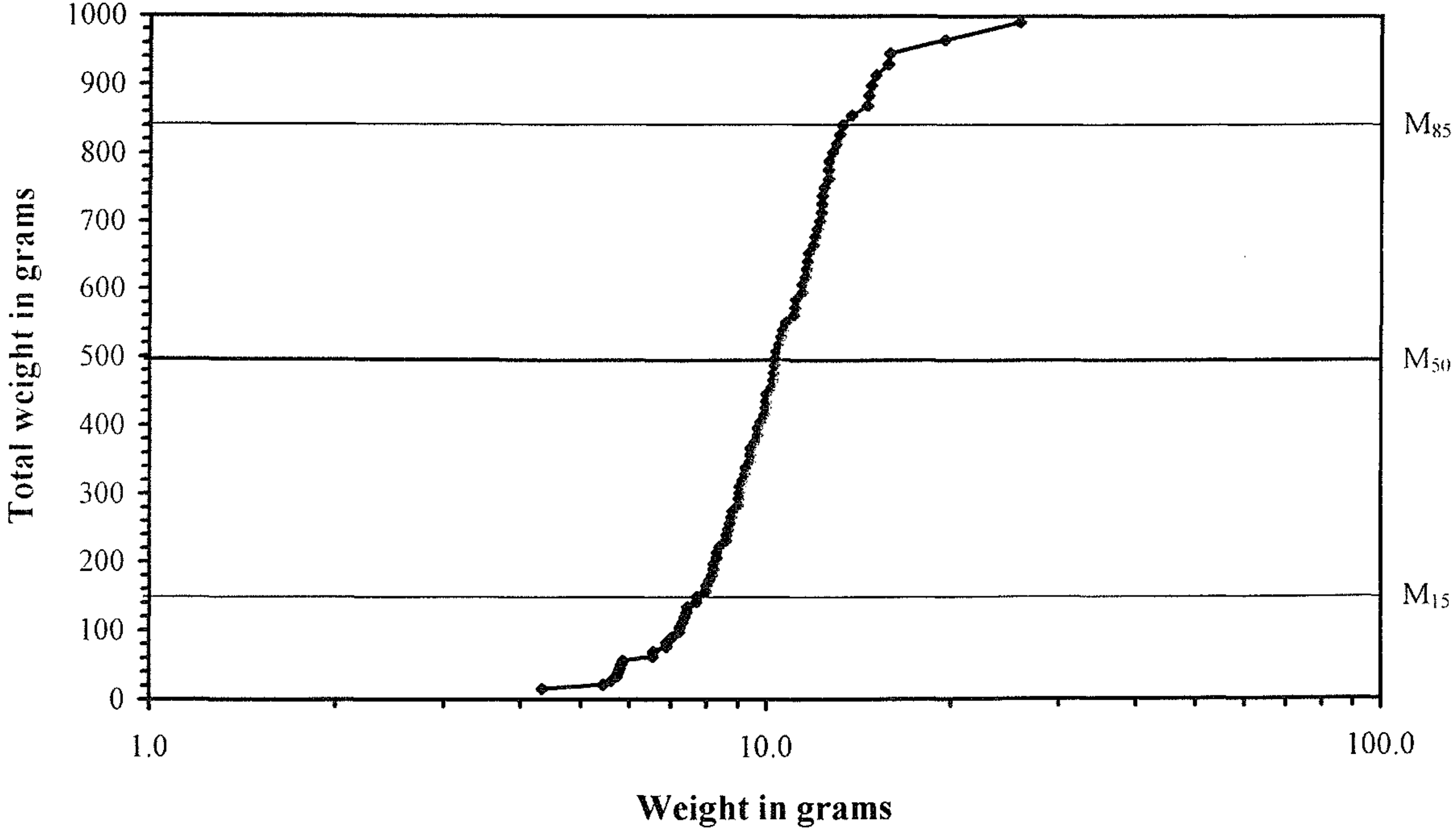

Mass distribution curve: D_{n50}= 23.1 mm ρ_s=1900 kg/m^3 gradation = 1.45

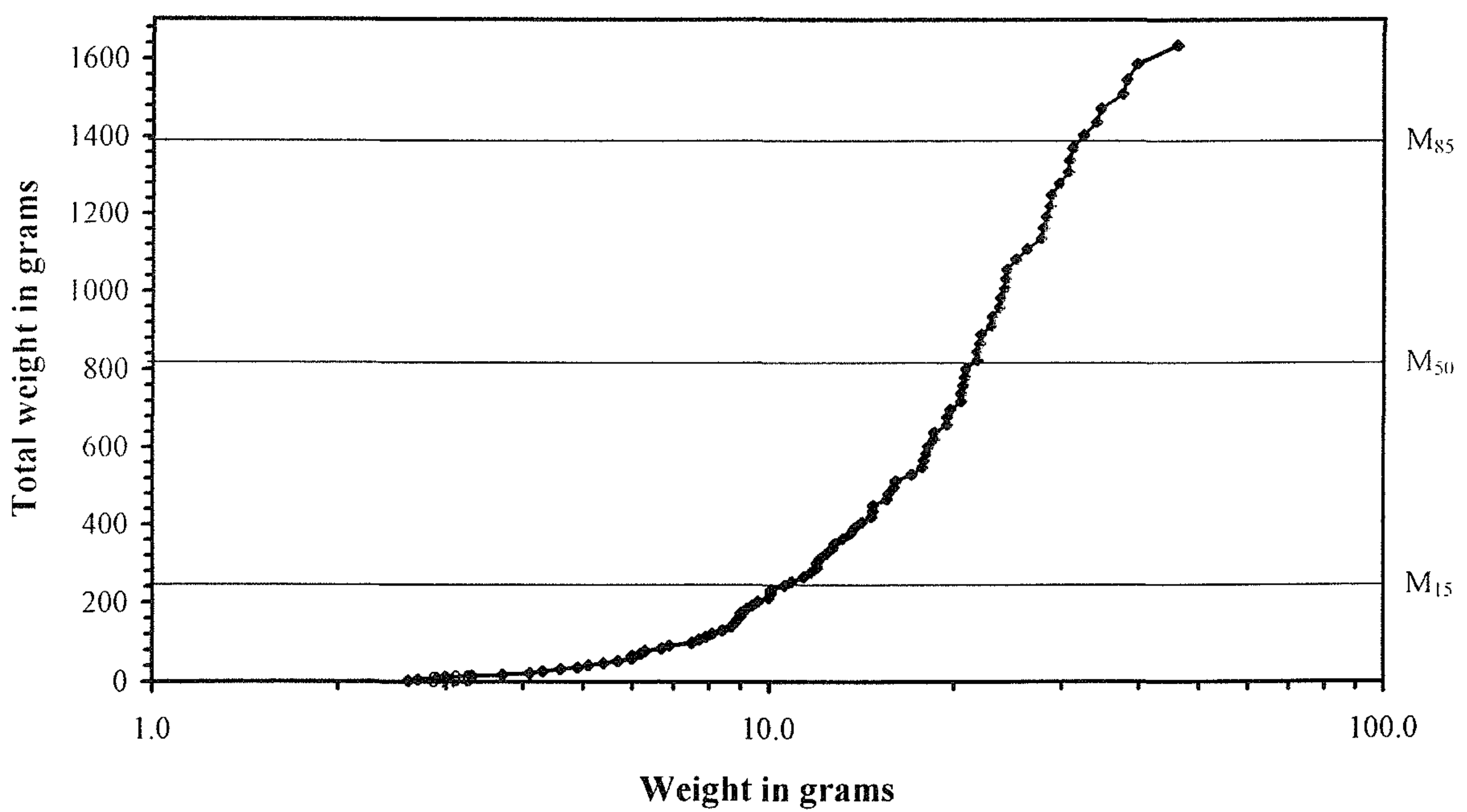

A3

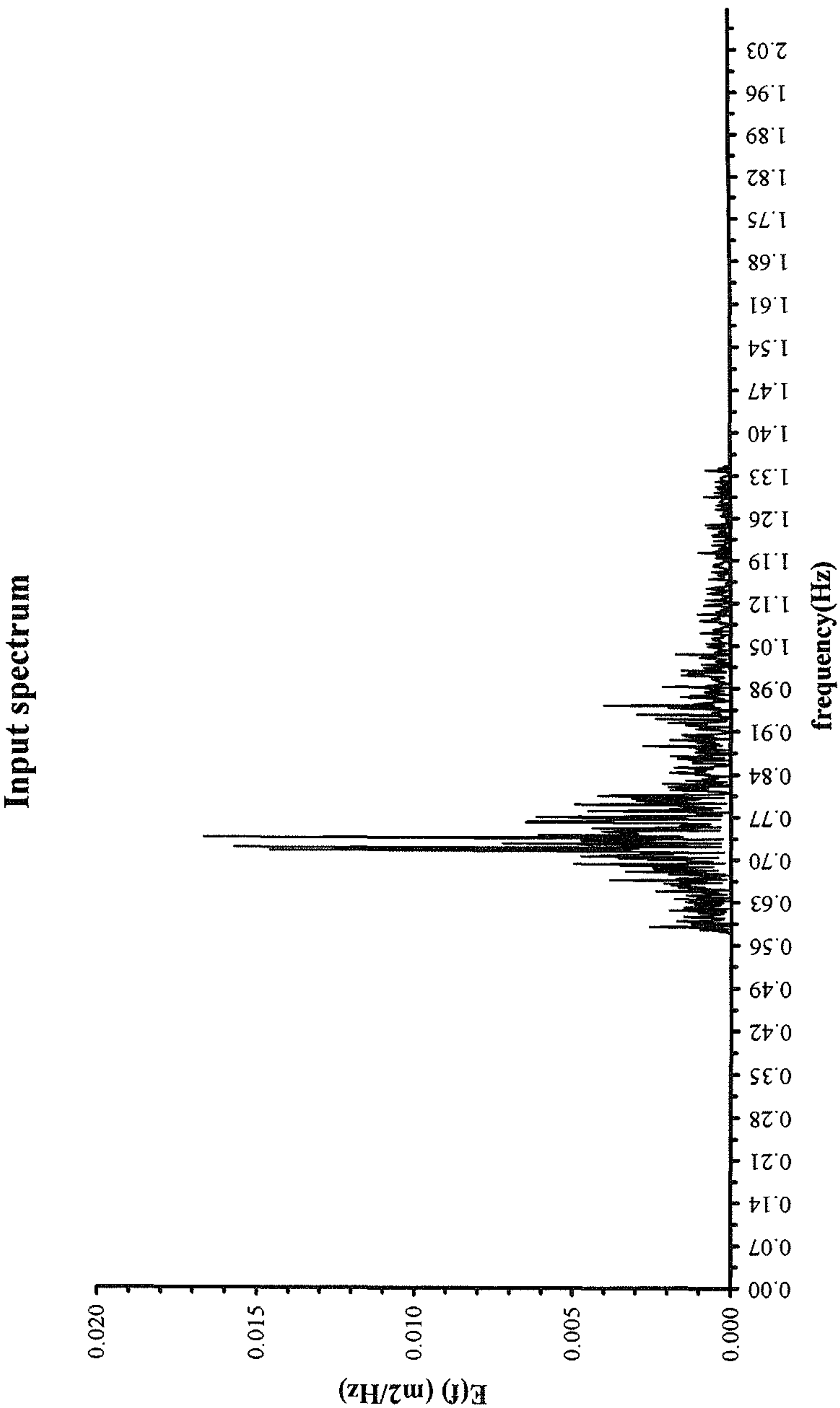
Input spectrum
frequency(Hz)
E(f) (m2/Hz)
0.000
0.005
0.010
0.015
0.020
0.00
0.07
0.14
0.21
0.28
0.35
0.42
0.49
0.56
0.63
0.70
0.77
0.84
0.91
0.98
1.05
1.12
1.19
1.26
1.33
1.40
1.47
1.54
1.61
1.68
1.75
1.82
1.89
1.96
2.03

A3

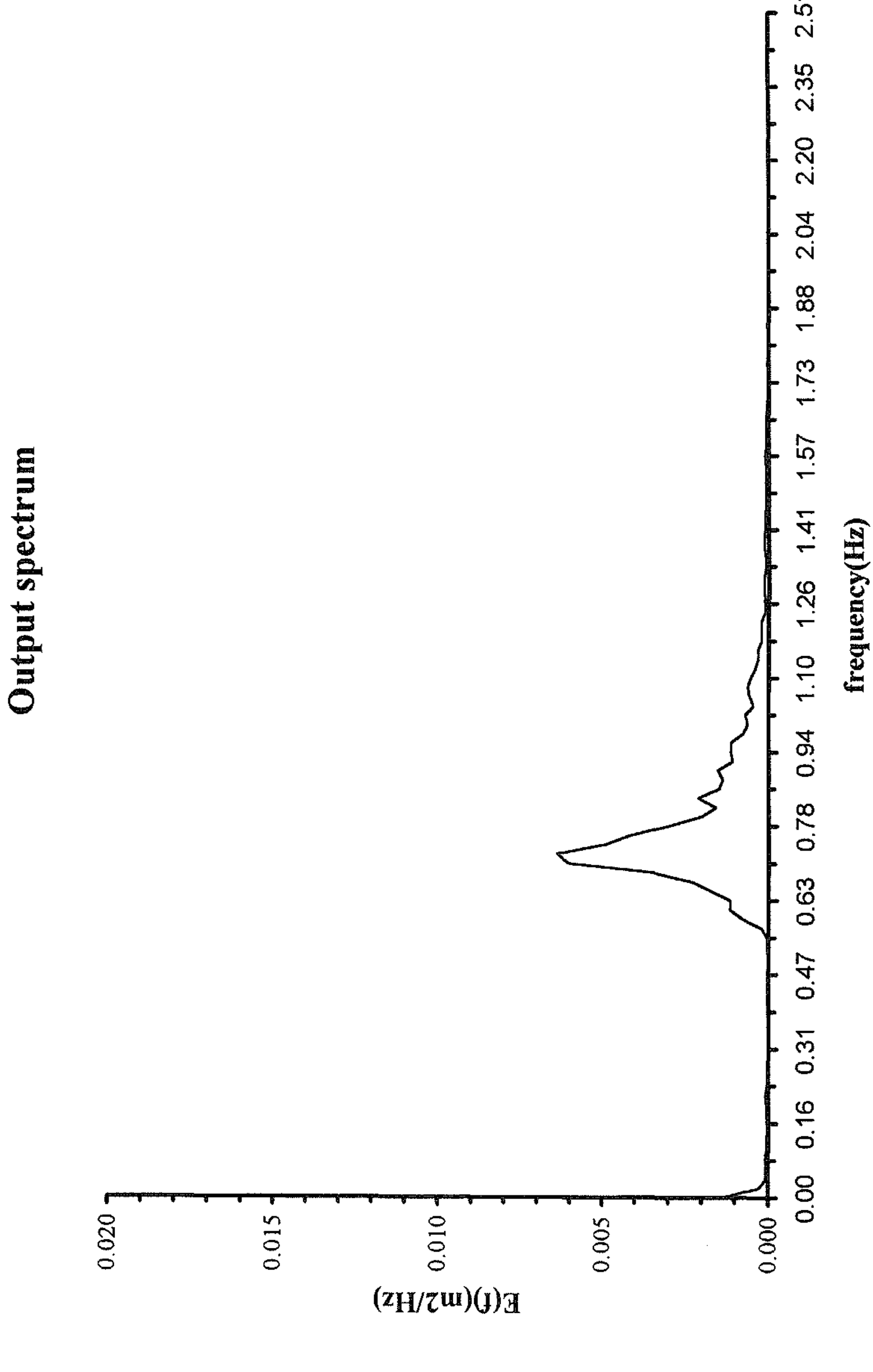

Output spectrum
E(f)(m2/Hz)
0.020
0.015
0.010
0.005
0.000
frequency(Hz)
0.00
0.16
0.31
0.47
0.63
0.78
0.94
1.10
1.26
1.41
1.57
1.73
1.88
2.04
2.20
2.35
2.51

A4 Photographs of tested materials


porfier
D_{n50} = 21.0 mm


basalt
D_{n50} = 15.1 mm


basalt
D_{n50} = 10.2 mm


brick
D_{n50} = 23.1 mm

A5 Photographs of breakwater cross section

A6 Photographs of damage results

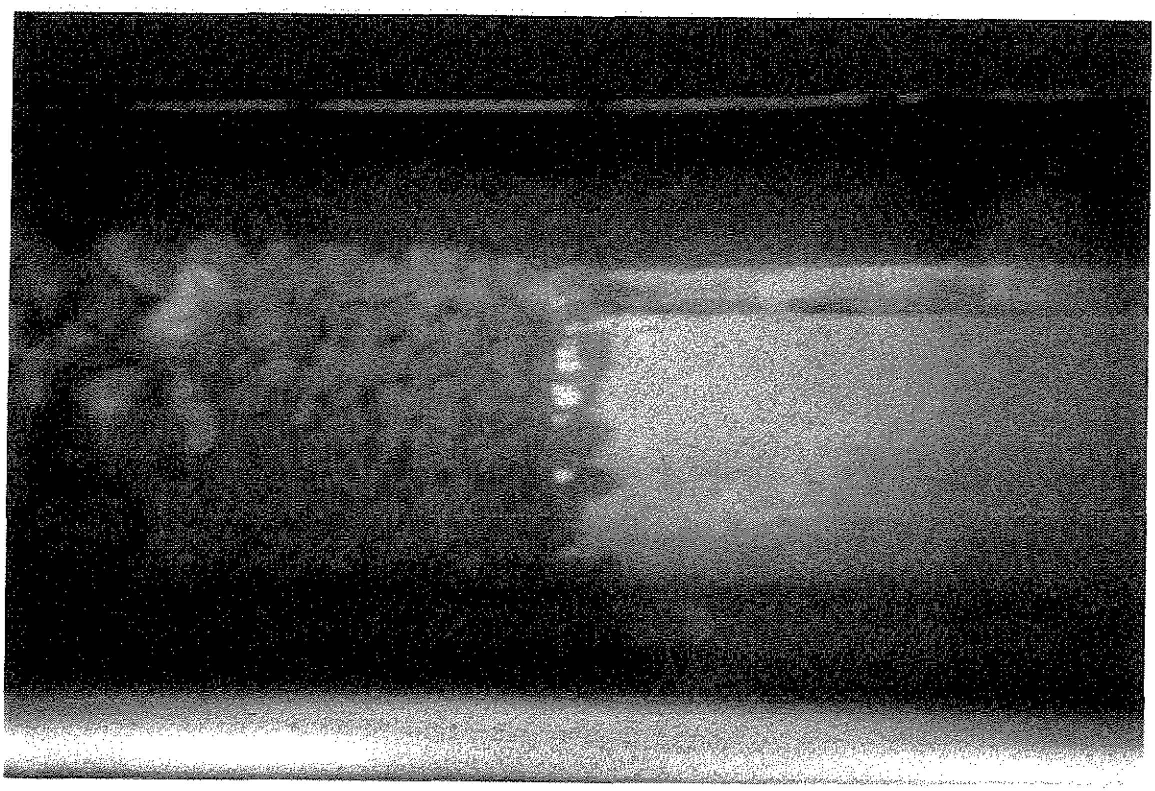

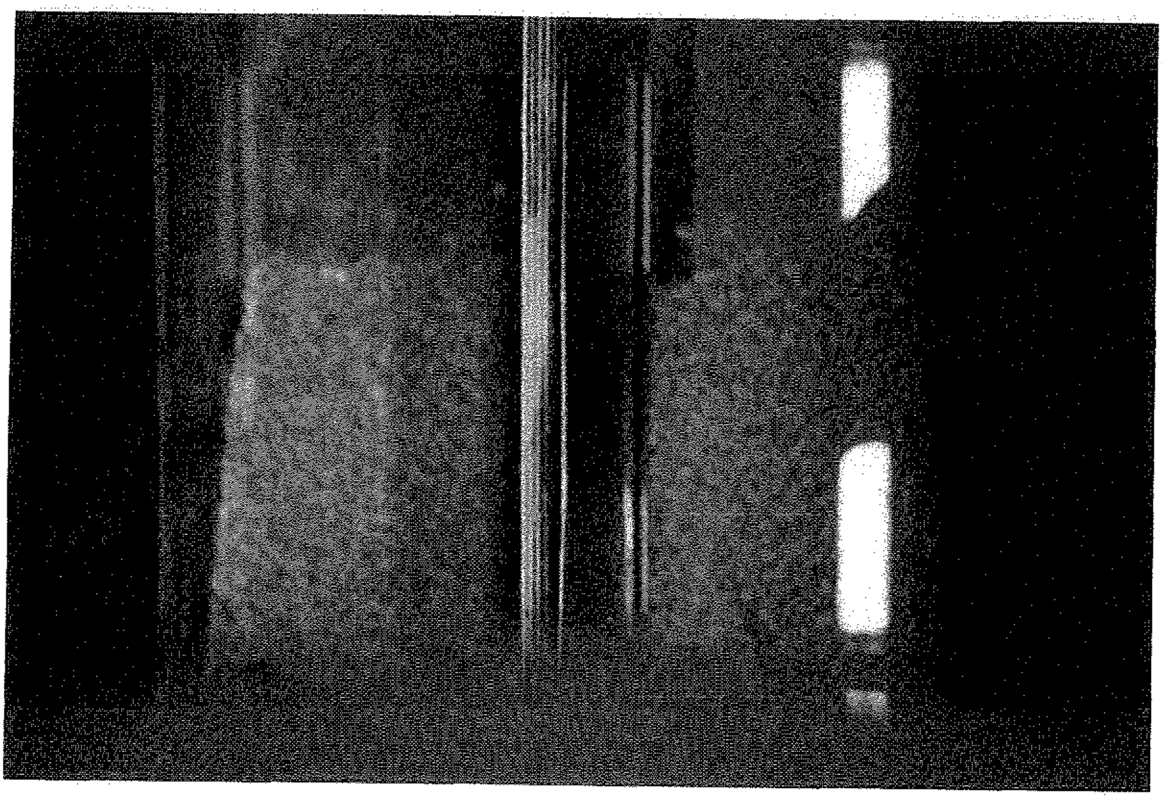

Appendix B

Contents

B1a

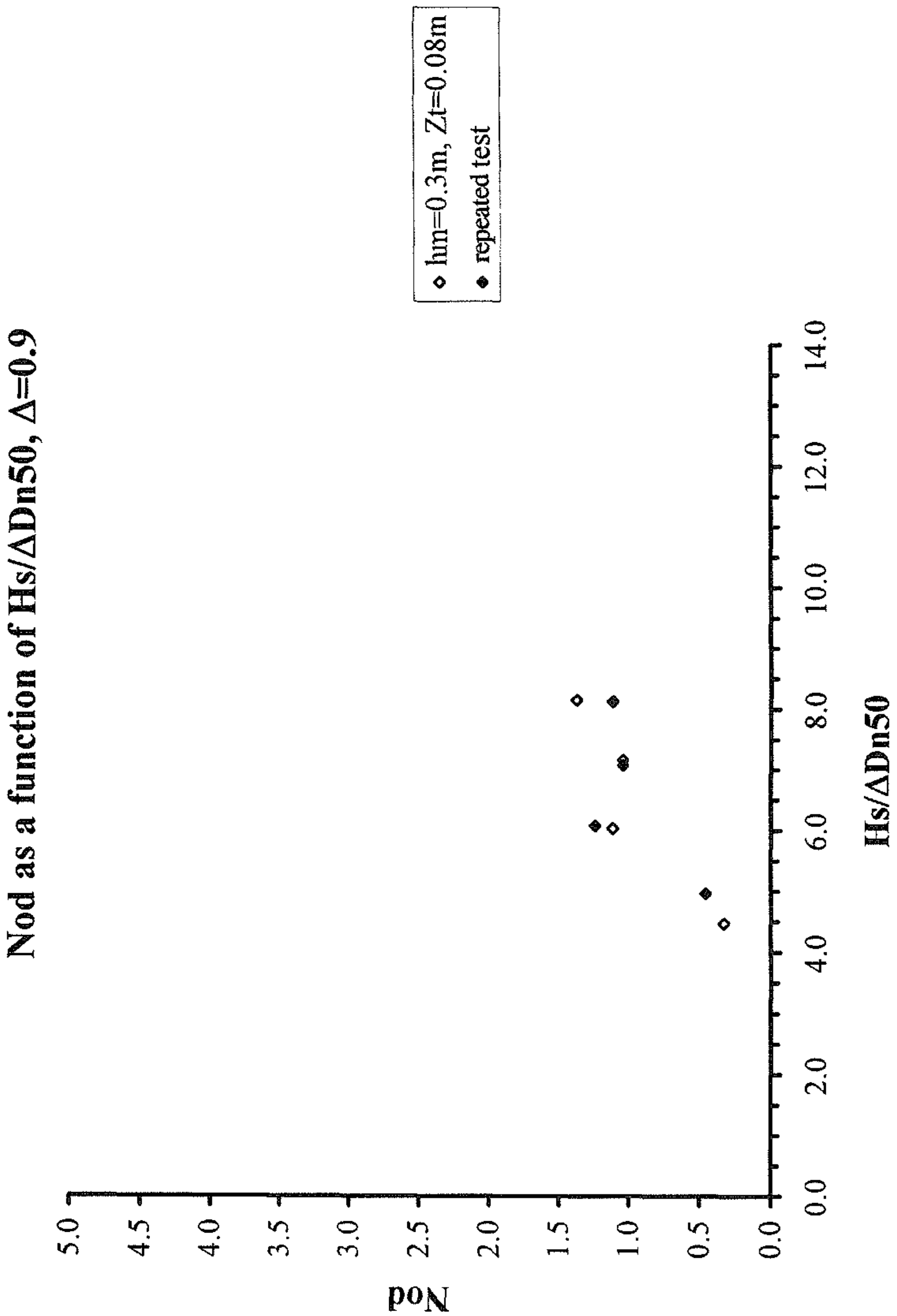

Nod as a function of Hs/ΔDn50, Δ=0.9
hm=0.3m, Zt=0.08m
repeated test
Nod
5.0
4.5
4.0
3.5
3.0
2.5
2.0
1.5
1.0
0.5
0.0
0.0
2.0
4.0
6.0
8.0
10.0
12.0
14.0
Hs/ΔDn50

B1b

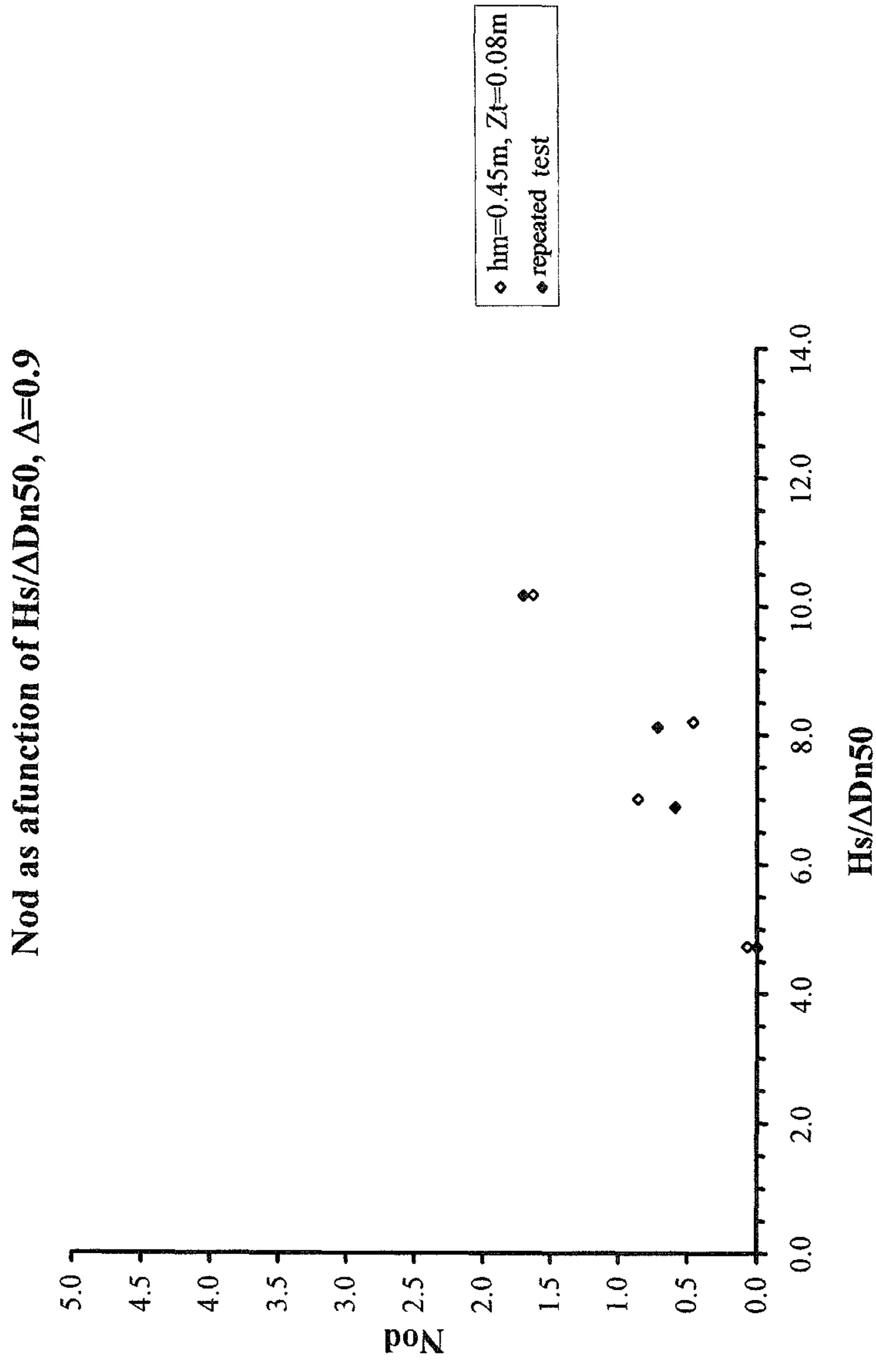

Nod as afunction of Hs/ΔDn50, Δ=0.9
hm=0.45m, Zt=0.08m
repeated test
Nod
5.0
4.5
4.0
3.5
3.0
2.5
2.0
1.5
1.0
0.5
0.0
0.0
2.0
4.0
6.0
8.0
10.0
12.0
14.0
Hs/ΔDn50

B1c

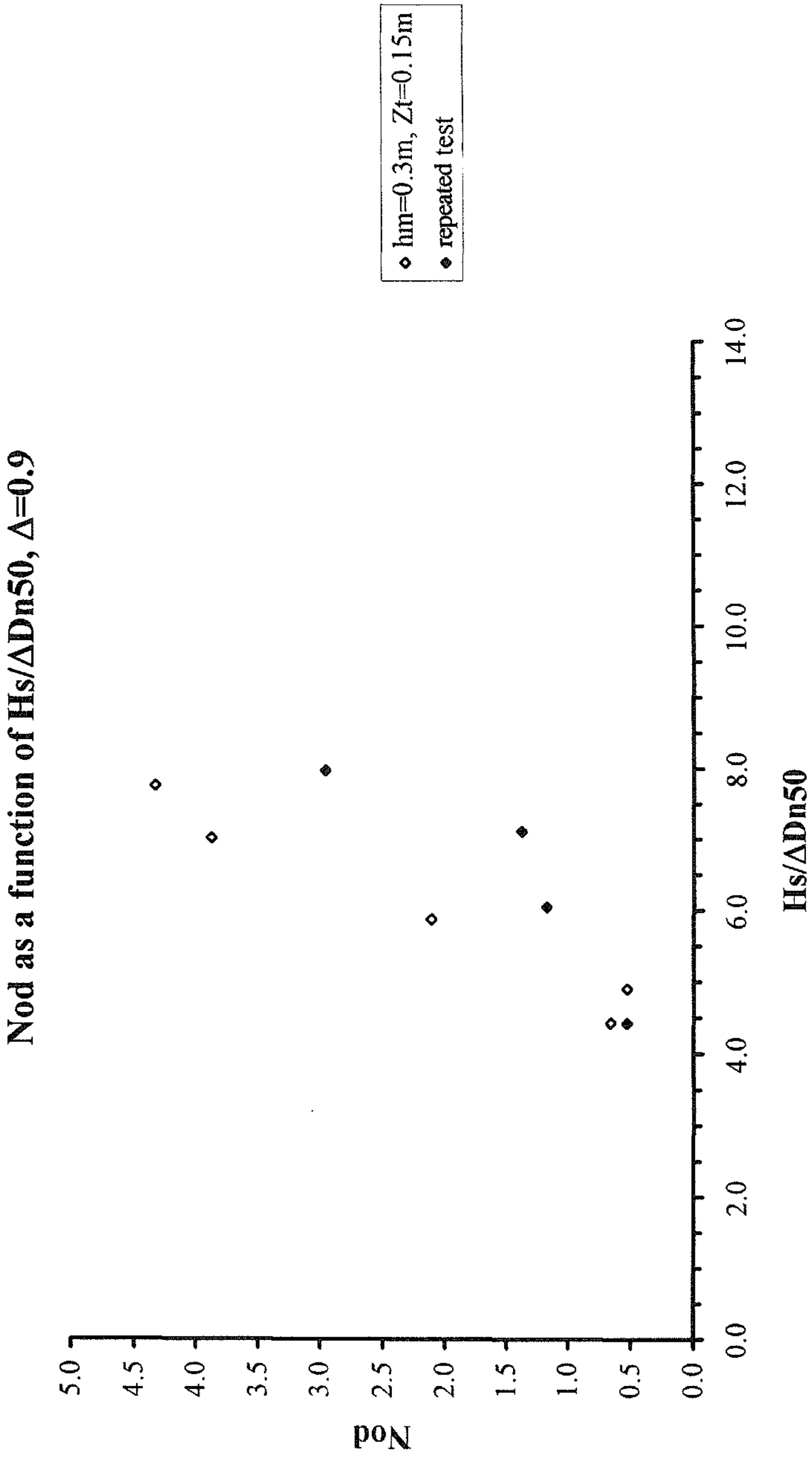

Nod as a function of Hs/ΔDn50, Δ=0.9
hm=0.3m, Zt=0.15m
repeated test
Nod
0.0
0.5
1.0
1.5
2.0
2.5
3.0
3.5
4.0
4.5
5.0
0.0
2.0
4.0
6.0
8.0
10.0
12.0
14.0
Hs/ΔDn50

Nod as afunction of Hs/ΔDn50, Δ=0.9

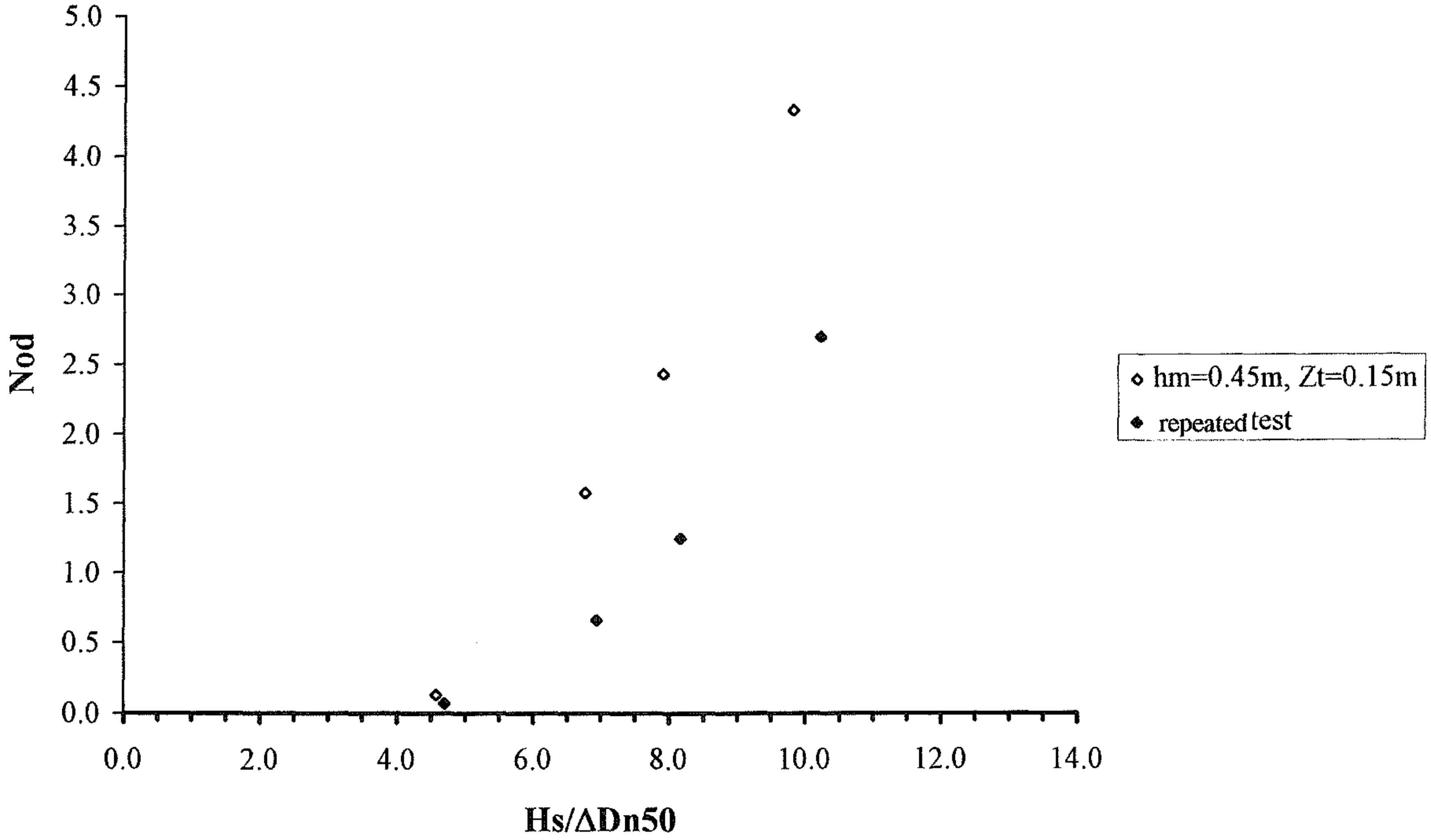

B1d

B2a

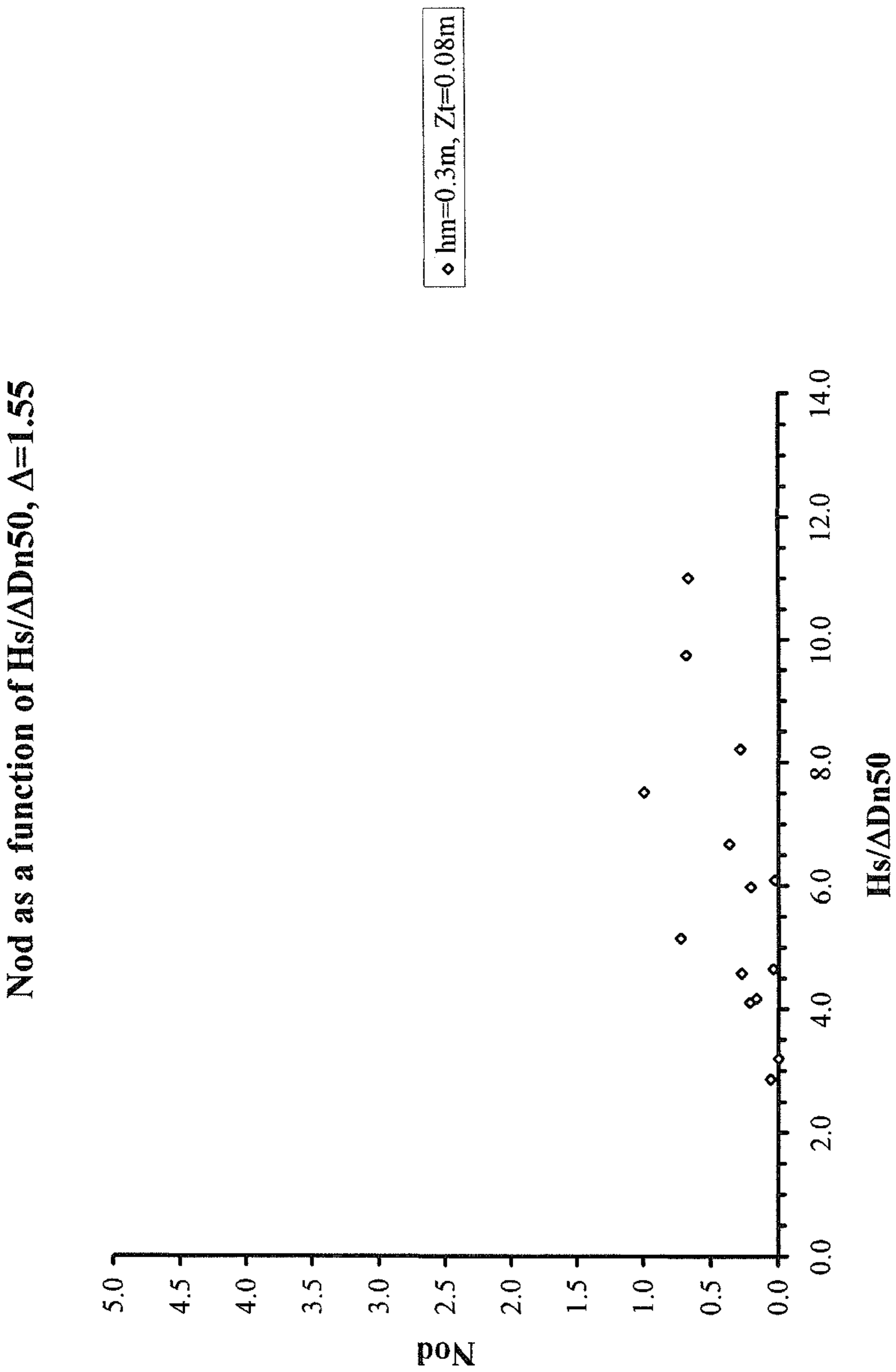
Nod as a function of Hs/ΔDn50, Δ=1.55
hm=0.3m, Zt=0.08m
Nod
5.0
4.5
4.0
3.5
3.0
2.5
2.0
1.5
1.0
0.5
0.0
0.0
2.0
4.0
6.0
8.0
10.0
12.0
14.0
Hs/ΔDn50

Nod as afunction of Hs/ΔDn50, Δ=1.55

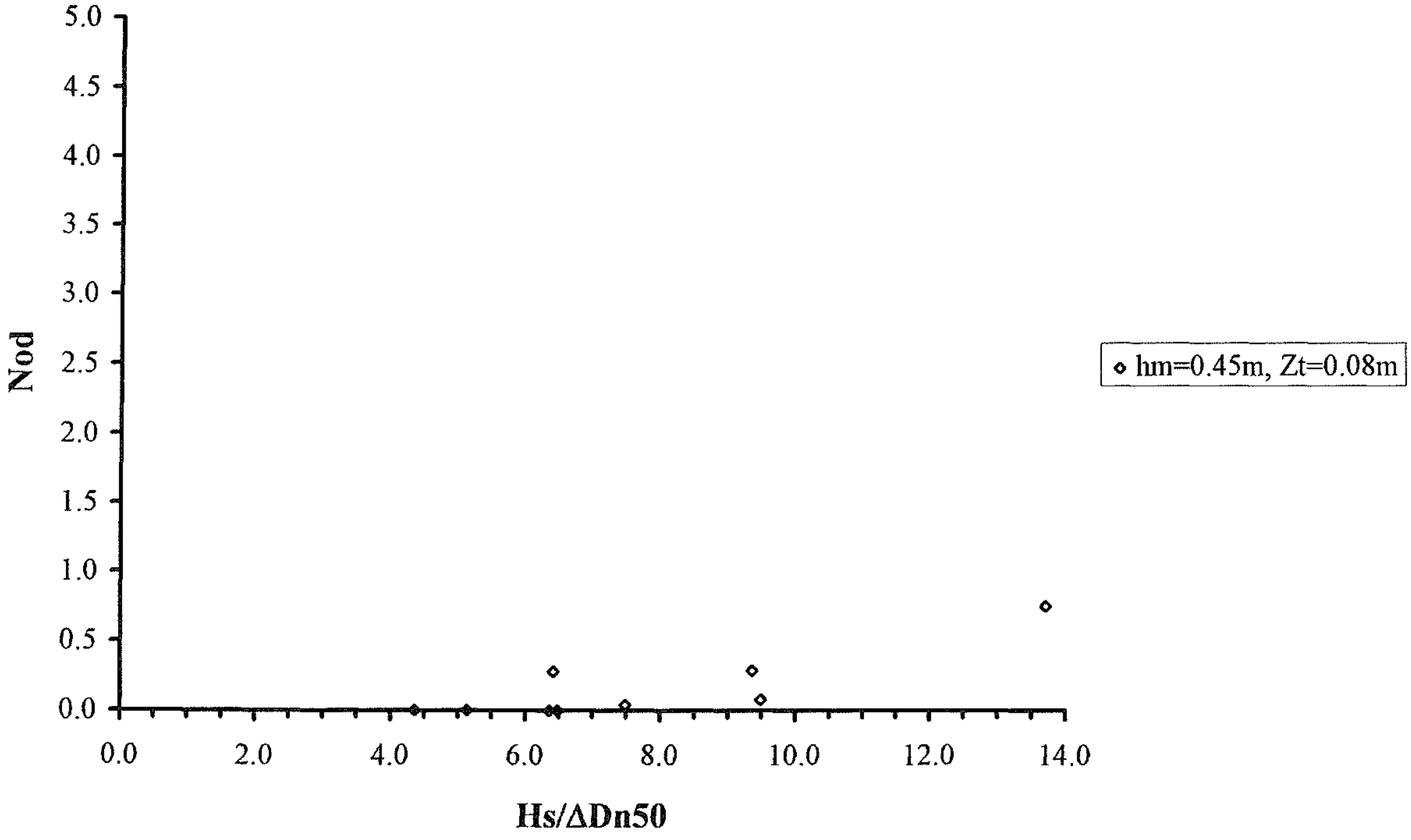

B2c

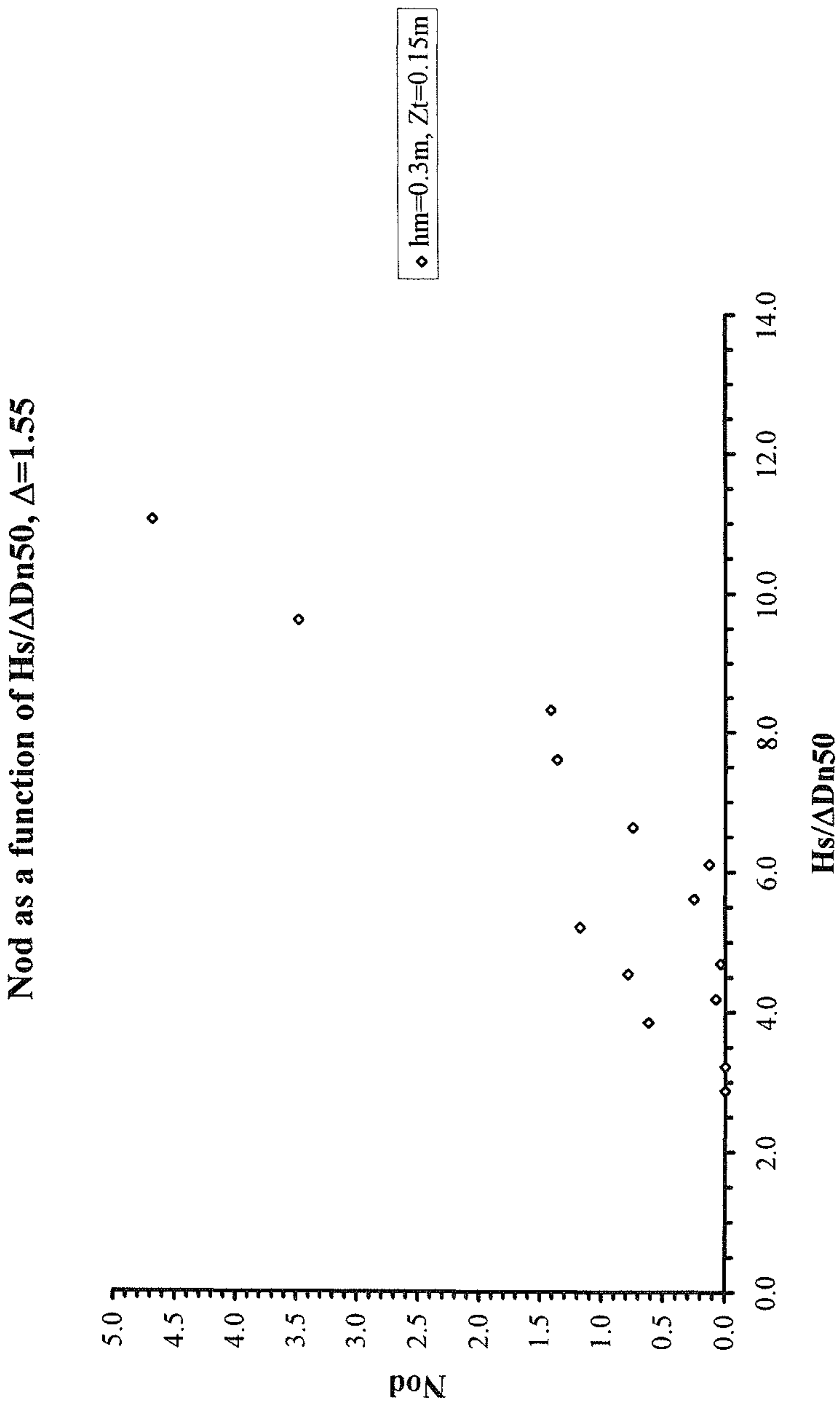
Nod as a function of Hs/ΔDn50, Δ=1.55
hm=0.3m, Zt=0.15m
Nod
Hs/ΔDn50
0.0
0.5
1.0
1.5
2.0
2.5
3.0
3.5
4.0
4.5
5.0
0.0
2.0
4.0
6.0
8.0
10.0
12.0
14.0

B2d

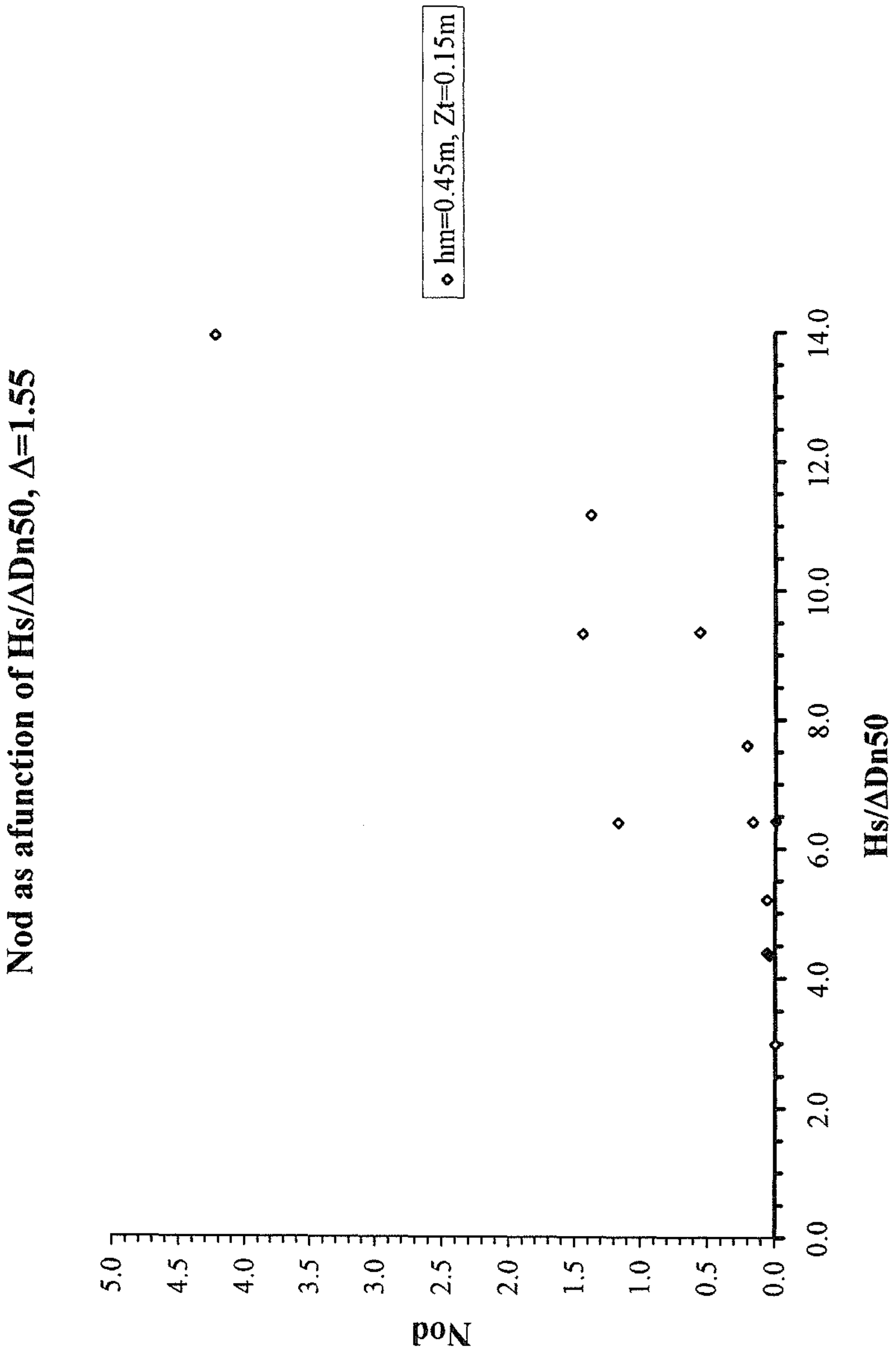

Nod as afunction of Hs/ΔDn50, Δ=1.55
hm=0.45m, Zt=0.15m
Nod
5.0
4.5
4.0
3.5
3.0
2.5
2.0
1.5
1.0
0.5
0.0
0.0
2.0
4.0
6.0
8.0
10.0
12.0
14.0
Hs/ΔDn50

B3a

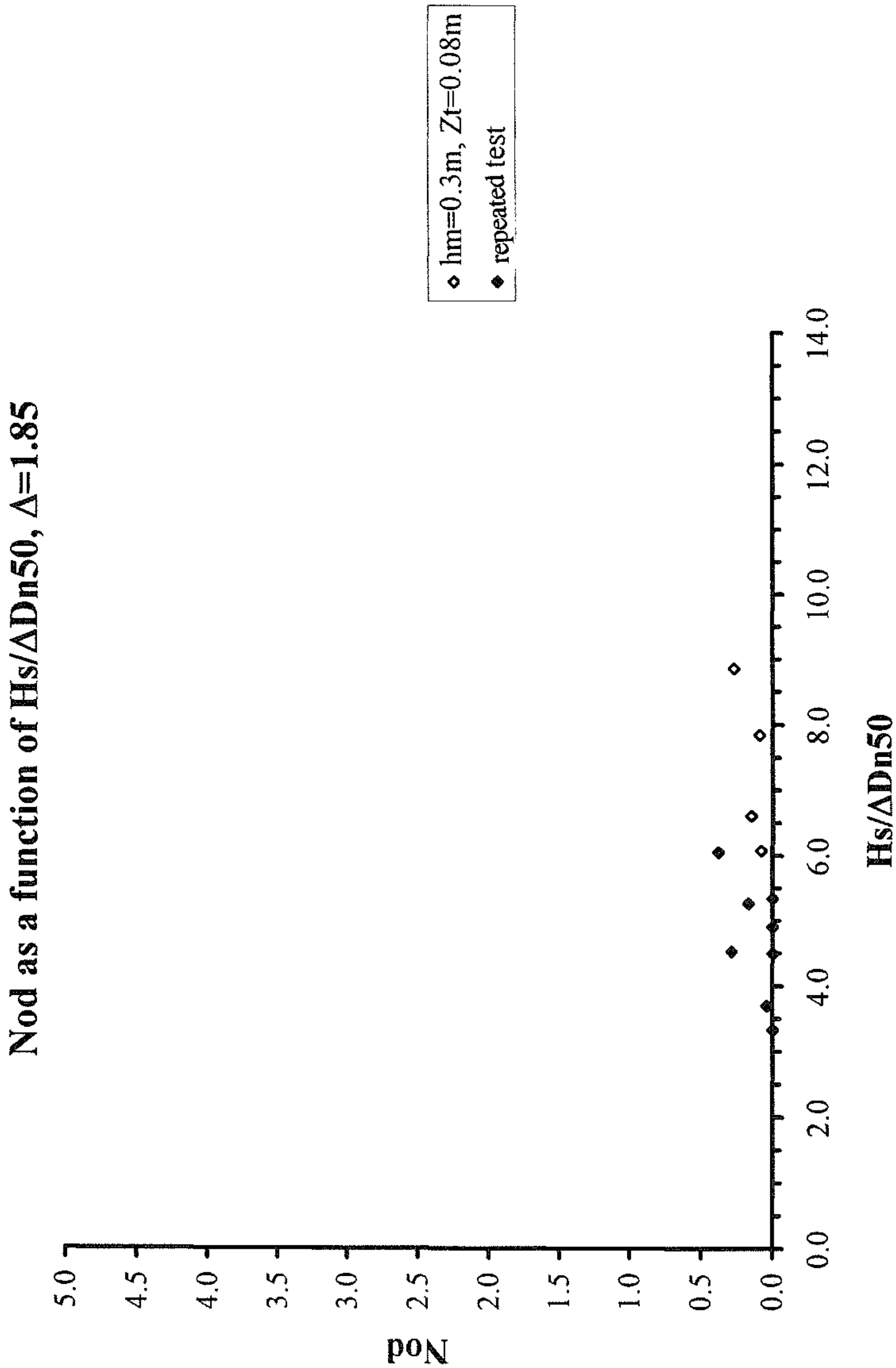
Nod as a function of Hs/ΔDn50, Δ=1.85
hm=0.3m, Zt=0.08m
repeated test
Nod
Hs/ΔDn50
0.0
0.5
1.0
1.5
2.0
2.5
3.0
3.5
4.0
4.5
5.0
0.0
2.0
4.0
6.0
8.0
10.0
12.0
14.0

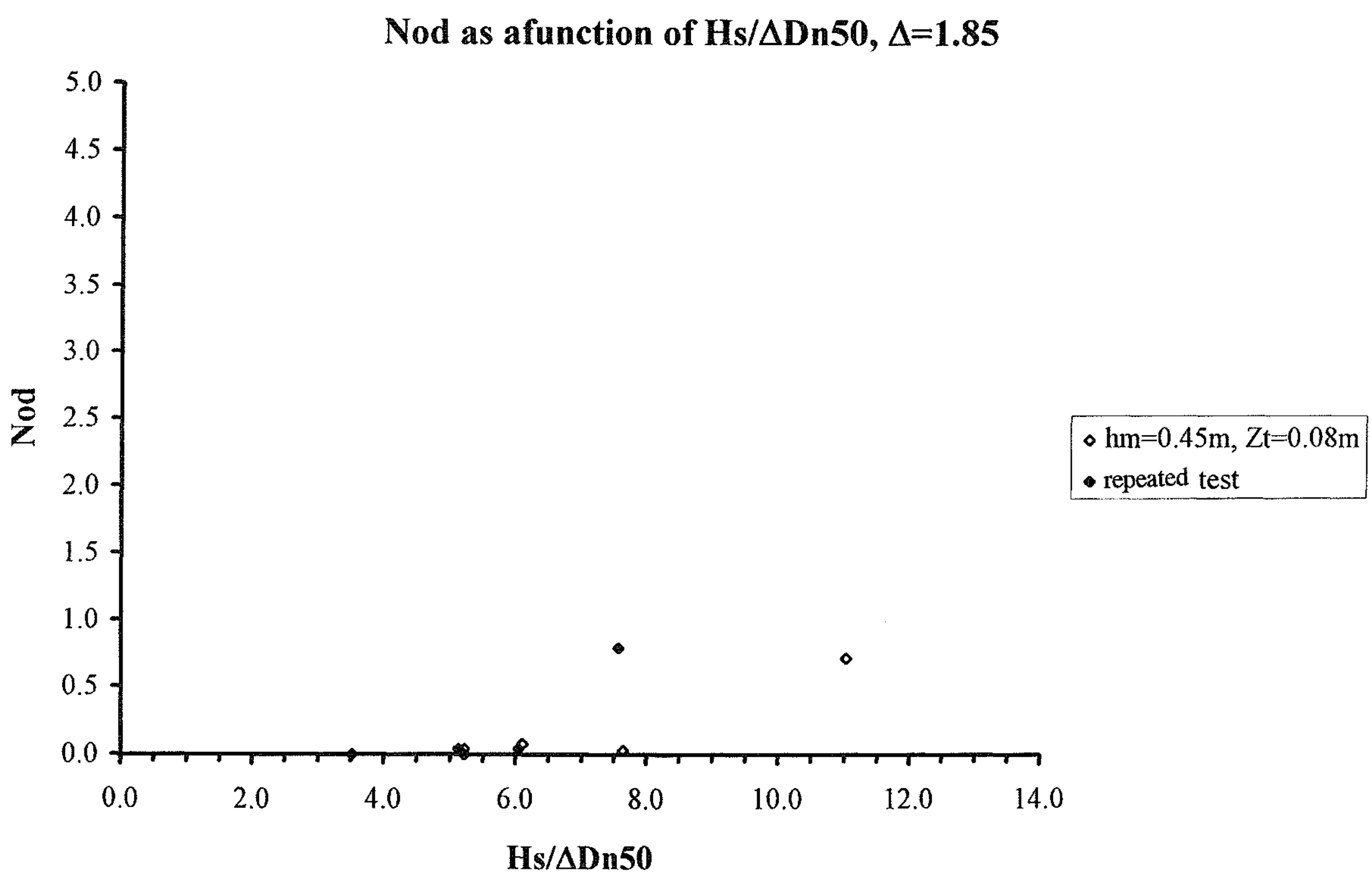
Nod as afunction of Hs/ΔDn50, Δ=1.85
Nod
5.0
4.5
4.0
3.5
3.0
2.5
2.0
1.5
1.0
0.5
0.0
0.0
2.0
4.0
6.0
8.0
10.0
12.0
14.0
Hs/ΔDn50
hm=0.45m, Zt=0.08m
repeated test

B3c

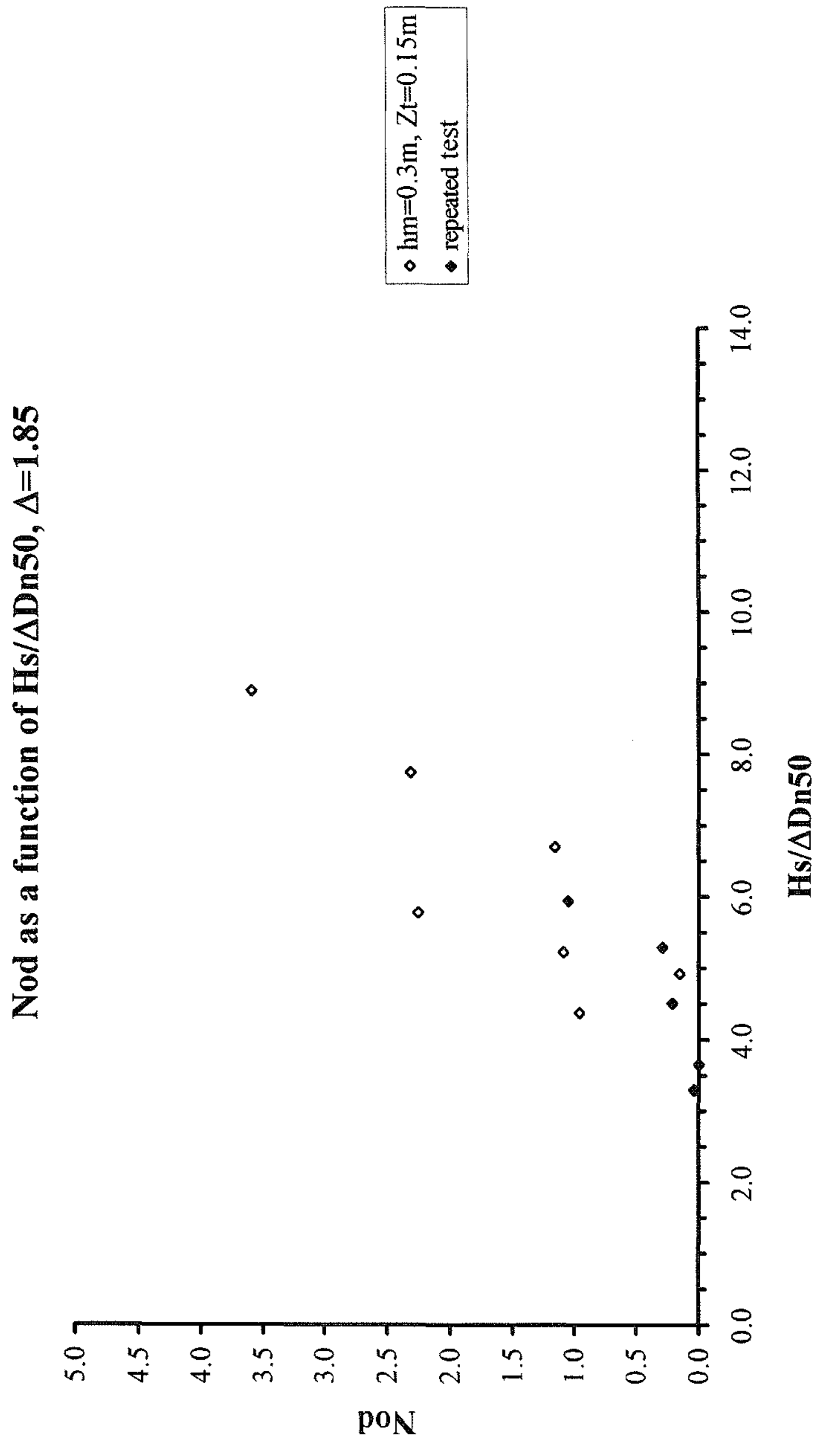

Nod as a function of Hs/ΔDn50, Δ=1.85
hm=0.3m, Zt=0.15m
repeated test
Nod
5.0
4.5
4.0
3.5
3.0
2.5
2.0
1.5
1.0
0.5
0.0
0.0
2.0
4.0
6.0
8.0
10.0
12.0
14.0
Hs/ΔDn50

B3d

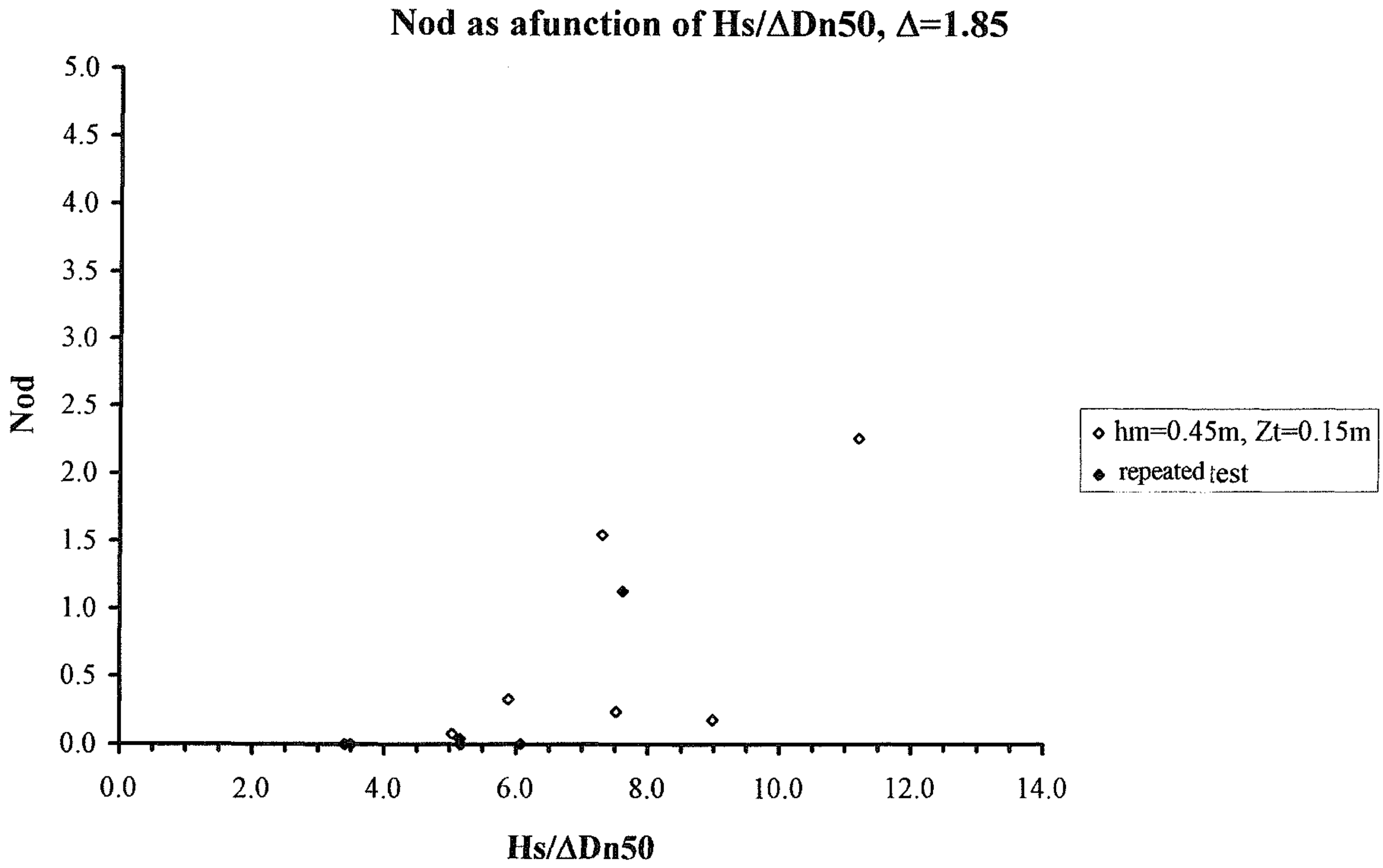
Nod as afunction of Hs/ΔDn50, Δ=1.85
Nod
5.0
4.5
4.0
3.5
3.0
2.5
2.0
1.5
1.0
0.5
0.0
0.0
2.0
4.0
6.0
8.0
10.0
12.0
14.0
Hs/ΔDn50
hm=0.45m, Zt=0.15m
repeated test

Appendix C

Contents

C1

teen po21

hm(m)	Zt(m)	Hsi(cm)	Δ	Tp(s)	Nod	ht/hm	Dn50(m)	ht(m)
0.3	0.08	9.3	1.55	1.34	0.06	0.733333	0.021	0.22
0.3	0.08	10.38	1.55	1.27	0	0.733333	0.021	0.22
0.3	0.08	13.35	1.55	1.59	0.22	0.733333	0.021	0.22
0.3	0.08	14.9	1.55	1.54	0.28	0.733333	0.021	0.22
0.3	0.08	16.75	1.55	1.69	0.73	0.733333	0.021	0.22
0.45	0.08	14.2	1.55	1.59	0	0.822222	0.021	0.37
0.45	0.08	16.72	1.55	1.49	0	0.822222	0.021	0.37
0.45	0.08	20.9	1.55	1.82	0.28	0.822222	0.021	0.37
0.45	0.15	9.72	1.55	1.37	0	0.666667	0.021	0.3
0.45	0.15	14.3	1.55	1.64	0.06	0.666667	0.021	0.3
0.45	0.15	16.95	1.55	1.49	0.06	0.666667	0.021	0.3
0.45	0.15	20.8	1.55	1.82	1.18	0.666667	0.021	0.3
0.3	0.15	9.35	1.55	1.37	0	0.5	0.021	0.15
0.3	0.15	10.48	1.55	1.27	0	0.5	0.021	0.15
0.3	0.15	12.53	1.55	1.59	0.62	0.5	0.021	0.15
0.3	0.15	14.8	1.55	1.54	0.79	0.5	0.021	0.15
0.3	0.15	16.95	1.55	1.69	1.18	0.5	0.021	0.15

teen po14.4

hm(m)	Zt(m)	Hsin(cm)	Δ	Tp(s)	Nod	ht/hm	Dn50(m)	ht(m)
0.3	0.08	9.3	1.55	1.34	0.17	0.733333	0.0144	0.22
0.3	0.08	10.38	1.55	1.27	0.04	0.733333	0.0144	0.22
0.3	0.08	13.35	1.55	1.59	0.21	0.733333	0.0144	0.22
0.3	0.08	14.9	1.55	1.54	0.37	0.733333	0.0144	0.22
0.3	0.08	16.75	1.55	1.69	1	0.733333	0.0144	0.22
0.45	0.08	14.2	1.55	1.59	0	0.822222	0.0144	0.37
0.45	0.08	16.72	1.55	1.49	0.04	0.822222	0.0144	0.37
0.45	0.08	20.9	1.55	1.82	0.29	0.822222	0.0144	0.37
0.45	0.15	9.72	1.55	1.37	0.04	0.666667	0.0144	0.3
0.45	0.15	14.3	1.55	1.64	0.17	0.666667	0.0144	0.3
0.45	0.15	16.95	1.55	1.49	0.21	0.666667	0.0144	0.3
0.45	0.15	20.8	1.55	1.82	1.45	0.666667	0.0144	0.3
0.3	0.15	9.35	1.55	1.37	0.08	0.5	0.0144	0.15
0.3	0.15	10.48	1.55	1.27	0.04	0.5	0.0144	0.15
0.3	0.15	12.53	1.55	1.59	0.25	0.5	0.0144	0.15
0.3	0.15	14.8	1.55	1.54	0.75	0.5	0.0144	0.15
0.3	0.15	16.95	1.55	1.69	1.37	0.5	0.0144	0.15

teen po9.8

hm(m)	Zt(m)	Hsin(cm)	Δ	Tp(s)	Nod	ht(m)	ht/hm	Dn50(m)
0.45	0.08	9.85	1.55	1.37	0	0.37	0.822222	0.0098
0.45	0.08	14.42	1.55	1.64	0.08	0.37	0.822222	0.0098
0.45	0.08	20.82	1.55	1.82	0.75	0.37	0.822222	0.0098
0.3	0.08	9.25	1.55	1.37	0.03	0.22	0.733333	0.0098
0.3	0.08	12.47	1.55	1.59	0.29	0.22	0.733333	0.0098
0.3	0.08	14.8	1.55	1.55	0.69	0.22	0.733333	0.0098
0.3	0.08	16.72	1.55	1.75	0.67	0.22	0.733333	0.0098
0.45	0.15	9.75	1.55	1.41	0	0.3	0.666667	0.0098
0.45	0.15	14.2	1.55	1.59	0.56	0.3	0.666667	0.0098
0.45	0.15	16.95	1.55	1.59	1.39	0.3	0.666667	0.0098
0.45	0.15	21.15	1.55	1.82	4.25	0.3	0.666667	0.0098
0.3	0.15	9.28	1.55	1.37	0.13	0.15	0.5	0.0098
0.3	0.15	12.62	1.55	1.59	1.42	0.15	0.5	0.0098
0.3	0.15	14.6	1.55	1.54	3.5	0.15	0.5	0.0098
0.3	0.15	16.78	1.55	1.76	4.71	0.15	0.5	0.0098

teen po21

ht/Dn50	function	N^0.15	Zt/hm	refl	number of removed stones		
10.47619	4.357218	0.655726	0.266667	0.195	1		
10.47619		0	0.266667	0.193	0		
10.47619	5.147151	0.796826	0.266667	0.228	4		
10.47619	5.540661	0.826178	0.266667	0.227	5		
10.47619	5.394676	0.95389	0.266667	0.291	13		
17.61905		0	0.177778	0.254	0		
17.61905		0	0.177778	0.247	0		
17.61905	7.7718	0.826178	0.177778	0.297	5		
14.28571		0	0.333333	0.229	0		
14.28571	6.699808	0.655726	0.333333	0.249	1		
14.28571	7.941381	0.655726	0.333333	0.244	1		
14.28571	6.233472	1.025138	0.333333	0.297	21		
7.142857		0	0.5	0.191	0		
7.142857		0	0.5	0.193	0		
7.142857	4.135627	0.930805	0.5	0.207	11		
7.142857	4.710496	0.965259	0.5	0.224	14		
7.142857	5.079681	1.025138	0.5	0.282	21		

teen po14.4

ht/Dn50	function	N^0.15	Zt/hm	refl	number of removed stones		
15.27778	5.435274	0.766597	0.266667	0.195	4		
15.27778	7.536924	0.617034	0.266667	0.193	1		
15.27778	7.558823	0.791285	0.266667	0.228	5		
15.27778	7.749288	0.86145	0.266667	0.227	9		
15.27778	7.50448	1	0.266667	0.291	24		
25.69444		0	0.177778	0.254	0		
25.69444	12.1404	0.617034	0.177778	0.247	1		
25.69444	11.27437	0.830538	0.177778	0.297	7		
20.83333	7.057698	0.617034	0.333333	0.229	1		
20.83333	8.357464	0.766597	0.333333	0.249	4		
20.83333	9.597157	0.791285	0.333333	0.244	5		
20.83333	8.813815	1.057317	0.333333	0.297	35		
10.41667	6.118626	0.684642	0.5	0.191	2		
10.41667	7.609535	0.617034	0.5	0.193	1		
10.41667	6.911398	0.812252	0.5	0.207	6		
10.41667	6.923223	0.957766	0.5	0.224	18		
10.41667	7.243816	1.048354	0.5	0.282	33		

teen po9.8

ht/Dn50	function	N^0.15	Zt/hm	refl	number of removed stones		
37.7551		0	0.177778	0.209	0		
37.7551	13.86577	0.684642	0.177778	0.239	3		
37.7551	14.3108	0.957766	0.177778	0.302	28		
22.44898	10.30424	0.590974	0.266667	0.188	1		
22.44898	9.88437	0.830538	0.266667	0.236	11		
22.44898	10.30093	0.945861	0.266667	0.251	26		
22.44898	11.68873	0.941697	0.266667	0.315	25		
30.61224		0	0.333333	0.232	0		
30.61224	10.1977	0.916702	0.333333	0.254	21		
30.61224	10.62086	1.050636	0.333333	0.245	52		
30.61224	11.20713	1.242391	0.333333	0.297	159		
15.30612	8.296572	0.736362	0.5	0.185	5		
15.30612	7.882397	1.054006	0.5	0.212	53		
15.30612	7.964983	1.20673	0.5	0.239	131		
15.30612	8.755502	1.261691	0.5	0.312	176		

C1

teenba15.1

hm(m)	Zt(m)	Hsin(cm)	Δ	Tp(s)	Nod	ht/hm	Dn50(m)	ht(m)
0.45	0.08	9.83	1.85	1.41	0	0.822222	0.0151	0.37
0.45	0.08	14.58	1.85	1.59	0.04	0.822222	0.0151	0.37
0.45	0.08	17.05	1.85	1.49	0.08	0.822222	0.0151	0.37
0.45	0.08	21.15	1.85	1.82	0.17	0.822222	0.0151	0.37
0.3	0.08	9.31	1.85	1.37	0	0.733333	0.0151	0.22
0.3	0.08	12.55	1.85	1.59	0	0.733333	0.0151	0.22
0.3	0.08	14.9	1.85	1.54	0	0.733333	0.0151	0.22
0.3	0.08	16.95	1.85	1.69	0.08	0.733333	0.0151	0.22
0.45	0.15	9.52	1.85	1.41	0	0.666667	0.0151	0.3
0.45	0.15	14.08	1.85	1.64	0.08	0.666667	0.0151	0.3
0.45	0.15	16.45	1.85	1.49	0.33	0.666667	0.0151	0.3
0.45	0.15	20.4	1.85	1.82	1.55	0.666667	0.0151	0.3
0.3	0.15	9.22	1.85	1.37	0.04	0.5	0.0151	0.15
0.3	0.15	10.2	1.85	1.27	0	0.5	0.0151	0.15
0.3	0.15	12.22	1.85	1.59	0.96	0.5	0.0151	0.15
0.3	0.15	14.58	1.85	1.49	1.09	0.5	0.0151	0.15
0.3	0.15	16.12	1.85	1.69	2.26	0.5	0.0151	0.15

refl	2 number of removed stones		
0.202	0		
0.236	1		
0.228	1		
0.297	19		
0.192	1		
0.21	7		
0.239	4		
0.31	9		
0.232	0		
0.253	1		
0.246	0		
0.298	27		
0.195	1		
0.199	5		
0.204	7		
0.218	25		
0.287			

teenba10.2

ht/Dn50	function	N^0.15	Zt/hm	refl	number of removed stones		
36.27451		0	0.177778	0.209	0		
36.27451	12.93079	0.590974	0.177778	0.239	1		
36.27451	11.61502	0.949924	0.177778	0.302	24		
21.56863		0	0.266667	0.188	0		
21.56863	8.783768	0.752339	0.266667	0.236	5		
21.56863	11.25521	0.696845	0.266667	0.251	3		
21.56863	10.7835	0.821683	0.266667	0.315	9		
29.41176		0	0.333333	0.232	0		
29.41176	9.321478	0.807294	0.333333	0.254	8		
29.41176	11.61735	0.773198	0.333333	0.245	6		
29.41176	9.917957	1.130098	0.333333	0.297	76		
14.70588	6.536758	0.752339	0.5	0.185	5		
14.70588	6.540618	1.022513	0.5	0.212	39		
14.70588	6.819582	1.134549	0.5	0.239	78		
14.70588	7.337949	1.21184	0.5	0.312	121		

teenba15.1

ht/Dn50	function1	N^0.15	1 number	Hsin2 (cm	Nodnieuw	Nod^0.15	function2	Zt/hm
24.50331		0	0	9.82	0	0		0.177778
24.50331	8.458627	0.617034	1	14.32	0.04	0.617034	8.307787	0.177778
24.50331	8.914812	0.684642	2	16.88	0.04	0.617034	9.792978	0.177778
24.50331	9.876302	0.766597	4	21.14	0.79	0.965259	7.839931	0.177778
14.56954		0	0	10.32	0.04	0.617034	5.987176	0.266667
14.56954		0	0	12.63	0.29	0.830538	5.44371	0.266667
14.56954		0	0	14.71	0.17	0.766597	6.86905	0.266667
14.56954	8.862526	0.684642	2	16.9	0.38	0.864903	6.994722	0.266667
19.86755		0	0	9.77	0	0		0.333333
19.86755	7.36191	0.684642	2	14.42	0.04	0.617034	8.365802	0.333333
19.86755	6.954087	0.846793	8	16.97	0	0		0.333333
19.86755	6.838042	1.067947	37	21.26	1.13	1.018502	7.472275	0.333333
9.933775	5.349008	0.617034	1	9.2	0.04	0.617034	5.337405	0.5
9.933775		0	0	12.58	0.21	0.791285	5.691137	0.5
9.933775	4.401309	0.993895	23	14.78	0.29	0.830538	6.370391	0.5
9.933775	5.152226	1.013011	26	16.57	1.05	1.007345	5.888375	0.5
9.933775	5.106227	1.130098	54					0.5

teenba10.2

hm(m)	Zt(m)	Hsin(cm)	Δ	Tp(s)	Nod	ht/hm	Dn50(m)	ht(m)
0.45	0.08	9.85	1.85	1.37	0	0.822222	0.0102	0.37
0.45	0.08	14.42	1.85	1.64	0.03	0.822222	0.0102	0.37
0.45	0.08	20.82	1.85	1.82	0.71	0.822222	0.0102	0.37
0.3	0.08	9.25	1.85	1.37	0	0.733333	0.0102	0.22
0.3	0.08	12.47	1.85	1.59	0.15	0.733333	0.0102	0.22
0.3	0.08	14.8	1.85	1.55	0.09	0.733333	0.0102	0.22
0.3	0.08	16.72	1.85	1.75	0.27	0.733333	0.0102	0.22
0.45	0.15	9.75	1.85	1.41	0	0.666667	0.0102	0.3
0.45	0.15	14.2	1.85	1.59	0.24	0.666667	0.0102	0.3
0.45	0.15	16.95	1.85	1.59	0.18	0.666667	0.0102	0.3
0.45	0.15	21.15	1.85	1.82	2.26	0.666667	0.0102	0.3
0.3	0.15	9.28	1.85	1.37	0.15	0.5	0.0102	0.15
0.3	0.15	12.62	1.85	1.59	1.16	0.5	0.0102	0.15
0.3	0.15	14.6	1.85	1.54	2.32	0.5	0.0102	0.15
0.3	0.15	16.78	1.85	1.76	3.6	0.5	0.0102	0.15

C1

teenbr23.1

hm(m)	Zt(m)	Hsin(cm)	Δ	Tp(s)	Nod	ht/hm	Zt/hm	ht(m)
0.45	0.08	9.83	0.9	1.41	0.07	0.822222	0.177778	0.37
0.45	0.08	14.58	0.9	1.59	0.86	0.822222	0.177778	0.37
0.45	0.08	17.05	0.9	1.49	0.46	0.822222	0.177778	0.37
0.45	0.08	21.15	0.9	1.82	1.64	0.822222	0.177778	0.37
0.3	0.08	9.31	0.9	1.37	0.33	0.733333	0.266667	0.22
0.3	0.08	12.55	0.9	1.59	1.12	0.733333	0.266667	0.22
0.3	0.08	14.9	0.9	1.54	1.05	0.733333	0.266667	0.22
0.3	0.08	16.95	0.9	1.69	1.38	0.733333	0.266667	0.22
0.45	0.15	9.52	0.9	1.41	0.13	0.666667	0.333333	0.3
0.45	0.15	14.08	0.9	1.64	1.58	0.666667	0.333333	0.3
0.45	0.15	16.45	0.9	1.49	2.43	0.666667	0.333333	0.3
0.45	0.15	20.4	0.9	1.82	4.34	0.666667	0.333333	0.3
0.3	0.15	9.22	0.9	1.37	0.66	0.5	0.5	0.15
0.3	0.15	10.2	0.9	1.27	0.53	0.5	0.5	0.15
0.3	0.15	12.22	0.9	1.59	2.11	0.5	0.5	0.15
0.3	0.15	14.58	0.9	1.49	3.88	0.5	0.5	0.15
0.3	0.15	16.12	0.9	1.69	4.34	0.5	0.5	0.15

Dn50(m)	ht/Dn50	function1	N^0.15	refl	Nod^0.15n	function2	Hsnieuw	Nodnieuw
0.0231	16.01732	7.045865	0.671065	0.202	0		9.82	0
0.0231	16.01732	7.173453	0.977631	0.236	0.923906	7.455225	14.32	0.59
0.0231	16.01732	9.21417	0.890049	0.228	0.951919	8.529392	16.88	0.72
0.0231	16.01732	9.445595	1.077027	0.297	1.083801	9.382122	21.14	1.71
0.0231	9.52381	5.288325	0.846793	0.192	0.890049	5.57714	10.32	0.46
0.0231	9.52381	5.934806	1.017145	0.21	1.034038	5.875061	12.63	1.25
0.0231	9.52381	7.114647	1.007345	0.239	1.007345	7.023924	14.71	1.05
0.0231	9.52381	7.768432	1.049499	0.31	1.017145	7.99189	16.9	1.12
0.0231	12.98701	6.218576	0.736362	0.232	0.671065	7.002859	9.77	0.07
0.0231	12.98701	6.323385	1.071022	0.253	0.939575	7.382087	14.42	0.66
0.0231	12.98701	6.925808	1.14246	0.246	1.034038	7.893886	16.97	1.25
0.0231	12.98701	7.873217	1.246302	0.298	1.160659	8.810574	21.26	2.7
0.0231	6.493506	4.720031	0.939575	0.195	0.909162	4.867343	9.2	0.53
0.0231	6.493506	5.396402	0.909162	0.199	1.025138	5.902607	12.58	1.18
0.0231	6.493506	5.25502	1.118516	0.204	1.049499	6.773889	14.78	1.38
0.0231	6.493506	5.722401	1.225532	0.218	1.176776	6.772894	16.57	2.96
0.0231	6.493506	6.221385	1.246302	0.287				

1number o	2number of removed stones		
1	0		
13	9		
7	11		
25	26		
5	7		
17	19		
16	16		
21	17		
2	1		
24	10		
37	19		
66	41		
10	8		
8	18		
32	21		
59	45		
66			

C2

	Hsin (m)	Hsin(m)	Zt	delta	ht	ht/Dn50	Hs/ΔDn50	Hs/ΔDn50
Dn50	Nod =0.5	Nod=1					Nod =0.5	Nod=1.0
0.021	0.161	0.18	0.08	1.55	0.22	10.47619	4.946237	5.529954
0.0144	0.156	0.182	0.08	1.55	0.22	15.27778	6.989247	8.154122
0.0098	0.147	0.167	0.08	1.55	0.22	22.44898	9.677419	10.99408
0.0151			0.08	1.85	0.22	14.56954		
0.0102	0.169	0.184	0.08	1.85	0.22	21.56863	8.956015	9.750927
0.0231	0.103	0.14	0.08	0.9	0.22	9.52381	4.954305	6.734007
0.021	0.235	0.26	0.08	1.55	0.37	17.61905	7.219662	7.987711
0.0144	0.222	0.232	0.08	1.55	0.37	25.69444	9.946237	10.39427
0.0098	0.196	0.216	0.08	1.55	0.37	37.7551	12.90323	14.21988
0.0151	0.222	0.258	0.08	1.85	0.37	24.50331	7.94702	9.235726
0.0102	0.2	0.218	0.08	1.85	0.37	36.27451	10.59883	11.55273
0.0231	0.154	0.184	0.08	0.9	0.37	16.01732	7.407407	8.850409
0.021	0.206	0.226	0.15	1.55	0.3	14.28571	6.328725	6.943164
0.0144	0.181	0.232	0.15	1.55	0.3	20.83333	8.109319	10.39427
0.0098	0.152	0.166	0.15	1.55	0.3	30.61224	10.00658	10.92824
0.0151	0.176	0.189	0.15	1.85	0.3	19.86755	6.30034	6.765706
0.0102	0.176	0.19	0.15	1.85	0.3	29.41176	9.326974	10.06889
0.0231	0.12	0.138	0.15	0.9	0.3	12.98701	5.772006	6.637807
0.021	0.136	0.145	0.15	1.55	0.15	7.142857	4.178187	4.454685
0.0144	0.142	0.158	0.15	1.55	0.15	10.41667	6.362007	7.078853
0.0098	0.112	0.124	0.15	1.55	0.15	15.30612	7.373272	8.163265
0.0151	0.132	0.141	0.15	1.85	0.15	9.933775	4.725255	5.047432
0.0102	0.112	0.128	0.15	1.85	0.15	14.70588	5.935347	6.783254
0.0231	0.092	0.107	0.15	0.9	0.15	6.493506	4.425204	5.146705

C3

Shields		ht/Dn50	Hs/ΔDn50		Rance and			ht/Dn50
d=u^2/Δg		21.407	10.107		Warren			10.517
		23.046	10.543		d=16u^2.5/T^0.5(Δg)^1.5			11.442
		26.511	11.429					13.431
		22.829	9.479					12.058
		36.968	19.231					16.253
		26.158	10.719					13.041
		29.955	11.596					15.231
		40.525	13.85					21.541
		35.753	11.596					19.86
		46.03	13.449					26.534
		43.374	20.059					19.272
		27.617	12.235					14.231
		37.679	14.666					20.316
		58.134	19.003					33.443
		48.154	15.27					28.654
		48.154	15.27					28.654
		62.823	27.921					30.32
		19.376	11.334					9.796
		17.572	10.732					8.763
		30.308	14.6					16.323
		24.752	11.774					13.802
		36.174	14.6					21.285
		28.126	19.167					12.356

C2

C3

ht/hm	hm	Reflection
0.733333	0.3	1.27
0.733333	0.3	1.27
0.733333	0.3	1.25
0.733333	0.3	
0.733333	0.3	1.32
0.733333	0.3	1.2
0.822222	0.45	1.3
0.822222	0.45	1.3
0.822222	0.45	1.3
0.822222	0.45	1.3
0.822222	0.45	1.3
0.822222	0.45	1.24
0.666667	0.45	1.3
0.666667	0.45	1.27
0.666667	0.45	1.25
0.666667	0.45	1.25
0.666667	0.45	1.26
0.666667	0.45	1.24
0.5	0.3	1.21
0.5	0.3	1.22
0.5	0.3	1.21
0.5	0.3	1.21
0.5	0.3	1.21
0.5	0.3	1.2

Rance and		ht/Dn50	Hs/ΔDn50
Warren		13.123	6.196
met refl		14.278	6.523
		16.759	7.224
u=w.r.1,5H			
		15.654	6.5
d=2.56u^2.5		23.369	12.157
		15.35	6.29
		17.927	6.94
		25.354	8.665
		23.376	7.581
		31.231	9.125
		25.529	11.806
		16.751	7.421
		25.35	9.868
		43.419	14.193
		37.201	11.797
		36.467	11.564
		40.163	17.85
		13.795	8.069
		12.089	7.384
		22.988	11.074
		19.437	9.246
		29.975	12.098
		17.765	12.106

AppC3

Hs/ΔDn50			Rance and			ht/Dn50	Hs/ΔDn50	
4.965			Warren			12.091	5.675	
5.235			d=14u^2.5/T^0.5(Δg)^1.5			13.077	5.982	
5.79						15.349	6.617	
5.007						13.78	5.722	
8.455						18.575	9.663	
5.344						14.904	6.107	
5.896						17.406	6.738	
7.362						24.618	8.413	
6.441						22.697	7.361	
7.753						30.324	8.86	
8.913						22.025	10.186	
6.305						16.265	7.205	
7.908						23.219	9.038	
10.932						38.22	12.493	
9.087						32.747	10.385	
9.087						32.747	10.385	
13.475						34.651	15.401	
5.73						11.195	6.549	
5.352						10.015	6.117	
7.863						18.655	8.987	
6.565						15.773	7.503	
8.591						24.325	9.818	
8.42						14.121	9.623	